

University of Louisville

ThinkIR: The University of Louisville's Institutional Repository

Electronic Theses and Dissertations

12-2021

Assessing the role of arsenic exposure and MIRNA-186 in skin tumorigenesis and chromosomal instability.

Angeliki Lykoudi
University of Louisville

Follow this and additional works at: <https://ir.library.louisville.edu/etd>



Part of the [Medical Pharmacology Commons](#), and the [Medical Toxicology Commons](#)

Recommended Citation

Lykoudi, Angeliki, "Assessing the role of arsenic exposure and MIRNA-186 in skin tumorigenesis and chromosomal instability." (2021). *Electronic Theses and Dissertations*. Paper 3743.
<https://doi.org/10.18297/etd/3743>

This Master's Thesis is brought to you for free and open access by ThinkIR: The University of Louisville's Institutional Repository. It has been accepted for inclusion in Electronic Theses and Dissertations by an authorized administrator of ThinkIR: The University of Louisville's Institutional Repository. This title appears here courtesy of the author, who has retained all other copyrights. For more information, please contact thinkir@louisville.edu.

ASSESSING THE ROLE OF ARSENIC EXPOSURE AND MIRNA-186 IN SKIN
TUMORIGENESIS AND CHROMOSOMAL INSTABILITY

By

Angeliki Lykoudi

B.S. in Molecular Biology and Genetics, 2018

Democritus University of Thrace, Greece

A Thesis

Submitted to the Faculty of the
School of Medicine of the University of Louisville

In Partial Fulfillment of the Requirements

For the Degree of

Master of Science in
Pharmacology and Toxicology

Department of Pharmacology and Toxicology

University of Louisville

Louisville, KY

December 2021

Copyright 2021 by Angeliki Lykoudi

All Rights Reserved

ASSESSING THE ROLE OF ARSENIC EXPOSURE AND MIRNA-186 IN SKIN
TUMORIGENESIS AND CHROMOSOMAL INSTABILITY

By

Angeliki Lykoudi

B.S. in Molecular Biology and Genetics, 2018

A Thesis Approved on

December 8, 2020

By the following Thesis Committee

Dr. J. Christopher States, Mentor and Thesis Director

Dr. Carolyn M. Klinge

Dr. Sandra S. Wise

ACKNOWLEDGEMENTS

I would like to express my sincere gratitude to my supervisor Dr. J. Christopher States, for his guidance, patience, and encouragement. I am also very grateful to Dr. Ana P.F Cardoso and Dr. Mayukh Banerjee for being great colleagues and precious friends. I am also thankful to Dr. Walter H. Watson, Dr. Yuxuan Zheng and other lab members for their assistance and constructive advice. I would also like to thank Dr. Sandra Wise for teaching me about cytogenetics and for her valuable help. I would like to thank Dr. Ceresa's, Dr. Damodaran's, Dr. Hein's, Dr. Wise's, and Dr. Yaddanapudi's labs for their kind assistance. Finally, I would like to thank my friends in the U.S. and Greece as well as my family for their love and support in all my endeavors.

ABSTRACT

ASSESSING THE ROLE OF ARSENIC EXPOSURE AND MIRNA-186 IN SKIN TUMORIGENESIS AND CHROMOSOMAL INSTABILITY

Angeliki Lykoudi

December 8, 2020

Chronic arsenic exposure through drinking water is a global health issue, affecting more than 200 million people. Arsenic is a group I human carcinogen and causes chromosomal instability (CIN). Arsenic exposure is the second most cause of skin cancer after UV radiation. MiR-186 is overexpressed in arsenic-induced squamous cell carcinoma relative to premalignant hyperkeratosis. Predicted targets of miR-186 are cell cycle regulators. Thus, we hypothesize that miR-186 overexpression drives malignant transformation of HaCaT cells by induction of CIN. Stable clones of HaCaT transfected with pEP-miR-186 expression vector or empty vector were maintained under puromycin selection were exposed to 0 or 100 nM NaAsO₂ and cultured for 29 weeks. HaCaT overexpressing miR-186 and exposed to NaAsO₂ showed growth ability in agar at 12 weeks and increased CIN in contrast to unexposed vector control cells. These cells also undergo epithelial to mesenchymal transition and form colonies in agar at 29 weeks. These results suggest that miR-186 overexpression exacerbates the arsenite-induced CIN and potentially is associated with accelerated skin carcinogenesis.

TABLE OF CONTENTS

CHAPTER 1: INTRODUCTION.....	1
1.1 Arsenic: An ambiguous and ubiquitous toxic metalloid.....	1
1.2 Arsenic distribution and contamination of drinking water.....	3
1.3 Absorption, Distribution, Metabolism and Excretion (ADME) profile of arsenic	4
1.4 Acute and chronic arsenic poisoning.....	7
1.5 Arsenic and disease	9
1.6 Arsenic-induced cancers	13
1.7 Arsenic-induced skin cancer.....	15
1.8 Modes of action in arsenic-induced carcinogenesis	16
1.9 MicroRNAs (miRNAs): Biogenesis, processing, and regulation of translation	23
1.10 Role of miRNAs in carcinogenesis	26
1.11 Dysregulated miRNAs in arsenic-induced cancers.....	28
1.12 Dysregulated miRNAs in arsenic-induced skin cancers	29
1.13 Association of miR-186 with carcinogenesis.....	31
1.14 The role of miR-186 in carcinogenesis through regulation of cell cycle	31
1.15 MiR-186 targets cell cycle proteins in arsenic-induced skin cancer.....	32
1.16 The biology of the spindle assembly checkpoint.....	33
1.17 Spindle assembly checkpoint and aneuploidy in carcinogenesis.....	36
1.18 HaCaT model of arsenic-induced skin carcinogenesis.....	37
1.19 Chromosomal instability	39
1.20 Mechanisms of chromosomal instability associated with carcinogenesis	43
1.21 Types of chromosomal instability associated with carcinogenesis.....	45
1.22 Metal-induced chromosomal instability as a driving force for carcinogenesis.....	48
1.23 Arsenic-induced chromosomal instability as a driving force for carcinogenesis ...	51
1.24 Aim of the thesis	54
CHAPTER 2: MATERIALS AND METHODS.....	55
2.1 Cell culture	55
2.1.1 HaCaT cells and arsenite exposure	55
2.1.2 HeLa cells	58
2.2 Cytogenetic analysis.....	58
2.2.1 Chromosomal damage staining.....	59
2.2.2 Karyotype analysis.....	59
2.3 RNA extraction.....	60
2.4 Western blot analysis.....	61

2.5 Flow cytometry cell cycle assay	62
2.6 Soft agar colony formation assay	62
2.7 Mycoplasma PCR assay	65
2.8 Statistical analysis	65
CHAPTER 3: RESULTS	66
3.1 Soft agar colony formation assay	66
3.2 Protein levels of epithelial-mesenchymal transition	70
3.3 Flow cytometry for cell cycle analysis	83
3.4 Protein levels of cell cycle proteins	87
3.5 Cytogenetic analysis for numerical and structural chromosomal alterations	94
CHAPTER 4: DISCUSSION.....	105
REFERENCES	117
CURRICULUM VITAE	137

LIST OF FIGURES

Figure 1: The biotransformation pathway of inorganic arsenic.....	6
Figure 2: miRNA biogenesis	265
Figure 3: miRNAs may act as tumor suppressor and oncogene.....	298
Figure 4: The molecular basis of spindle assembly checkpoint (SAC)	36
Figure 5: Schematic overview of chronic culture and exposure to 0 or 100 nM.....	60
Figure 6: Schematic overview of the protocol for the soft agar colony formation assay.	67
Figure 7: Soft agar colony formation assay.....	70
Figure 8: HeLa cells as positive control.....	772
Figure 9 : Western blots for epithelial markers at 12 weeks.....	75
Figure 10 : Western blots for mesenchymal markers at 12 weeks.....	78
Figure 11 : Western blots for epithelial markers at 29 weeks.....	81
Figure 12 : Western blots for mesenchymal markers at 29 weeks.....	84
Figure 13 : Flow cytometry for cell cycle analysis.....	88
Figure 14 :Western blots for cell cycle proteins at 12 weeks.....	993
Figure 15 : Western blots for cell cycle proteins at 29 weeks.....	95
Figure 16 : Total structural and numerical chromosomal abnormalities.....	98
Figure 17: Representative karyotypes of unexposed cells at 9 weeks.....	102
Figure 18: Representative karyotypes of arsenic exposed cells at 9 weeks.....	103
Figure 19: Most common structural chromosomal abnormalities.....	105
Figure 20: MiRNA-186 induces structural chromosomal abnormalities.....	106
Figure 21: Clonal variability in miRNA-186 induced structural chromosomal instability.....	107

CHAPTER 1: INTRODUCTION

1.1 Arsenic: An ambiguous and ubiquitous toxic metalloid

Heavy metals are ubiquitous in the environment and heavy metal-induced environmental pollution is a global health hazard. Arsenic is a prevalent natural pollutant and the 20th most common element in the earth's crust (IARC Working Group on the Evaluation of Carcinogenic Risks to Humans., 2012). It is ranked first on the Agency for Toxic Substances and Disease Registry (ATSDR) Substance Priority List for more than 20 years (ATSDR, 2017). Arsenic is a toxic metalloid and acknowledged carcinogen. In 1973, arsenic was classified as a group I human carcinogen by the International Agency for Research on Cancer (IARC) [2]. Arsenic is also clastogenic and it causes chromosomal instability (CIN) both *in vitro* and *in vivo* [3]. CIN is a hallmark of carcinogenesis, and it is associated with poor prognosis, metastasis, and therapeutic resistance [4]. The molecular mechanism by which arsenic induces CIN-mediated carcinogenesis is yet to be delineated [5]. Arsenic has also an atherogenic potential according to epidemiologic studies that have shown an association between elevated arsenic levels in drinking water and an increased risk of atherosclerosis and cardiovascular diseases [6] [7]. It is also reported that sodium arsenate induces developmental malformations in a variety of experimental animals after subjecting mothers to administration of teratogenic levels of arsenate [8].

Arsenic has been used since ancient times, both as a poison and a medicine. It is a component of Chinese, Tibetan, Vietnamese, and Indian traditional medicines [9]. Arsenicals also are still used to treat some tropical diseases [9]. It is tasteless, colorless,

and odorless, characteristics making arsenic a powerful poison throughout history. On the other hand, potassium bicarbonate-based arsenic solutions were widely used to treat asthma, convulsions, and psoriasis [10] [11]. Organic arsenic preparations such as melarsoprol are widely used for the treatment of African trypanosomiasis [12]. Arsenic was also approved by Food and Drug Administration (FDA) in 2001 for the treatment of acute promyelocytic leukemia (APL) [13]. Trisenox is indicated for induction of remission in patients with APL who are refractory to, or have relapsed from, retinoic acid chemotherapy or have t(15;17) chromosomal translocation [13]. Moreover, arsenic trioxide when used in combination with cisplatin (PDD) or doxorubicin (ADM) on hepatocellular carcinoma, improved therapeutic effectiveness, and surmounted drug resistance [14]. Also, it has been shown that cisplatin treatment alone, induces xeroderma pigmentosum group C (XPC) expression [15]. XPC plays a role in the global genomic nucleotide excision repair pathway, which detects and eliminates bulky adduct DNA damage in the entire genome [16]. The latter could suggest that the cisplatin-resistant cells are due to cisplatin-induced XPC expression [17]. However, cotreatment of cisplatin-resistant ovarian carcinoma cells with arsenic suppressed the cisplatin-induced XPC expression, thereby sensitizing wild-type p53-expressing cells to cisplatin and increasing cellular and DNA platinum accumulation [18].

So, there is a paradox about arsenic, since it is a well-established toxicant and carcinogen, but it is also used in medical applications, and specifically as a treatment for APL. However, carcinogenicity is observed in patients who received arsenic treatment, and its use has declined over the years. Thus, more investigation on arsenic's mechanisms of toxicity is crucial for delineating its toxic effects and its usage as a cancer chemotherapeutic agent.

1.2 Arsenic distribution and contamination of drinking water

Environmental arsenic contamination can be from natural or industrial sources, such as arsenic-based pesticides, wood preservatives, feed additives, chemical warfare, and industrial waste [19]. Ingestion is the primary source of exposure, and the main source is drinking water. The World Health Organization (WHO) and the Environmental Protection Agency (US EPA) have set the maximum contaminant level (MCL) at 10 ppb ($\mu\text{g/L}$) (in 2008). However, it is estimated that more than 200 million people consume water contaminated with arsenic above the recommended limit [20]. Exposure to arsenic levels that exceed the MCL for more than six months, leads to arsenicosis [21]. Also, in a study performed in Inner Mongolia, China, it was shown that skin lesions improved after drinking low arsenic-containing water for 1 year [21]. However, a 5-year follow-up showed no more improvement of skin lesions [22]. Countries of South Asia and the Americas, including Bangladesh, India (West Bengal), Taiwan, China and Argentina, Mexico, Bolivia, Chile respectively, are highly affected by arsenic poisoning through consumption of contaminated drinking water [23]. Specifically, more than 70 million people in the Ganges River delta, spanning Bangladesh and West Bengal in India, consume very high levels of arsenic via their drinking water, ranging from 40 $\mu\text{g/L}$ to 2 mg/L [24] [25]. Also, in central and western China, ground and surface water contain arsenic levels as high as 969 $\mu\text{g/L}$ and arsenic metabolites were detected in residents' urine samples [26] [27]. Arsenicosis and high risk for a wide range of chronic arsenic exposure-associated health complications are observed in the populations mentioned above [28] [29]. Most commonly, skin manifestations occur, for example, Blackfoot disease is reported frequently [30]. The latter is a dry gangrene resulting from ischemic changes in the toes accompanied by ulcers [30]. Arsenic contamination is also a prevalent issue in the United States, since the EPA limits arsenic in public water supplies, but not in private wells. Approximately, 15 % of the total population rely on

domestic wells as a main water source [31] [32]. Thus, it is estimated that 2.9 million people are at high risk due to contaminated (more than 10 ppb) private well water consumption in the United States [33].

The most common route of arsenic exposure is through ingestion of naturally contaminated food and water. An accurate measurement of the absorbed dose of arsenic in tissues, is challenging, because of variation among individuals, like gender, individual genetics, interactions with specific agents and occupational exposures [34]. The average blood arsenic level in people exposed to high levels of arsenic in their drinking water for approximately 18 years, has been reported to be 100 nM and is referred to as “physiologically relevant” [35] (see 2.1.1.).

1.3 Absorption, Distribution, Metabolism and Excretion (ADME) profile of arsenic

The main route of arsenic exposure is through ingestion and both pentavalent and trivalent soluble arsenic compounds are absorbed from the gastrointestinal tract (GI tract). Also, absorption of arsenic in inhaled airborne particles is dependent on the solubility and size of the particles. The main site of arsenic metabolism is the liver, and methylation is critical for arsenic metabolism. Frederick Challenger was the first to suggest arsenic methylation as a major metabolic pathway [36]. Arsenic metabolism is characterized by two main types of reactions: 1) reduction reactions of pentavalent to trivalent arsenic by arsenate reductase and glutathione (GSH) [37]. 2) oxidative methylation reactions in which trivalent forms of arsenic are sequentially methylated to form mono-, di- and trimethylated products by arsenite (III) methyltransferase (AS3MT), using S-adenosyl methionine (SAM) as the methyl donor [38] (Figure 1).

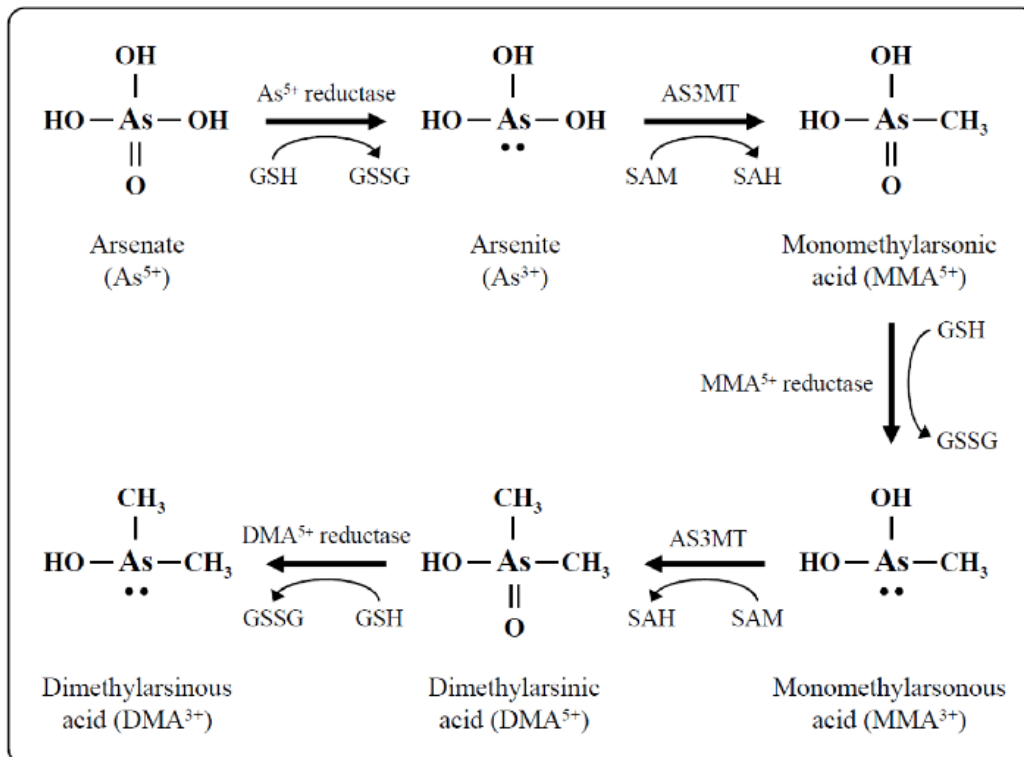


Figure 1: The biotransformation pathway of inorganic arsenic in the human body [39]

Methylation of inorganic arsenic facilitates the excretion of arsenic from the body because the products MMA^{III} (monomethylarsonous acid), DMA^{III} (dimethylarsinic acid) and DMA^V (dimethylarsenic acid) are readily excreted in urine [40].

Moreover, Frederick Challenger and his colleagues described the arsenic methylation pathway, however, alternative schemes for arsenic methylation including glutathione-or protein-conjugated intermediates have been also suggested [41]. Specifically, it has been proposed that trivalent arsenic persists during methylation reactions and that oxidation to pentavalent arsenic occurs after methylation [41] [42]. In this alternative pathway, the arsenic-glutathione complexes are the major substrates for arsenite (III) methyltransferase (AS3MT) and inorganic arsenic triglutathione (iAs^{III} (GS)₃) is produced and methylated to form, MMA^{III}(GS)₂ and DMA^{III}(GS).

Methylation of arsenic is also considered to be a bioactivation and detoxification pathway depending on the condition of arsenic exposure and its levels. Bioactivation process is suggested to occur in case of long-term arsenic exposure, but in cases of acute exposures, it may be a detoxification pathway [41]. All arsenic metabolites are toxic to different extents. Reports have shown that MMA^{III} and DMA^{III} are more cytotoxic and genotoxic than arsenite [43] [44]. Also, it has been found that MMA^{III} and DMA^{III} bind differentially with zinc finger peptides and proteins [45] and they can inhibit the activities of many enzymes in human hepatocytes, epidermal keratocytes and bronchial epithelial cells respectively [41] [44]. So, the products of arsenic metabolism exert toxic effects and they are not just by-products.

Studies in humans suggest the existence of various AS3MT polymorphisms among individuals which affect its activity [46]. Also, ingested organoarsenicals such as, MMA^V DMA^V and arsenobetaine are much less extensively metabolized and more rapidly eliminated in urine than inorganic arsenic in both experimental animals and humans [47]. Finally, some studies have also indicated that the arsenic methylating capacity varies

depending on the tissue and the highest amount of arsenic methylating activity is in the cytosol of testes, followed by kidney, liver, and lungs [48] [49]. So, arsenic retention and tissue distribution depend on the bioconversion to methylated metabolites and determines its toxic and carcinogenic potential [50].

The distribution of the different arsenic species depends on the animal or plant species to which arsenic is administered and the different types of cells within the same organism [41]. Rodent models are used for most of the toxicological studies of arsenic effects. However, the ADME profile of arsenic differs significantly between rodents and humans. Specifically, in rodents, during oxidative methylation, DMA^V can be converted into trimethylarsine oxide (TMAO^V) [41]. Strain specific differences have also been observed in rodents' arsenic metabolism. For example, C57BL/6J mice are more susceptible to oxidative hepatic injury compared with 129X1/SvJ mice after acute arsenic exposure [51]. So, species and strain metabolic differences should be considered during the experimental design, and data extrapolation to humans.

1.4 Acute and chronic arsenic poisoning

Arsenic toxicity depends on its dose and duration of exposure. Most cases of acute arsenic poisoning occur from accidental ingestion of insecticides or pesticides and less commonly from attempted suicide [52]. The symptoms of acute poisoning include, abdominal pain, toxic cardiomyopathy, skin rash, hematological abnormalities, peripheral neuropathy, and seizures [53] [54]. Usually, small amounts (less than 5 mg) cause vomiting, dehydration, hypotension, and diarrhea but resolve after 12 hours without treatment [52]. However, ingestion of large arsenic amounts requires treatment, such as chelation therapy, gastric lavage, or administration of intravenous fluids. The lethal dose of arsenic in acute poisoning ranges from 100 mg to 300 mg [55] or 0.6 mg/kg/day [52].

So, depending on the quantity consumed, death can occur within 24 hours to four days. For example, a study showed that a 23-year-old male who voluntarily took 300 mg of arsenic daily, survived only 8 days [53]. For the acute arsenic poisoning diagnosis, a twenty-four-hour urine test is more reliable than a blood test because arsenic is cleared from the blood within 24 hours. Detection of urinary arsenic levels higher than 50 µg/L are indicative of acute arsenic toxicity (Agency for Toxic Substances and Disease Registry) [56].

Chronic exposure to arsenic results in multisystem disease and the most serious health complications are cardiovascular disease and cancer [57] [52]. Chronic arsenic poisoning causes dermatological changes, such as skin lesions (hyperkeratosis) and changes in skin pigmentation [52]. Gastrointestinal complications also occur, including diarrhea and vomiting. Also, chronic arsenic exposure increases the risk for cardiovascular, neurodegenerative, and malignant diseases [52]. Long-term toxicity is frequently observed in workers who are exposed to low levels chronically through their occupation. Arsenite readily binds thiol or sulfhydryl groups in tissue proteins of the liver, lungs, kidney, and skin [52], thus these tissues are the most affected organs of arsenic toxicity. Specifically, keratin-rich tissues (skin, hair, and nails) have high content of cysteine residues and arsenic accumulates in keratinocytes due to its reactivity with cysteine thiol groups [58] [59]. So, arsenic levels analysis in hair and nails are useful indicators for evaluating the time of arsenic exposure [60]. In individuals who have no known arsenic exposure, the concentration of arsenic in hair and nails ranged from 0.02 to 0.2 mg/kg [61] [62]. In contrast, areas of West Bengal with arsenic concentration more than 50 µg/L in drinking water, the arsenic level in hair ranged from 3 to 10 mg/kg [63]. Unfortunately, there is no effective treatment, although chelation therapy can be used occasionally, to mitigate the toxic effects [64].

Thus, arsenic can cause multisystem diseases and both the dose and duration of exposure are critical for either the chronic or acute toxicity outcome. Also, different tissues and organs are affected depending on chronic or acute exposure, and diagnosis and treatment differ, respectively.

1.5 Arsenic and disease

Epidemiological evidence has linked chronic arsenic exposure with several severe health conditions, including, cardiovascular disease, diabetes, pulmonary disease, neurotoxicity, pregnancy complications, teratogenicity, developmental effects, and cancers [65]. There is large amount of epidemiological data showing arsenic as a common cause of disease [66]. One large study followed more than 165,000 individuals from 17 municipalities in the Viterbo region of Italy for 20 years, showed that those consuming groundwater with arsenic levels higher than 20 µg/L, had an 83% increased risk of lung cancer and heart disease [66] [67]. Also, individuals consuming water with levels higher than the US EPA maximum contaminant limit of 10 µg/L, had a 47% increase in risk for chronic obstructive pulmonary disease (COPD) [66] [67]. A smaller study in US that followed 3575 Americans between 1989 and 2008, showed that those exposed to levels exceeding 61 µg/L, were 65% more likely to have cardiovascular disease and 71% more likely to have coronary artery disease [68]. Another study in Bangladesh showed that the mortality rate for cardiovascular disease was 214.3 per 100,000 person years in people drinking water containing <12 µg/L arsenic, compared with 271.1 per 100,000 person years in people drinking water with ≥ 12.0 µg/L arsenic [57]. There is a dose-response relation between exposure to arsenic in well water and mortality from heart diseases as well as a significant synergistic interaction between arsenic exposure and cigarette smoking in mortality from ischemic heart disease [57].

To investigate the potential for in utero arsenic exposure to accelerate the onset of cardiovascular disease, pregnant ApoE-knockout mice (ApoE^{-/-}) were exposed to arsenic in their drinking water [69]. Exposure of pregnant dams to arsenic exacerbates atherosclerotic lesion formation in the offspring in ApoE^{-/-} mice [69]. Early post-natal exposure to 49 ppm arsenic for 7 weeks through drinking water increased the atherosclerotic lesion formation by 3- to 5-fold in the aortic valve and the aortic arch [70]. Further exposure of ApoE^{-/-} mice to 1, 4.9 and 40 ppm of arsenic for 13 weeks increased the lesion formation and macrophage accumulation in a dose-dependent manner [70]. Also, when mice were exposed for 21 weeks and then withdrawal of arsenic for 12 weeks followed, decreased lesion formation was observed compared with mice continuously exposed to arsenic [70]. Expression of pro-inflammatory chemokines and cytokines as well as markers of oxidative stress were significantly increased in lesions of arsenic-exposed ApoE^{-/-} mice [70]. It was also shown that methylated arsenicals are proatherogenic and that arsenic (3) methyltransferase (As3MT) is required for arsenic to induce reactive oxygen species and promote atherosclerosis [71]. Methylated arsenicals can also cause changes in plaque components toward a more unstable, rupture-prone phenotype [71].

In utero or childhood exposure to arsenic is also strongly associated with severe diseases. Animal experiments have shown that arsenic is a transplacental carcinogen in mice and transplacental exposure leads to tumor formation in offspring [72]. Strong evidence of arsenic toxicity due to early life exposure comes from Chile. Specifically, in 1958, a new city water supply was installed in the city of Antofagasta in northern Chile [73]. This water supply was using water from the Toconce and Holajar rivers, which contained 800 and 1,300 µg/L of arsenic, respectively [73]. The exposure stopped in 1970 by an arsenic-removal plant and the arsenic concentration dropped to 110 µg/L for about 10 years and reduced further since then [73]. From 1958 to 1970, more than

125,000 residents were exposed to high levels of arsenic through their drinking water [73]. Studies on mortality among adults 30-49 years of age showed increased mortality due to lung cancer, bronchiectasis, myocardial infarction, and kidney cancer among people born during the high-exposure period [74] [75] [76]. Also, another study on investigation of all causes of death in young adults following early-life exposure in drinking water to approximately 870 µg/L of arsenic in Antofagasta, showed increases in mortality in young adults from liver, larynx cancer and chronic renal failure [73]. Additionally, two infants who were not related to each other from Antofagasta died from myocardial infarction in 1973 [77]. The autopsies showed that the two infants had arteriosclerosis and arsenic tests showed traces of arsenic in their hair and tissues [77]. Pathologic analysis showed no demonstrable etiologic evidence in the vascular lesions, so the connection with arsenic, as in Blackfoot disease, should be considered [77].

A cohort study in Bangladesh revealed a dose-dependent increase in lower respiratory tract infection (LRTI) in relation to maternal arsenic exposure [78]. Specifically, the study included 1,552 live-born infants of women in Matlab, Bangladesh. Inorganic arsenic in maternal urine samples was measured [78]. After birth, information on symptoms of LRTI was collected monthly. The results of the monthly check showed that the estimated risk of LRTI increased by 69% in the participants whose mothers had urinary arsenic concentration ranging from 262 to 977 µg/L, compared with offspring of mothers whose exposure was less than 39 µg/L [78].

Chronic arsenic exposure via drinking water with arsenic concentrations as low as 10-50 µg/L can also cause peripheral neuropathy [79]. The impairment is observed mainly in sensory fibers and less frequently in motor fibers [80]. Sural nerve biopsies showed a reduction in both myelinated and unmyelinated fibers as well as axonal degeneration of peripheral nerves because of chronic arsenic exposure [81]. Arsenic-induced peripheral neuropathy may recover in the long term; however, CNS impairments

are less likely to recover [79]. It has been shown that arsenic trioxide significantly decreased the activity of serum acetylcholinesterase in a dose-dependent manner [82]. The decreased acetylcholinesterase activity caused cholinergic crisis, which is probably associated with peripheral neuropathy or CNS damage [82] [83]. The latter is the most possible mechanism of arsenic-induced neurotoxicity [83].

Arsenic induces neural tube defects (NTDs) when given to animal models during organogenesis [84]. A study from India showed a national NTDs rate of 4.4/1000[84]. With a birth cohort of approximately 26 million livebirths in India, this translates to 114,000 cases of NTDs per year [84]. Also, marked variations were observed between regions in China, where the prevalence of NTDs in the Northern Regions was 4.5/1000 births, compared to 1.1/1000 in the Southern Regions [84] [85]. Due to the high rates of NTDs in the Northern Regions, the health authorities took active measures by promoting periconceptional folic acid supplementation [85]. Also, environmental factors that contribute to high incidence of NTDs in China and India, should be considered and if found, these factors should be reduced [85]. In the search for environmental causes for NTDs, exposure to arsenic has been suggested as a risk factor [84] [86]. The Times of India has reported that ~19% of Indians consume water with lethal levels of arsenic [84]. Also, most of the Chinese and Indian populations rely of rice as a dietary sample and rice is a major source of arsenic exposure [84]. Rice is not very efficient in absorbing arsenic from soil and it can absorb up to 10 times more arsenic than other crops [87]. Several studies have showed the association of environmental exposure to arsenic with high incidence of NTDs. For example, analysis of gene expression in the neural tube of arsenic-exposed embryos indicated that there was a significant dysregulation in a group of genes directly involved in the mitochondrial process of energy production during organogenesis [86]. A study from Bangladesh also showed that maternal consumption of

high levels of arsenic via drinking water and rice, reduced the efficacy of folic acid in the prevention of NTDs [84] [88].

Thus, arsenic exposure affects many organs and systems in a dose-dependent manner and chronic arsenic exposure should be considered as a cause of many commonly occurring severe diseases. Regulating arsenic levels in drinking water and food and assessing the risk of exposure in areas that arsenic occurs in levels that exceed 10 µg/L, would be crucial for disease prevention and control.

1.6 Arsenic-induced cancers

Arsenic causes several cancers, such as lung, bladder, kidney, liver and nonmelanoma skin cancer [2]. Arsenic is classified as a group I human carcinogen by the International Agency of Research on Cancer (IARC) since 1980 [89]. The latter means that there is sufficient evidence of carcinogenicity to humans [90]. Despite evidence in humans, animal models fail to replicate these observations. The lack of an animal model has made it difficult to determine the exact mode(s) of action underlying arsenic-induced carcinogenicity and these mechanisms of actions are yet to be delineated [90].

Arsenic is a unique carcinogen because there is sufficient evidence of carcinogenic risk by both inhalation and ingestion [89]. In a detailed study spanning a 7-year period, it was shown that several patients had premature death due to cancer and had serious arsenic skin lesions prior to that [89]. Data from Taiwan indicate that there is increased risk of internal cancers from arsenic exposure through drinking water [89]. Specifically, in a study of 8102 residents from an arsenic endemic area in Northeastern Taiwan, the association between ingested arsenic and risk of cancers of urinary organs was positive [91]. Additionally, a US study showed that there was an increased risk of bladder cancer

in smokers that were exposed to arsenic in drinking water near 200 µg/L compared with smokers exposed to lower arsenic levels [92].

Another study in Chile showed a positive correlation between ingestion of inorganic arsenic and lung cancer [89] [93]. It was also shown that cigarette smoking plus ingestion of arsenic had a synergistic effect for the development of lung cancer [93]. A significant dose-response relationship between arsenic concentration in water and incidence of lung and bladder cancers has been shown for both men and women [94]. Interestingly, the increased risk of lung cancer associated with arsenic is suggested to be cancer subtype specific [90]. For instance, lung squamous cell carcinoma (SCC) incidence had decreased worldwide and is associated with cigarette smoking. However, in Bangladesh, no decline in lung SCC cases in non-smokers is observed and lung SCC is the predominant histological subtype in areas with arsenic concentration above 100 µg/L [95].

A crucial relationship between arsenic exposure and skin cancer has been observed [89]. It has been reported that arsenite can play a synergistic role in UV-induced skin cancers [89]. Skin cancer in patients consuming arsenic-based medications was first reported by Sir Jonathan Hutchinson in 1887 [96]. Bowen's disease (intraepithelial carcinoma or carcinoma *in situ*), basal cell carcinoma (BCC) and squamous cell carcinoma (SCC) are the most common malignancies found in patients with chronic exposure to arsenic [90]. Merkel cell carcinoma, a rare and aggressive cutaneous neoplasm, has been also reported at a lower frequency [97].

So, chronic exposure to arsenic can not only cause non-malignant diseases (see 1.5) but also several cancers, affecting mainly the skin, lung, and urinary bladder. The focus of this thesis is on arsenic-induced skin cancer since it is the most prevalent cancer caused by arsenic.

1.7 Arsenic-induced skin cancer

The second most common cause of skin cancer is chronic arsenic exposure [98]. Arsenic is a leading cause of skin cancer in areas where people are exposed to high levels of arsenic in their drinking water and food [98]. An increased frequency of skin cancer following treatment with Fowler's solution (1% potassium arsenite) for various hematological disorders was first observed in 1982 [99]. Arsenic-induced skin toxicity symptoms first manifest as changes in the skin pigmentation including raindrop-shaped lesions and diffuse dark brown lesions cancer [100]. The latter are frequently followed by arsenical keratosis in the palms, soles, and trunk, and even by cutaneous malignancies [98] [101]. These lesions are considered a diagnostic criterion of arsenicosis [90].

Chronic arsenic exposure is associated with different types of skin cancer, progressing from premalignant hyperkeratosis (HK) to Bowen's disease, BCC and SCC (see 1.6). Arsenic-induced skin cancer has a different pattern of pathology and progression to malignancy compared to sunlight-induced skin cancer [100]. The premalignant lesions for both arsenic-induced BCC and SCC are arsenic hyperkeratosis, whereas the premalignant lesions for sunlight-induced SCC are actinic keratoses [100]. Also, sunlight causes BCC, SCC, and malignant melanoma, while arsenic exposure does not cause malignant melanoma [100]. Specifically, keratosis in areas of the body that are not exposed to the sun is the most distinguishing cutaneous manifestation of arsenic-induced skin lesions [102]. Dysplasia in the keratotic lesions is an intermediate stage between premalignancy and malignancy and are immediate predecessors to Bowen's disease and SCC [103]. The most commonly occurring malignant lesions in arsenicosis are Bowen's disease and superficial BCC [102]. Specifically, BCC is not invasive while SCC can be metastatic cancer, which tends to progress in later stages of arsenic exposure [102]. Arsenic-induced Bowen's disease can appear 10 years after

arsenic exposure, whereas BCC and SCC can have a latency period of 20 or 30 years [104].

Exposure of normal human epidermal keratinocytes to varying noncytotoxic concentrations of inorganic arsenic causes gene expression changes in pathways involved in oxidative stress and proliferation as well as increased transcriptional levels of keratinocyte growth factors [105]. Also, arsenic toxicity can be potentiated by other environmental carcinogens. *In vitro* studies combining arsenic and UV showed significant oxidative damage in arsenic-treated cells compared to controls [106]. For instance, arsenic-exposed people with a history of smoking, may be more prone to develop skin lesions than nonsmokers [107]. Additionally, arsenic acts as a cocarcinogen with UV light in a synergistic mode of action [107]. Models using UV exposure of mice with concomitant drinking water arsenic revealed rapid skin tumor formation, larger tumor size and a greater percentage of invasive SCCs than control mice [108].

1.8 Modes of action in arsenic-induced carcinogenesis

The mechanisms of arsenic-induced carcinogenesis are not completely elucidated and there are several proposed mode of actions including inhibition of DNA repair, altered epigenetics (DNA methylation, miRNA expression), co-mutagenicity, oxidative stress and chromosomal instability (numerical and structural chromosomal abnormalities). [109].

Many studies have described arsenic's ability to cause oxidative and nitrosative stress via the production of reactive oxygen species (ROS) and reactive nitrogen species (RNS) [98] [110]. Arsenic-induced genotoxicity in Chinese hamster ovary cells and epidermal keratinocytes showed the presence of hydroxyl and hydrogen peroxide ROS and confirmed the significance of ROS and the reduction of intracellular thiols,

particularly glutathione, in the toxicity of arsenic [111]. Also, another study showed that when arsenic-treated human-hamster hybrid cells were compared to mitochondria-depleted controls, the latter exhibited the necessity for mitochondria in arsenic-mediated ROS production [98] [112]. This suggests that mitochondrial damage is required for arsenic-induced DNA damage to occur [112]. Also, the human neutrophil cytochrome b light chain (CYBA) protein, which is a critical subunit of NADPHO (nicotinamide adenine dinucleotide phosphate oxidase) complex, was upregulated by arsenic exposure in vascular smooth muscle cells [113]. Arsenic exposure contributes further to oxidative stress by stimulating the translocation of Ras-related C3 botulinum toxin substrate 1 protein (Rac1) and thus activating NADPHO [114]. Monomethylarsonous acid (MMAsIII) also readily binds the thiol moiety of nitric oxide synthase (NOS), which inhibits NOS function and thus reduces the availability of NO [115]. Additionally, chronic arsenic exposure has been associated with systemic nitric oxide (NO) depletion and arsenic-induced dysregulation of NO metabolism is implicated in high frequency of atherosclerosis and peripheral vascular disease to individuals chronically exposed to high levels of arsenic [116] [98]. These findings show that arsenic induces oxidative stress through various mechanisms.

Arsenic causes genotoxicity and it is responsible for disrupting chromosomes and DNA strands [98]. Arsenic-induced genomic instability is multi-factorial and involves molecular crosstalk across various cellular pathways [117]. Genomic instability can be caused through DNA damage, aberrant DNA repair, telomere dysfunction, mitotic arrest, and apoptosis [117]. Also, epigenetic dysregulation could contribute to genomic instability such as altered promoter methylation and miRNA dysregulation [117]. One study with 60 residents of West Bengal in India showed significantly increased incidence of chromosomal aberrations and sister chromatid exchange in lymphocytes from DNA of arsenic-exposed individuals [118]. Chronic arsenic exposure modulates DNA

methylation, histone maintenance, mRNA, and miRNA expression [119]. Altered DNA methylation has been related to arsenic's ability to generate ROS and deplete methyl group donors such as S-adenosylmethionine (SAM). Tri- and pentavalent arsenic species receive methyl groups from SAM to form di- and monomethylated arsenic. So, these methylated arsenics reduce the available pool of SAM and directly methylate DNA in an abnormal manner [90] [98] [120]. Also, arsenic-treated prostate epithelial cells showed a significant suppression of SAM levels occurred with decreased methionine adenosyltransferase 2A (converts methionine to SAM) expression [120]. Cellular arsenic adaptation is a dynamic process involving decreased SAM recycling and this disruption in metabolism may have an impact on arsenic-induced oncogenesis [120]. Also, analysis of bladder cancers from patients with high arsenic exposure showed a low rate of tumor protein 53 (TP53) mutations present in patients who had used hair dyes, suggesting that arsenic exposure did not promote mutagenesis in humans [121]. Arsenic exposure alone is not sufficient to induce cancer in adult animals but arsenic acts as a co-carcinogen and enhances tumorigenesis after exposure to other agents such as UV radiation [108] [122]. TP53 mutation is known to be a driver for UV-induced squamous cell carcinoma and arsenic-induced increase in sunlight-induced mutagenesis was shown in rodent studies [108]. However, arsenic-induced skin tumors showed neither TP53 mutations nor mutations associated with UV light exposure [123].

Moreover, arsenic impacts many cellular DNA repair mechanisms. Specifically, it inhibits nucleotide excision, base excision repair, and mismatch repair pathways [124] Poly (ADP-ribosyl)ation of nuclear proteins following DNA damage is catalyzed by poly (ADP-ribose) polymerase 1 (PARP1) and it is required for the dissociation of nuclear proteins so that base excision repair proteins can access the damaged site and repair the DNA [125]. Long term exposure to low arsenic levels (0.1 μ M) led to poly (ADP-ribosyl)ation of TP53 and PARP1 in HaCaT cells [126] [125]. It is known that after DNA

damage induced by a genotoxic agent, activated TP53 induces expression of cyclin dependent kinase inhibitor 1A (CDKN1A aka p21^{CIP1/WAF1}), which then causes cell cycle arrest allowing for damaged DNA to be repaired before cell cycle further progresses (reviewed in [125]). However, studies showed decreased expression of CDKN1A mRNA and protein after concomitant exposure to arsenic and another genotoxic agent. The latter suggests the inactivation of TP53 function following its poly (ADP-ribosyl)ation induced by arsenite [125] [126]. A study on the effect of arsenic and its metabolites on base excision repair pathway in human A549 lung cancer cells showed that arsenite at 10 μ M or greater significantly decreased the levels of DNA ligase IIIa (LIG3) [127]. Dimethylarsinic acid (DMA^V) starting at 5 μ M decreased human 8-oxoguanine DNA glycosylase-1 (OGG1) activity [127]. Monomethylarsonic acid (MMA^V) and arsenite also decreased the X-ray cross complementing protein 1 (XRCC1) levels at 2.5 and 5 μ M respectively [127]. Additionally, low concentration of arsenite (10 nM) inhibited PARP1 in HeLa cells and increased the number of DNA strand breaks by H₂O₂ [128]. Arsenite targets the zinc finger motifs containing three or more cysteine residues in DNA repair proteins, such as xeroderma pigmentosum group A (XPA) and PARP1 [129] [130], which are essential DNA repair enzymes [117]. Thus, repair of oxidative DNA damage is inhibited [125]. Also, inhibition of PARP1 activity by arsenite was shown in HaCaT cells treated with UV light and this effect was diminished after adding zinc (II) ions [131] [125]. Arsenic displaces phosphate in ATP and covalently binds with sulfhydryl moieties of DNA repair machinery enzyme [132]. Particularly, arsenite (> 5 μ M) inhibits O6-methyl-guanine-DNA methyltransferase, and PARP-1 [132]. Also, polymorphisms of the DNA repair pathway genes, such as the excision repair cross-complementation group 2 (*ERCC2*), tumor protein 53 (*p53*), apurinic/apyrimidinic endonuclease 1 (*APE1*), X-ray repair cross complementing 3 (*XRCC3*) and Nijmegen breakage syndrome (*NBS1*) have been associated with risk of development of arsenic-induced skin lesions [117]. Arsenic

also promotes genomic instability by interfering with telomere function [117]. Many *in vitro* and *in vivo* studies have shown that at low doses of arsenic, telomerase activity and telomere length are maintained, while at higher doses, telomerase activity is decreased with telomeric DNA attrition and apoptosis [117]. Arsenic can also induce some positive regulators of telomerase and cell proliferation like heat shock proteins (such as Hsp90), oncogenes (such as MYC proto-oncogene (*c-myc*)) and some growth factors (such as epidermal growth factor (EGF)) and these could be mechanisms of arsenic-induced alteration of telomerase activity [117]. Hence, the altered telomere states due to arsenic exposure is thought to be a major reason for arsenic-induced senescence [117].

Moreover, the anaphase promoting complex/cyclosome (APC/C) which regulates progression through mitosis and entry into G1 phase is known to be perturbed by arsenic. Specifically, arsenic disrupts mitosis and delays transit through M phase in SV40-transformed human skin fibroblasts [133]. Disruption of the APC/C by arsenite is consistent with the observation of disruption of mitotic progression by arsenite [125] [133]. Also, studies showed that mitotic arrest induced in A375 malignant melanoma cells by arsenite is associated with the phosphorylation of the BUB1 mitotic checkpoint serine/threonine kinase B (BUBR1) [134] [135]. Phosphorylation of BUBR1 occurs during spindle checkpoint activation by mitotic disrupting agents [135]. Spindle checkpoint activation by arsenite resulted in stabilization of cyclin B and securin, thus inhibiting mitotic exit [134]. Arsenite also promoted activating Thr161 phosphorylation on cyclin dependent kinase 1 (CDK1) and reduced inhibitory phosphorylation at Tyr15, leading to increased CDK1 activity that maintains spindle checkpoint activation and further inhibits exit from mitosis [136]. The transcription of signaling kinase genes upstream of TP53 was also decreased in ovarian cells after arsenic exposure: ATM serine/threonine kinase (*ATM*) was down two-fold; ATR serine/threonine kinase (*ATR*), three-fold; and checkpoint kinase 1 (*CHEK1*). Thus, arsenite exposure downregulates

transcription of many DNA damage signaling genes, possibly contributing to disrupted DNA damage responses [125]. In summary, arsenic interferes with the DNA damage response at multiple levels and disrupts cell cycle control mechanisms. Thus, arsenic is a genotoxic agent with many deleterious effects and some of these mechanisms could be implicated in genomic instability observed in arsenic-induced tumors [117].

There is also evidence that arsenic plays a role in the disruption of the innate and cell-mediated immune responses [98]. Studies showed an association between lower respiratory tract infections and diarrhea in individuals with a history of chronic arsenic exposure [137]. Arsenic reduces the pulmonary antibacterial defenses mediated by innate immune cells in rodents [98]. Also, arsenic-exposed mice exhibited greater influenza virus infectivity because of inhibited T cell function, when compared to controls [138]. Impaired immune responses were reported among patients treated with therapeutic arsenic trioxide (ATO) since they were found to have a greater incidence of herpes simplex and herpes zoster infection among multiple myeloma and colon cancer patients treated with ATO [139]. Some mechanisms by which arsenic mediates disruption of immune responses includes the unfolded protein response (UPR) [98]. Specifically, UPR is a homeostatic mechanism that is activated in response to an increased number of unfolded or misfolded proteins present in the endoplasmic reticulum (ER) lumen. Studies have shown that arsenic exposure upregulates sensors of the UPR pathway in the epidermis of SKH-1 mice [98]. Treatment with antioxidants such as N-acetylcysteine (NAC) decreased the arsenic-induced cutaneous inflammation of these mice, providing evidence of the involvement of ROS in UPR activation [140]. So, ER stress in arsenic toxicity could be a possible mechanism by which this metalloid altered cellular differentiation leading to cutaneous inflammation [98]. Also, ATO treatment disrupted murine macrophage function by simultaneously generating ROS and activating the UPR pathway [98].

Many of the adverse effects caused by arsenic are mediated by aberrant activation of various signal transduction pathways. Arsenic directly binds sulfhydryl (SH) moieties, and this interaction may occur in over 200 known human proteins [141]. Most pathways affected by arsenic may lead to the activation of oncogenes, the inhibition of tumor suppressors, and/or the upregulation of inflammatory pathways [98]. Arsenic activates the canonical Hippo pathway that is responsible for cell survival and proliferation and implicated in many malignancies [142]. Yes-associated protein (YAP) is a known component of the Hippo signaling pathway and dephosphorylated, it acts as a transcription factor in the regulation of epithelial cell proliferation [98]. A downstream target of the dephosphorylated YAP is a downstream effector of Sonic hedgehog (Shh) pathway, which has been implicated in arsenic-induced basal cell carcinoma [143]. Additionally, arsenic-mediated ROS have been found to promote nuclear factor kappa-light-chain-enhancer (NFκB) mediated apoptosis [144]. Also, arsenic exposure induces the overexpression of epidermal growth factor receptor (EGFR) [145] and increased level of EGFR ligand mRNAs, specifically HB-EGF, which is upregulated in many colorectal, cervical, breast and gastric cancers [146]. Furthermore, exposure to arsenite promotes epithelial to mesenchymal transition (EMT) and angiogenesis by increasing signaling through the β -catenin vascular endothelial growth factor pathway [88]. Arsenic also activates the mineral dust induced gene (MDIG), also known as myc-induced nuclear antigen 53 and nucleolar protein 62 by upregulating Jun-N-terminal protein kinase (JNK) and signal transducer and activator of transcription 3 (STAT3) pathways [98]. MDIG is an oncogene that has been linked to lung, breast, colon, gastric, renal, and esophageal squamous cell carcinomas [147]. Hence, arsenic's ability to perturb signal transduction makes it an important carcinogen in many cancers.

1.9 MicroRNAs (miRNAs): Biogenesis, processing, and regulation of translation

MicroRNAs are part of the epigenome and play a significant role in the regulation of gene expression at the post-transcriptional level [148]. miRNAs are endogenous short non-coding RNAs (containing ~22 nucleotides) and are transcribed by RNA polymerase II as miRNA genes or in protein coding genes embedded in introns [149]. It is estimated that miRNAs target more than 60 % of protein-coding regions and silence genes post-transcriptionally by guiding Argonaute (AGO) proteins to mRNA targets [150].

The biogenesis of the mature miRNA is a two-step process (Figure 2) [151] [152].

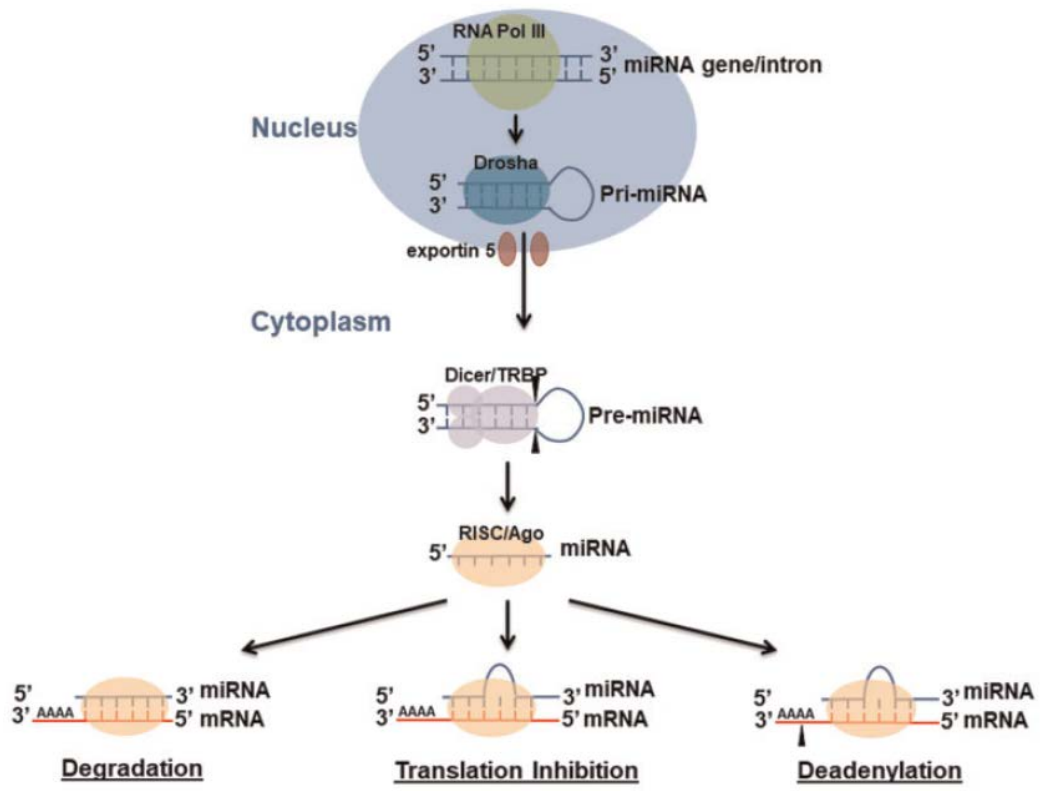


Figure 2: miRNA biogenesis occurs in both the nucleus and the cytoplasm and the regulation of their target mRNAs [150] [153].

Initially, the pri-miRNA, which is the nascent miRNA transcript, is cleaved in the nucleus by the microprocessor complex containing the double-stranded RNA-specific ribonuclease Drosha, into pre-miRNA (~85 nucleotide pre-mRNA hairpin) (Figure 2) [153]. The cleaved pre-miRNA is then transported from the nucleus to the cytoplasm by exportin 5 where it is processed to ~21-25 nucleotide single-stranded mature miRNA by a protein complex consisting of Dicer (a helicase with RNase motif) and TRBP (HIV-1 TAR RNA binding protein) (Figure 2) [152] [154]. Dicer and TRBP recruit AGO2 and other argonaute proteins to mediate the assembly of the RNA-induced silencing (RISC) complex [152] [154]. RISC is a ribonucleoprotein complex that binds to one of the miRNA strands and guides the miRNA to the target mRNA to regulate translation [153].

MiRNAs target cytosolic mRNAs by forming complementary base pairing, typically with the 3' untranslated regions (UTRs) of the target mRNAs within the RISC complex. The complementary sequences in UTRs with which miRNAs bind, are known as seed regions. The hybridization of miRNAs to seed regions leads to decreased translation, deadenylation or degradation of the mRNA [155] [156]. In cases of perfect base pairing of miRNAs with the seed regions of their target mRNA, the mRNA is degraded. However, imperfect base pairing leads to repression of mRNA translation and restoration of translation is possible when the repressor miRNA is degraded [157].

MiRNAs play a complex and crucial role in many biological processes (cell proliferation, apoptosis, response to therapy, diseases, development) and can create complex feedback regulatory loops in a cell [158] [159]. A single miRNA can target hundreds of mRNAs and each mRNA can be targeted by multiple miRNAs in different regions [159] [157]. MiRNAs also can bind to the 5'-UTR or the open reading frame (ORF) regions, creating a complex network of interactions [159]. Some miRNAs may also regulate gene families by targeting regions within their genes [160]. For example, it has been shown that many zinc finger genes (ZNFs) are regulated at the post-

transcriptional level by miRNAs, which directly target their coding regions [160]. So, there is a complex mechanism of miRNA/mRNA interplay, which should be considered in studies of gene regulation and expression [160].

1.10 Role of miRNAs in carcinogenesis

Several studies have linked aberrant miRNA expression or dysregulated expression of components of miRNA processing machinery (i.e. Dicer, Drosha, RISC complex) with different cancers [161], [162] [163]. Studies have shown the association of dysregulated miRNA expression with lung, cervical, oral, squamous cell carcinoma (SCC) [161], breast, colon, prostate, and thyroid cancers [164]. MiRNA dysregulation can affect tumor development, progression, and response to therapy (drug resistance) [165]. Specifically, miRNAs dysregulation in cancer involves targeting of oncogenes and tumor suppressors, resulting in changes in gene expression, stem cell biology, angiogenesis, epithelial-mesenchymal-transition, and metastasis [165]. Thus, miRNAs can act either as novel oncogenes by suppressing tumor suppressor genes, or as tumor suppressor genes by suppressing oncogenes (Figure 3) [1] [166] [167].

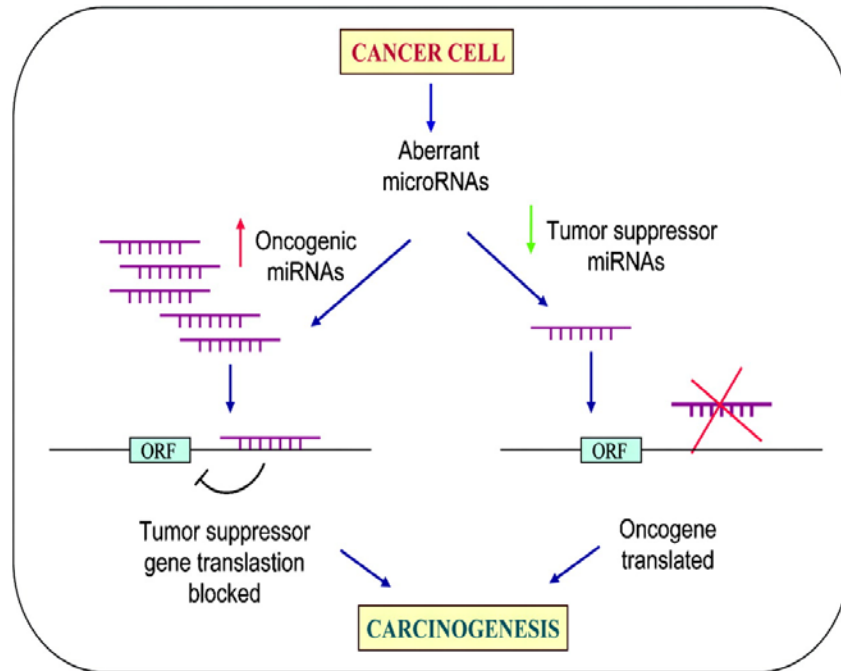


Figure 3: miRNAs may act as tumor suppressors and oncogenes leading to carcinogenesis [1]

For example, in Burkitt lymphoma cells, miRNA let-7a downregulates expression of the proto oncogene *MYC* reverting the *MYC*-induced cell growth [168]. Studies have also shown the regulation of *MYC* and *RAS* expression by let-7a microRNA family in lung and colon cancers [169] [170]. Alternatively, overexpression of miR-504 decreases TP53 expression levels, resulting in decreased TP53-mediated apoptosis, and cell cycle arrest in response to stress [171]. Thus, the impact of miRNAs on carcinogenesis is significant and miRNAs may function as potential biomarkers for prognosis, diagnosis, and therapy [165] [158]. MiRNAs can also be dysregulated in response to environmental stress. Several studies have shown that various arsenic concentrations and different times of exposure can alter the miRNA expression profile in arsenic-induced cancers in different cell lines both *in vitro* and *in vivo* [172] [173].

1.11 Dysregulated miRNAs in arsenic-induced cancers

Exposure to environmental chemicals has been associated with altered miRNA expression profile and carcinogenesis [174]. For example, arsenic alters both the mRNA and miRNA expression levels in arsenic-induced cancers and transformed cell lines [173] [175]. The impact of arsenic exposure on altered miRNA responses was first reported in 2006, when it was shown that miRNA profiles are altered by folate deficiency and arsenic exposure [174]. Also, there is evidence for the therapeutic potential of arsenic in leukemia by regulating miRNAs as well as exploiting the synergistic effects of miRNAs and arsenic trioxide (ATO) for leukemia chemotherapy [176] [177]. Specifically, the combination of miRNA-15a/16-2 and ATO induced apoptosis in BCR-ABL positive myelogenous leukemia cells (K562) and could be a potential treatment of chronic myeloid leukemia [176]. Moreover, anti-miR-21 sensitizes leukemic K562 cells to arsenic trioxide by inducing apoptosis [177]. Several reports have also shown that expression of

let-7 miRNA family and miRNA-200 are altered in response to exposure to various arsenic doses and arsenicals in several arsenic-induced tumors [165]. These studies suggest that miRNA expression plays a crucial role in arsenic-induced carcinogenesis by either promoting or inhibiting malignant transformation.

1.12 Dysregulated miRNAs in arsenic-induced skin cancers

Chronic exposure to arsenic has been linked to cancer development in different organs and tissues. Skin is the major target for arsenic toxicity [178]. Arsenic-exposed keratinocytes have been shown to exhibit differential miRNAs expression profile [179]. Specifically, exposure of human immortalized keratinocytes (HaCaT cells) to 500 nM sodium arsenite for 4 weeks resulted in overexpression of miR-21, miR-200a, and miR-141 [179]. MiR-21 and miR-200a have been reported to be associated with most human tumors [179] [180] and miR-141 family is associated with epithelial-mesenchymal transition (EMT) during malignant transformation and cancer progression [179]. Analysis of human serum samples from individuals exposed to arsenic in West Bengal, India, showed that miR-21 is overexpressed in exposed individuals compared with nonexposed [175]. Also, in the arsenic exposed group, the levels of miR-21 are even higher in individuals with skin lesions compared to individuals without skin lesions [175]. *In vitro*, when HaCaT cells were exposed to 0.05 ppm of sodium arsenite for 8 weeks, miR-21 levels were upregulated [175]. Banerjee et al., 2017 also showed that PTEN (phosphatase and tensin homolog) and PDCD4 (programmed cell death 4) levels, which are tumor suppressor downstream targets of miR-21, were decreased with miR-21 overexpression. The latter findings suggest that miR-21 possibly contributes to arsenic-induced skin lesions in exposed individuals and transformation in HaCaT cells *in vitro* [150]. Moreover, accumulating evidence has shown that let-7 miRNA family functions as

tumor suppressors and regulate various biological processes, such as cell proliferation, cell cycle, migration, and stem cell biology [181].

Overexpression of let-7c inhibits arsenite-induced acquisition of cancer stem cell like properties and neoplastic transformation of HaCaT cells [182]. Exposure of HaCaT cells to 1 μ M arsenite for 15 weeks leads to neoplastic transformation and transformed HaCaT cells had decreased levels of let-7 family miRNAs [182]. The levels of let-7c were also decreased in a time-dependent manner in acute exposure experiments [182] [183].

Analysis of skin lesions from individuals chronically exposed to high levels of arsenic (59-172 ppb) in their drinking water in West Bengal, India showed altered miRNA profile [183]. Differential miRNA expression patterns were observed when comparing expression in three premalignant HK (hyperkeratosis) lesions and six malignant lesions (three squamous cell carcinoma (SCC) and three basal cell carcinoma (BCC)) [183]. This study [183] showed the differential expression of 35 miRNAs in arsenic-induced premalignant and malignant lesions. Specifically, the differential expression was shown in phenotypic and stage-related manner, for example, expression of miR-425-5p and miR-433 were higher in both BCC and SCC relative to HK, which suggests that upregulated levels of miR-425-5p and miR-433 are associated with progression from premalignant to malignant lesions [183].

The studies described above show that miRNA dysregulation is one of the effects of arsenic-induced toxicity and plays a vital role in the malignant transformation of human keratinocytes. Since skin is the primary target organ of arsenic toxicity and there is aberrant miRNA expression profile, studies that assess the effects of different miRNAs throughout the transformation process are critical during the investigation of mechanisms of arsenic-induced skin cancer.

1.13 Association of miR-186 with carcinogenesis

MiR-186 may play a crucial role in various biological processes and may act as an oncogenic or tumor-suppressor miRNA. The likely role of miR-186 in carcinogenesis has been reported and dysregulated miR-186 levels can either promote or inhibit tumorigenesis [184] [150]. MiR-186 was found to be highly upregulated in some cases of squamous cell carcinoma induced by chronic arsenic exposure via drinking water, relative to non-malignant hyperkeratosis [109] [183]. On the other hand, the inhibitory effect of miR-186 has been demonstrated on melanoma cell growth, migration, and invasion *in vitro*, exerting tumor suppressor function in human malignant melanoma cells (CMM) [184]. Moreover, it has been shown that the level of pituitary tumor transforming gene (PTTG1) (also known as securin) expression correlates with clinicopathological features and patient survival in non-small cell lung cancer (NSCLC) and promotes NSCLC cell invasion under miR-186 modulation [185]. Also, aberrant miR-186 expression occurs in metastatic melanoma [186] and metastatic pancreatic cancer [187]. Baffa et al. indicated that miR-186 was differentially expressed in paired primary and metastatic cancers [188]. Leidinger et al. showed that miR-186 in combination with other miRNAs was a biomarker that distinguished melanoma patients from healthy individuals [189]. According to the studies mentioned above, there is strong evidence that miR-186 plays a significant role in carcinogenesis and is associated with either progression or inhibition of cancer.

1.14 The role of miR-186 in carcinogenesis through regulation of cell cycle

Dysregulation of miR-186 is also involved in chromosomal instability, which is a hallmark of carcinogenesis. The ambiguous role of miR-186 in carcinogenesis via regulation of cell cycle has been reported. Downregulation of miR-186 promoted cell cycle progression and proliferation in non-small cell lung cancer (NSCLC), resulting in

adverse prognosis [185]. On the other hand, upregulated miR-186 targeted cyclin D1 (CCND1), and cyclin-dependent kinases 2 (CDK2) and 6 (CDK6), arresting cells in G1/S checkpoint and inhibiting growth of lung cancer cells [185]. Also, it has been shown both *in vivo* and *in vitro*, that miR-186 suppress protein phosphatase 1B (PPM1B). PPM1B is a phosphatase that dephosphorylates cyclin-dependent kinases (CDKs) and overexpression of PPM1B is reported to cause cell-growth arrest. Suppressed PPM1B by miR-186 promotes G1/S cell cycle transition, driving cell cycle progression in bladder cancer [190]. On the other hand, miR-186 also negatively regulated cell growth through cell cycle arrest and apoptosis in malignant fibroblasts [191]. The reports mentioned above, suggest a contradictory role of miR-186 in carcinogenesis via regulation of cell cycle.

1.15 MiR-186 targets cell cycle proteins in arsenic-induced skin cancer

Preliminary results have shown that chronic arsenic exposure induces miR-186 expression [109]. Upregulated miR-186 suppresses securin, which is one of its targets [185] [109]. Normally, securin binds to and inhibits a protease called separase, which, when released, following securin degradation, cleaves cohesins that hold the sister chromatids together, thus initiating anaphase [192]. Therefore, suppressed securin levels, because of overexpression of miR-186, allows anaphase progression and contributes to aneuploidy by promoting premature chromatid separation [109]. Securin's suppression facilitates progression from metaphase to anaphase but also contributes to chromosomal instability, which is a defining characteristic of most human cancers [193].

Arsenic induces mitotic arrest associated with securin stabilization [134]. It has been suggested that miR-186 overexpression in chronic arsenic exposure could mitigate securin stabilization and contribute to escape from arsenic induced mitotic delay [109].

Also, dysregulated securin could cause aberrant chromatid segregation, resulting in aneuploidy and carcinogenesis [109] [5]. The latter suggests that miR-186 dysregulation could be involved in chromosomal instability, which is a feature of carcinogenesis [5] [193].

Bioinformatic analysis using the DIANA miRPath V3.0, has shown that miR-186 is predicted to target mRNAs of proteins that regulate the cell cycle and are components of the spindle assembly checkpoint (SAC) and anaphase promoting complex (APC), including: budding uninhibited by benzimidazoles 1 (BUB1), cell division cycle 27, (CDC27), and BUB1-related protein 1 (BUBR1) [194]. Ectopic expression of miR-186 in HaCaT cells induces significant increase in chromosome number and in structural chromosomal abnormalities [5]. The latter occurs because miR-186 targets and suppresses BUB1, a mitotic checkpoint serine/threonine kinase, which plays a role in the establishment of the mitotic spindle checkpoint and proper chromosome segregation. Specifically, overexpression of miR-186 causes aneuploidy in HaCaT cells, which is further increased with chronic arsenite exposure [5]. Overall, the studies described above, suggest that miR-186 plays an essential role in arsenic-induced skin carcinogenesis and contributes to chromosomal instability.

1.16 The biology of the spindle assembly checkpoint

The successful attachment of chromosomes, through its sister kinetochores, to microtubules of the mitotic spindle, is crucial for error-free chromosome segregation [195]. Genomic stability and proper chromatid separation are ensured by monitoring the kinetochore-microtubules interactions and the spindle assembly checkpoint (SAC) [196]. The presence of unattached or improperly attached kinetochores, is the signal for SAC activation, and it functions as a platform for the assembly of the mitotic checkpoint complex (MCC). The MCC signals inhibition of the metaphase to anaphase transition (Figure 4) [196].

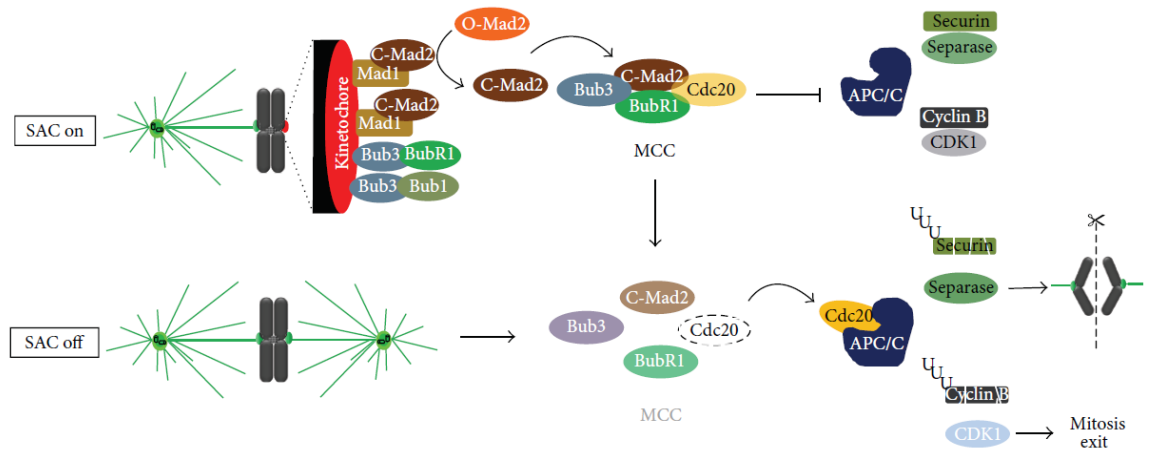


Figure 4: The molecular basis of spindle assembly checkpoint (SAC) signaling [196]

The MCC consists of the highly conserved proteins: mitotic arrest deficient 2 like 1 (MAD2), BUBR1 and budding uninhibited by benzimidazoles 3 (BUB3) in association with CDC20 [196]. CDC20 is a coactivator of the E3 ubiquitin ligase anaphase promoting complex/ cyclosome (APC/C) [197]. Once MCC is activated, cell division cycle 20 (CDC20) is unable to activate the APC/C, preventing anaphase onset by inhibiting securin degradation by the ubiquitin/protease system (Figure 4) [196]. This way, sister-chromatid cohesion is maintained, and the cell cycle is arrested. A single free kinetochore can activate the SAC transduction pathway and sustain a mitotic arrest, because the inhibitory signal that comes from the unattached kinetochore is further amplified within the cytoplasm [198]. The catalytic conformational conversion of MAD2 causes the diffusion and amplification of the inhibitory signal [196]. The binary complex MAD1- “closed” MAD2 at unattached kinetochores, acts as a scaffold for a continuous conversion of the cytosolic “open” MAD2 into “closed” MAD2. The latter can bind CDC20 and inhibit APC/C activity [196] [199] [200]. A “closed” MAD2-dependent CDC20 conformational change allows the binding of CDC20 with the N-terminus of BUBR1 bound to BUB3, which in turn inhibits the APC/C activity and anaphase onset (Figure 4) [201]. When all kinetochores have aligned, the MCC disassembles and CDC20 is released [196] (Figure 4). CDC20 activates the APC/C, leading to securin and cyclin B degradation. APC/C catalyzes the poly-ubiquitylation of securin and cyclin-B, leading to ubiquitin-mediated proteolysis. Securin degradation leads to the activation of the protease separase, which cleaves cohesins, leading to sister-chromatid separation [196] (Figure 4). Cyclin B degradation decreases the cyclin-dependent kinase (CDK1) activity, which results in mitotic exit [196]. Thus, by stabilizing securin and cyclin B, the SAC prevents premature sister-chromatid separation in the presence of unattached kinetochores, and maintains the mitotic state, respectively.

Some other components of SAC are the kinases BUB1, monopolar spindle 1 (MPS1), and aurora B, which are essential for proper checkpoint signaling [196]. BUB1 forms a constitutive complex with BUB3 and is required for kinetochore recruitment of BUBR1, MAD1, and MAD2 [202]. BUB1 also inhibits APC/C via CDC20 phosphorylation [203]. BUB1 phosphorylates members of the MCC and activates it, inhibiting APC/C activation [196]. BUB1 binds to the kinetochore and delays mitosis in response to spindle disruption, so BUB1 is critical to high fidelity chromosome segregation [184]. Loss of function mutations or absence of BUB1 results in chromosomal instability and premature senescence. Deletions have been identified in some aneuploid tumor cell lines and primary tumors [204]. Kinetochore targeting of MAD1 and MAD2 is also

dependent on MPS1 which is essential for aurora B kinase activation [205]. Aurora B recruits BUB1 and MAD2 to the kinetochore and has an important role in correcting aberrant kinetochore-microtubule attachments by sensing and destabilizing improper kinetochore-microtubule attachments, reducing aneuploidy [206] [207].

1.17 Spindle assembly checkpoint and aneuploidy in carcinogenesis

Disrupted mitosis results in chromosomal instability and aneuploidy which is a common feature of human tumors and a contributory factor in tumorigenesis [208] [209]. The cell must ensure that each daughter cell only receives one copy of each chromosome, in order to maintain the same karyotype in every cell. The latter is regulated by SAC; thus, a compromised SAC will result in aneuploid cells, with either extra or fewer chromosomes, a state that contributes to tumorigenesis [196]. An impaired MCC is associated with an increase in aneuploid cells, however cells may still be able to divide and survive [196]. The chromosome gain or loss is known as chromosomal instability (CIN), a hallmark of carcinogenesis correlated with poor patient prognosis [210].

Chronic SAC activation is frequently used in chemotherapy and is based on the use of microtubule-targeting agents, which by disrupting microtubule dynamics, elicit a long-term SAC response that often results in mitotic cell death [196] [211]. However, some cells can escape cell death and exit mitosis (mitotic slippage) [212]. The cell fate (either mitotic slippage or mitotic cell death) is dependent on the efficiency of the apoptotic machinery and the threshold of cyclin B degradation [213]. If the apoptotic machinery is activated during the mitotic arrest, before cyclin B reaches a threshold of degradation, then the cell dies [213]. On the other hand, if the threshold of cyclin B degradation is reached before activation of apoptotic machinery, then mitotic exit occurs [213]. All the

above show that a fine-tuning of SAC activity is essential for cell survival, since an impaired SAC can favor tumorigenesis but the absence or chronic activation of SAC results in apoptosis in normal and cancer cells [210].

1.18 HaCaT model of arsenic-induced skin carcinogenesis

HaCaT cells are a spontaneously immortalized human keratinocyte cell line that maintains full epidermal differentiation capacity and was established in 1988 from adult male human skin [214]. HaCaT cells have unlimited growth potential and express differentiation-specific keratins (keratin-1 and 10) and other markers including involucrin and filaggrin [214]. They do not have a tumorigenic phenotype *in vitro* and they are not invasive *in vivo* [214]. HaCaT cells exhibit normal differentiation and provide a promising tool for studying regulation of keratinization in human cells [214]. These cells were initially hypodiploid with unique stable marker chromosomes indicating monoclonal origin [214]. In passage 2, most cells were hypodiploid with an average of 44 chromosomes resulting from full or partial monosomies of chromosomes involved in the formation of marker chromosomes [214]. All metaphases had the XO sex chromosome constitution (lacking the Y chromosome) and were partially monosomic for the short arm of chromosomes 3, 9 and 4 [214]. In later passage, they were monosomic for the whole chromosome 4 [214]. They were also trisomic for the long arm of chromosome 9 (i[9q]) [214]. Three individual marker chromosomes (M1: t(3q4q), M2: i[9q] and M3: del(4q28)) were present in 100% of the cells and indicated the clonal origin of this cell line [214]. The presence of these marker chromosomes could be used to validate the authenticity of the cells and exclude cross-contamination with other human cell lines. At passage 5 a hypotetraploid stem line evolved with a range of 72-88 chromosomes, including duplication of the early marker chromosomes and the presence of a fourth marker

chromosome M4:[4p18q] which replaced the M3: del(4q28) [214]. These cytogenetic changes were linked to changes in growth control, since improved adaptation to growth ability under modified culture conditions was observed [214]. The significance of chromosomal alterations in different stages in cell transformation is not yet fully established [214]. HaCaT cells exhibit unbalanced aneuploidy and their cytogenetic changes are essential for the early disturbances in growth control resulting in prolonged life span [214].

HaCaT cells malignantly transformed by chronic incubation in low concentration of sodium arsenite are a very well-established *in vitro* model to study arsenic-induced skin carcinogenesis. Specifically, continuous exposure of HaCaT cells to 100 nM of sodium arsenite for 28 weeks induced malignant transformation [215] [161]. After 28 weeks of chronic arsenic exposure, HaCaT cells exhibited unique morphological alterations with frequent occurrence of giant multinuclear cells, which are common during malignant transformation and are present in tumors [216]. Also, there was a marked increase in secretion of active matrix metalloproteinase 9 (MMP-9) in arsenic-exposed cells and MMP-9 extracellular activity was 2.3-fold higher in arsenic-treated cells compared to control [161]. Arsenic-treated cells expressed higher levels of keratin-1, keratin-10, involucrin and loricrin, which are markers of keratinocyte differentiation and skin keratinization, compared to control cells [161]. Malignant transformation was further confirmed after inoculation of these transformed cells into nude mice and the development of aggressive squamous cell carcinoma (SCC) [215] [161]. Also, long-term low dose exposure of HaCaT to sodium arsenite induces progressive aberrant DNA methylation profile, associated with developing tumors in Balb/c mice [217]. Another study showed that following sodium arsenite exposure for 30 passages, HaCaT cells acquired a cancer stem-like phenotype [218]. Arsenic-treated cells also became tumorigenic in nude mice compared to nontreated cells and they exhibited a higher

growth rate and an increase in colony-forming efficiency [218]. The verification of malignant transformation of HaCaT cells following chronic arsenic exposure was performed after passage-matched HaCaT and arsenic-treated HaCaT cells were intradermally injected into athymic nude mice [219]. None of the mice injected with the parental HaCaT cells developed tumors at the injection site, while all injected mice with arsenic-treated cells developed tumors, which expressed stem cell markers [219]. Also, arsenic-treated cells were more invasive than nontransformed HaCaT cells *in vitro* [219]. Moreover, under regular growth conditions, lower concentrations of arsenic (0.05-0.5 $\mu\text{mol/L}$) increased HaCaT cell viability and proliferation while exposure to higher concentrations (3 $\mu\text{mol/L}$) decreased cell viability and proliferation [220]. Thus, HaCaT is a well-established model in the study of the effects of chronic arsenic exposure and its association with skin carcinogenesis.

1.19 Chromosomal instability

Chromosomal instability (CIN) is defined as a form of genomic instability that leads to both numerical and structural chromosomal alterations [221]. Healthy human cells contain two sets of 23 chromosomes, one set inherited from each parent, having a total of 46 chromosomes [222]. Euploid is the state of having 46 chromosomes while aneuploidy is the state of having fewer or more chromosomes [222]. In other words, aneuploidy is a state in which the number of chromosomes in a cell or organism deviates from multiples of the haploid number of chromosomes [222] [221]. Numerical CIN includes the gain or loss of whole chromosomes and can be due to mistakes in the distribution of DNA to daughter cells during mitosis. Structural CIN is caused by gains, losses or translocations or parts of one or multiple chromosomes, without necessarily changing the number of chromosomes [222]. The generation of structural and numerical abnormalities can be visible as mis-segregated chromosomal material during mitosis,

where duplicated chromosomes are divided between the two daughter cells [223]. Several proteins regulate mitosis and assure accurate chromosome segregation, however mistakes in mitosis can occur and lead to CIN [224]. For instance, errors in attachment of spindle microtubules to a chromosome leads to mis-segregation of that chromosome, leading to numerical chromosomal abnormality [224]. Additionally, attachment of multiple spindle microtubules from opposing sides/daughter cells can “tear apart” a chromosome, causing the two daughter cells to either gain or lose part of that chromosome, leading to structural chromosomal abnormality [224] [223]. CIN can also be caused by processes preceding mitosis, for instance due to faulty DNA damage, repair or replication stress [225] [226].

There are different types of CIN, including chromosomal translocations, dicentric, ring and double minute chromosomes. Specifically, a chromosomal translocation is a type of chromosomal rearrangement in which two non-homologous chromosomes exchange genetic material [227]. The process of exchange involves breakage of each chromosome at a specific point (breakpoint), followed by fusion of the fragments generated by these breaks [227]. A simple case is the reciprocal translocation between two chromosomes; however, translocations can involve three or more chromosomes. Also, if no genetic material is lost, translocations are known as “balanced” [227]. A known example of a reciprocal translocation is in the case of chronic myelogenous leukemia, in which there is the reciprocal translocation (t(9;22)(q34;911) [228]. This translocation leads to the appearance of the Philadelphia chromosome and the BCR-ABL fusion gene consisting of the breakpoint cluster region (BCR) gene and abelson murine leukemia viral oncogene homolog 1 (ABL1) gene. This fused gene codes for a tyrosine kinase, which is targeted by tyrosine kinase inhibitors and thus achieving remission of the disease [228].

Dicentric chromosomes are products of genome rearrangement that places two centromeres on the same chromosome [229]. Normally, each chromosome contains a single region of centromeric DNA where the centromere and kinetochore are assembled [229]. However, genome rearrangements can lead to fusion of two different chromosomes, often resulting in a dicentric chromosome on which two centromeres are linked [229]. Dicentric chromosomes can be quite stable in mitosis and inherited through meiosis [229]. Dicentric's stability can be due to centromere inactivation, where one of the centromeres becomes nonfunctional or inactive and, in this case, a dicentric chromosome segregates as a functionally monocentric chromosome during cell division [230]. Inactive centromeres of dicentric chromosomes lack key centromere and kinetochore proteins, such as histone H3-like centromeric proteins (CENP-A, CENP-C, and CENP-E), however the mechanism of centromere inactivation remains unclear [230]. Many dicentric chromosomes have been observed in humans and associated with birth defects such as Turner Syndrome and Down Syndrome and with other reproductive abnormalities [229]. Dicentrics can occur between any two chromosomes, but some types are more prevalent than others [229]. For example, Robertsonian translocations (ROBs) and isochromosome X_i(X) [231]. ROBS involve any two of the ten acrocentric chromosomes (13, 14, 15, 21, and 22) [231]. Rob(13;14) and rob(14;21) account for approximately 85% of dicentric ROBs found [232]. ROBs are whole-arm transfers between homologous or non-homologous chromosomes and they may be monocentric or dicentric (in dicentric the second centromere is often inactivated) [232]. Dicentric ROBs are the most common human chromosome abnormality, about 1/1000 in newborns [232].

Ring chromosomes (RCs) are circular DNA molecules, typical for many prokaryotes, eukaryotic plastids, and mitochondria but rare in the nucleus of eukaryotic genomes [233]. McClintock and Rhoades noted that RCs are unstable in the cell cycle, can

change their size, become lost or increase their copy number [234]. The presence of RCs in humans often leads to abnormal development [233]. RCs are formed because of two double-strand DNA breaks, for example after exposure to ultraviolet radiation [235] or after nuclear disasters (the number of RC carriers increased after the Chernobyl disaster) [236]. Two broken ends are combined and form a RC and chromosome ends without centromere are lost [233]. The formation of RC by two double-strand DNA breaks can lead to the loss of genetic material and gene monosomy [237]. Also, RCs can be formed by the fusion of the telomeric or subtelomeric regions without loss of genetic material, thus RC carriers are often healthy but have reduced fertility. [238] [237]. Additionally, RCs formation can occur through inverted duplication associated with a deletion (inv dup del rearrangements), which may be stabilized by circularization [233]. The frequency of RCs in the human population is about 1 in 50,000 embryos [239] and about 50% of RC carriers do not have significant symptoms [240]. The clinical manifestations of RCs are similar with corresponding syndromes induced by genetic material deletion and accompanying monosomy [233].

Double minutes are extrachromosomal circular DNA (eccDNA) and found in the context of chromothripsis, a catastrophic event in which one or a few chromosomes are shattered into pieces, then reassembled in an unnatural order and orientation via non-homologous end joining [241] [242]. Double minutes lack centromeres; thus, they are unequally segregated to daughter cells at cell division [242]. EccDNA amplification can increase copy number of oncogenes and significantly enhance and maintain tumor heterogeneity [243]. Despite their important roles in tumorigenesis, it is unclear how double minutes evolve and how they contribute to the dynamics of tumor heterogeneity [243].

Thus, there are many types of CIN and each of them is implicated in different diseases. Mechanisms of CIN and types of CIN implicated in carcinogenesis are described in the next section (1.20).

1.20 Mechanisms of chromosomal instability associated with carcinogenesis

Most solid tumors exhibit aneuploidy and aneuploidy was first associated with tumors in the late 19th century [221]. Cancer CIN results in a high rate of change of chromosome number and structure and generates intratumour heterogeneity [244]. The majority of solid tumors exhibit CIN and it is associated with both poor prognosis and therapeutic resistance [245]. Structural and numerical CIN are frequently found in solid tumors [225] and this co-occurrence can be induced through defective mitotic checkpoint function or chromosome attachment to the mitotic spindle, or via pre-mitotic defects such as faulty DNA repair and replication [246].

There are various mechanisms through which tumor cells lose mitotic fidelity and exhibit CIN [225]. Depletion of cohesins or of the cohesion regulators and separase (which cleaves cohesion to initiate anaphase) using RNA interference increases the numbers of tetraploid cells, frequently observed in tumor genomes [247]. Also, tetraploid cells arise when separase is overexpressed, indicating that disturbances of cohesion cause chromosome segregation errors in tumor cells [248]. For example, high levels of separase are observed in breast cancer tumor samples, which exhibit CIN, compared with normal tissue controls [249]. Additionally, large-scale sequencing of tumor genomes shows that cohesin genes are rarely mutated [250]. Moreover, impairments of the spindle assembly checkpoint (SAC) can significantly increase the likelihood for chromosome mis-segregation, meaning that mutations in SAC genes can cause CIN [221]. Some breast tumor cell lines have decreased levels of the SAC protein (mitotic arrest deficient 2) MAD2 [251], and mutations in the gene encoding mitotic checkpoint

serine/threonine kinase (BUB1) have been identified in colon cancer cell lines [252]. Experiments in mice support the association of CIN with defective SAC activity in carcinogenesis. Heterozygous mice with mutations in specific SAC genes displayed elevated chromosome mis-segregation rates compared with control animals and had increased tumor incidence later in life [253] [254]. For example, mice heterozygous for Mad2 gene mutations develop spontaneous lung tumors after 18 months [253] and mice with hypomorphic Bub1 alleles display an increase in hepatocellular carcinomas, lung adenocarcinomas, sarcomas, and lymphomas after 19 months [255]. These results of tumor formation in many of these transgenic mouse models suggests that chromosomal instability promotes tumorigenesis [221].

Another mechanism of chromosomal instability associated with carcinogenesis is due to defects in kinetochore-microtubule attachment dynamics [221]. The centromere-localized Aurora B kinase is a central controller of the regulation of kinetochore-microtubule dynamics [221]. Inhibition of this kinase renders the attachment of microtubules to kinetochores irreversible [256]. One of the targets of Aurora B is the Ndc80 complex and members of the kinesin-13 family of microtubule-depolymerizing enzymes [257]. Loss of function of these targets eliminates stable kinetochore-microtubule attachments and contributes to CIN [221]. It was shown that kinetochore-microtubule attachments were more stable in tumor cells with CIN than in a chromosomally stable diploid cell line [257]. CIN cancer cells displayed hyperstable kinetochore-microtubule attachments in prometaphase, or metaphase, or both [221]. Overexpression of kinesin-13 reduced kinetochore-microtubule attachment stability and restored chromosome segregation to cancer cells that otherwise exhibited CIN [257]. This provides evidence that the excessively stable kinetochore-microtubule attachments are the cause of CIN in many cancer cells [221]. Additionally, components of the anaphase promoting complex (APC/C) are frequently mutated in cancer cells and these

cells show high rates of lagging chromosomes in metaphase [258]. Depletion of APC increased kinetochore-microtubule stability and induced lagging chromosomes in stable diploid cells [257]. The latter was rescued by overexpression of proteins that promoted kinetochore-microtubule dynamics [257].

Defects in cell-cycle regulation can account for CIN observed in tumors [221]. For example, F-box and WD repeat domain containing 7 (FBXW7) is a ubiquitin ligase that targets cyclin E for degradation and thus regulates the G1-S cell cycle transition [259]. FBXW7 is mutated in many cancers, including ~12% of colorectal cancers which exhibit CIN, however the role of FBXW7 in CIN remains unclear [259]. Another example is the retinoblastoma (Rb) tumor suppressor protein, which regulates the transcriptional activator E2F [260]. One target of E2F is the Mad2 gene and loss of Rb results in overexpression of Mad2, which has been shown to include CIN [260].

Thus, CIN can occur due to defects in multiple levels of chromosomal regulation and understanding the various mechanisms of CIN associated with carcinogenesis would be crucial for diagnosis, prognosis and even therapeutic design.

1.21 Types of chromosomal instability associated with carcinogenesis

Different types of chromosomal instability are involved in carcinogenesis and many different cancers display characteristic chromosomal abnormalities. This section is focused on describing examples of dicentrics, rings, double minute chromosomes and translocations and their implication in different malignancies.

Dicentric chromosomes have been identified in hematological malignancies, including the recurrent dic(17;20) [261] and dic(5;17) [262] in myelodysplastic syndrome (MDS) and acute myeloid leukemia (AML) as well as the dic(9;20) [263] in acute lymphoblastic leukemia [264]. These dicentrics occur usually due to unbalanced reciprocal translocations, with breakpoints often described at or near the centromere

[265]. Most dicentric chromosomes appear to have a range of breakpoints on both chromosomes, but the dic(9;20) has been shown to have breakpoints within a single gene on 9p, *PAX5*, creating a fusion gene between this gene and a number of different genes on 20q [266]. Thus, dicentric chromosomes frequently occur in various cancers and may contribute to the malignant phenotype and clonal evolution [264].

Ring chromosomes (RCs) formation, formation of chromosome bridges, isochromosomes, deletions, polyploidy etc. are present in many tumors [233]. Chromosomal abnormalities are a hallmark of cancer cells [233]. Specific rearrangement, including RCs are frequently markers of tumors [233]. For example, fat tissue tumors known as “atypical lipomas” and well-differentiated liposarcomas” often have RCs [267]. Also, some tumors of mesenchymal origin exhibit RCs in more than 70% of cells [268]. Overall, RCs occur in approximately 10% of epithelial cancers and less than 10% in hematopoietic neoplasias [268]. In leukemias, the presence of ring chromosomes seems to be associated with poor prognosis in most but not all cases [268]. The majority of hematopoietic neoplasias that exhibits RCs is acute non-lymphoblastic leukemia, in which the chromosomes forming the corresponding ring could not be clearly defined [268]. RCs are very typical in certain low or borderline malignant mesenchymal tumors, such as dermatofibrosarcoma protuberans, parosteal osteosarcoma, low-grade malignant fibrous histiocytoma and atypical lipomatous tumors [269]. Thus, RCs serve as cytogenetic hallmarks and are used in determining proper diagnosis [270].

Double minutes are frequently found in many different tumor types, especially in brain tumors [271]. Double minutes are associated with resistance to targeted cancer therapy [272]. G-banding revealed regions lacking patterns that might identify their origin in other chromosomes of normal parental cell karyotypes [271]. Chromosome banding applied to neuroblastoma cells led to the discovery of the homogeneously staining regions

(HSRs), which are distinctive regions stained uniformly [271]. HSRs were initially described in human neuroblastoma and methotrexate-resistant hamster cells [273]. HSRs in methotrexate-resistant cells were considered to involve intrachromosomal amplification of the dihydrofolate reductase gene, the target enzyme of methotrexate [273]. Many reports imply a relationship between double minutes and HSRs [274]. Both double minutes and HSRs display pale staining with G-banding [271]. Also, double minutes and HSRs were reported as mutually exclusive since some cell lines contained subpopulations with double minutes or HSRs but rarely both [275]. The latter suggests that double minutes and HSRs were alternative manifestations of the same biological phenomenon [271]. There is biochemical evidence supporting the relationship between double minutes and HSRs [271]. In Chinese hamster cells stably resistant to methotrexate, the gene for the target enzyme dihydrofolate reductase was amplified in an HSR on chromosome 2 [276] [271]. In stably resistant mouse cells, HSRs were also the chromosomal sites of dihydrofolate reductase gene amplification [277] [271]. On the other hand, mouse cell lines unstably resistant to methotrexate contained unstably amplified dihydrofolate reductase genes associated with double minutes [278]. These reports correspond well with cytogenetic indications that HSRs were attached to chromosomes with stable centromeres, while double minutes were without centromeres [271]. Thus, gene amplification can be alternatively associated with chromosomal HSRs in case of stable phenotypes or with double minutes in case of unstable phenotypes [271].

Breast and ovarian cancers, but also various types of lung cancers and colon carcinomas, showed the highest percentages of double minute positive cases (breast cancer: 18%, ovarian cancer: 29%, colon cancer: 44%) [279]. Double minute chromosomes were also observed in 20%-30% of small cell lung cancers (SCLC) and 10%- 20% of non-small cell lung cancers (NSCLC) [279]. There are also reports on the

association of double minutes with MYC proto-oncogene (MYC) or epidermal growth factor receptor (EGFR) amplification in some cases of lung cancer [280]. Specifically, MYC amplification occurs in 15%-30% of SCLC and in 5%-10% of NSCLC [280]. Moreover, more than 20% of glioma cases are carriers of double minute positive cells [279]. The amplified EGFR gene is the most frequently located on the double minute positive cells in human gliomas [279]. Also, double minutes are very frequent in neuroblastomas, approximately 30% of advanced tumor stages and they carry amplified copies of the MYCN gene [281]. Additionally, Marinello et al reported that double minute chromosomes occurred in 40 of 320 patients with hematologic diseases [282]. Amplification of MYC associated with double minutes frequently occurs in acute myeloid leukemia (AML) and is linked with poor prognosis [279] [282].

There is evidence of a possible link between chromosomal instability and metastasis [222]. Aneuploid tumors were more often a higher grade and stage and were associated with decreased patient survival in several types of cancer [283] [284] [222]. A meta-analysis of 141,163 breast cancer cases showed that patients with aneuploid breast cancer had worse survival compared to patients with a diploid tumor [285]. Also, chromosomal instability was associated with breast cancer containing lymph node metastasis [285]. A meta-analysis on colorectal cancer (CRC) indicated that aneuploidy was linked to higher tumor stage in most of the studies analyzed [286]. Another study on gastric cancer found an increase in aneuploidy in distant metastases [287]. Thus, there is evidence of correlation of chromosomal instability and metastasis.

1.22 Metal-induced chromosomal instability as a driving force for carcinogenesis

Heavy metals are generally considered to be weak mutagens, if mutagenic at all and CIN is reported to be the driving force for metal-induced carcinogenesis [288] [289].

Exposure to chemical agents can destabilize the numbers and structure of chromosomes, alter regulators of chromosome segregation, and disturb DNA synthesis and repair [288]. Arsenic, cadmium, chromium, nickel, beryllium, and cobalt are considered as carcinogenic metals and lead is also suggested as a probable carcinogen [289]. A description of the association of various metals with carcinogenesis is following in this section. A more detailed discussion of arsenic induced CIN as a mechanistic event in carcinogenesis is in section 1.23.

Cadmium is an environmental contaminant and exposure to cadmium also occurs through cigarette smoking [290]. It is a known human carcinogen, and cadmium exposure increases the risk for lung, kidney, liver, bladder, stomach, and prostate cancers [291]. Cadmium carcinogenesis has been linked to CIN and microsatellite instability (MIN) [291]. Specifically, cadmium induces sister chromatid exchange and inhibits mismatch repair activity in various cells [292] [291]. Cadmium also produces depolymerization of the actin cytoskeleton in several cultured cell lines [293]. Finally, cadmium also causes failure of kinetochores to attach to the spindle apparatus either by alteration of its proteins or by altered chromatid separation in anaphase [294].

Hexavalent chromium is a well-established human lung and bladder carcinogen, but the mechanism of chromium-induced carcinogenesis is not fully understood [289]. A suggested key mechanism is that hexavalent chromium causes CIN, which further leads to neoplastic transformation [295]. Specifically, studies show that chronic exposure to hexavalent chromium impacts DNA repair and induces centrosome amplification, which then leads to numerical and structural chromosomal abnormalities [295]. Hexavalent chromium-induced lung and bladder tumors have been characterized by MIN and CIN [295]. MIN was detected in 79% of chromium-induced lung tumors, while only 15% of non-exposed lung tumors had increases in MIN [296]. Loss of heterozygosity (LOH) was observed at 6 different loci in 50-75% of chromium-induced lung tumors, while this was

not observed in non-exposed tumors [296]. Moreover, lymphocytes of chromate workers exhibited increased CIN, as well as high number of bi-nucleated cells [297]. The latter is consistent with cell culture studies showing increased bi-nucleated cells and changes in chromosomes' structure in various cell lines exposed to hexavalent chromium [298]. Also, cell culture studies have shown that exposure to hexavalent chromium for more than 24 h, causes SAC bypass [299], centrosome amplification [300] and defects in the homologous recombination (HR) pathway [301]. All of these can affect chromosomal stability, causing numerical and structural aberrations. Xie et al 2007 showed that bronchial cells malignantly transformed by lead chromate exhibited increased levels of aneuploidy and centrosome amplification [302]. Long-term exposure to hexavalent chromium also induced a concentration-dependent increase in aneuploid metaphases in primary and immortalized human urothelial cells [303].

Beryllium has long been implicated in lung carcinogenesis; however, the mechanism of beryllium-induced lung cancer remains unclear [289]. Some in vitro assays have shown that beryllium suppresses the dynamic instability of microtubules [304], suggesting a potential mechanism for an aneuploid effect [304].

Cobalt is considered a possible human lung carcinogen [289]. Cobalt chloride induces aneuploidy in lymphocytes in the chromosomes 13, 14, 15, 21, 22 and Y [305]. Also, hamsters intraperitoneally injected with cobalt chloride exhibited aneuploidy in bone marrow and testes [305]. Occupational exposure to cobalt refinery workers caused increased chromosome loss [305]. The etiology of cobalt-induced CIN is unclear, but DNA damage and repair inhibition are suggested mechanisms of CIN in carcinogenesis due to cobalt exposure [305]. A study in human skin cells exposed to 2 ppb cobalt chloride showed that keratinocytes exhibited increased aneuploidy (more than 46 chromosomes) compared with unexposed cells [306].

Lead is a probable carcinogen and characterized as an aneugenic agent in both cell cultures and epidemiologic studies [289] [307] [308]. A pilot study in Poland, consisting of 9-year-old children (n=92) showed that exposure to lead causes increase in micronuclei (MN) formation in their hematopoietic cells [308]. MN formation may predispose these children to hematopoietic malignancies and was also correlated with elevated blood lead levels [308]. Also, in Chinese hamster lung cell cultures inorganic lead compounds caused micronuclei formation and aneuploidy [307]. The aneuploidy is likely a result of destabilized microtubules causing the assembly/disassembly steady state to shift to microtubule disassembly due to inhibition of tubulin assembly [307] [309] [289].

Nickel is a carcinogenic metal causing lung and nasal cancers, mainly due to occupational exposure [289]. Several studies have shown that nickel causes chromosomal damage, but the mechanism of action remains unclear [289]. Specifically, studies in human cells showed an increase of kinetochores positive micronuclei after 24-26 h treatment of nickel sulfate and nickel chloride [310]. Another study showed that after 72 h of exposure to nickel sulfate, hamster cells had increases in the production of aneuploid metaphases, MN formation and an increase in cells exhibiting errors in chromosome segregation, including lagging chromosomes, chromatin bridges and asymmetrical segregation [311].

1.23 Arsenic-induced chromosomal instability as a driving force for carcinogenesis

As mentioned in section 1.1, arsenic is clastogenic and it causes CIN both *in vitro* and *in vivo* [3]. The molecular mechanism by which arsenic induces CIN-mediated carcinogenesis is yet to be delineated. In section 1.8, suggested mechanisms of arsenic

induced CIN are described in detail. This section contains examples of how arsenic causes CIN and its association with tumorigenesis.

Arsenic exposure is associated with lung, skin, liver, and bladder cancer [289]. Several studies have shown that arsenic causes CIN and disrupts the normal progression of mitosis which can lead to polyploidy or structural chromosomal abnormalities [312]. Specifically, chronic exposure to arsenic, both *in vitro* and *in vivo*, results in structural changes, including chromosome end to end fusion, abnormal sister chromatid separation, and aberrant chromosome segregation [117]. Arsenic induces lagging chromosomes, suggesting a disruption of microtubule assembly dynamics [313]. Arsenic exposure may disrupt microtubule assembly through interaction with the sulfhydryl groups of tubulins, leading to mitotic spindle complex malfunction [314] [315]. Arsenic also bypasses the SAC, resulting in premature anaphase and the induction of diplochromosomes and tetraploidy in subsequent cell divisions [313]. Additionally, arsenic can cause centrosome amplification and it has been detected through the formation of multi polar spindles and immunofluorescent staining of centrosomes [316] [312]. Arsenite induces mitotic arrest by disrupting centrosome function [317]. Specifically, arsenite disrupts heat shock proteins, involved in both kinetochore and centrosome organization, increasing centrosome abnormalities, and inducing mitotic arrest [317]. Also, arsenic exposure has long been known to induce MN which can contain either whole chromosomes or fragments of chromosomes, as indicated by *in situ* hybridization [109]. Specifically, exposure to arsenite causes MN formation and binucleated in human colon carcinoma cells in [318].

A study in Argentina and Chile examining chromosomal alterations in bladder tumor DNA in 123 patients who had been exposed to arsenic in their drinking water, showed that the total number of chromosomal alterations was higher in individuals exposed to higher arsenic levels [319]. These chromosomal alterations were mostly observed in

metastatic tumors, raising the possibility that bladder tumors from arsenic-exposed patients may behave more aggressively than tumors from unexposed patients [319]. Additionally, dicentric chromosomes and DNA hypomethylation (which enhances CIN) were observed in V79-C13 Chinese hamster cells by short term exposure to 10 μ M sodium arsenite [320]. These chromosomal alterations persisted even after the exposure was withdrawn and the CIN propagated within the cell population [320]. Arsenic exposed individuals with Bowen's disease (skin carcinoma *in situ*) were more likely to have significantly higher CIN in their peripheral blood lymphocytes than individuals with arsenic-induced non-malignant skin lesions [321]. Micronuclei formation was higher in individuals with arsenic-induced Bowen's disease compared to those with non-cancer skin lesions [322]. There is also evidence that an increased frequency of chromosomal aberrations in peripheral lymphocytes is predictive of increased risk of cancer [321]. The increase of CIN in patients with Bowen's disease is consistent with results of previous studies performed in Taiwan and in Europe, which showed an association of CIN with cancer risk in an arsenic-induced black foot disease region in Taiwan [323] and with arsenic-induced stomach cancer in Central Europe [324].

Thus, there are various mechanisms by which arsenic causes CIN and there is evidence of CIN in arsenic-induced tumors. Elucidation of the types of chromosomal abnormalities caused by arsenic and how CIN drives the arsenic-induced carcinogenesis, is crucial for a better understanding of arsenic toxicity and for therapeutic design to treat arsenic-induced cancers.

1.24 Aim of the thesis

Previous study of differential miRNA expression in squamous cell carcinoma (SCC) caused by chronic arsenic exposure in drinking water relative to that of premalignant hyperkeratotic lesions, showed that miR-186 was highly expressed in some SCC relative to hyperkeratosis [325] (see section 1.13). Also, HaCaT cells that overexpressed miR-186 and were exposed to sodium arsenite showed increased levels of aneuploidy and structural chromosomal abnormalities, including dicentric, rings and double minute chromosomes, compared to vector control transfected and unexposed HaCaT cells [5].

Given the introduction of this thesis; specifically, the role of miR-186 in carcinogenesis through regulation of cell cycle (see section 1.14) and the role of arsenic-induced CIN as a driver of carcinogenesis (see sections 1.8 and 1.23), the focus of my master's degree project was to assess the role of arsenic exposure and miR-186 in skin carcinogenesis and chromosomal instability. Specifically, the hypothesis that miR-186 overexpression drives malignant transformation of HaCaT cells by induction of chromosomal instability, is tested in my master's degree research project. The methods that were used to test this hypothesis are described in chapter 2.

CHAPTER 2: MATERIALS AND METHODS

2.1 Cell culture

2.1.1 HaCaT cells and arsenite exposure

Human immortalized keratinocytes, HaCaT cells were the kind gift of the Dr. TaiHao Quan (University of Michigan Ann Arbor). The identity of the cells was confirmed by STR (Short Tandem Repeat) mapping (Genetica DNA Laboratories/LabCorp, Burlington, NC). HaCaT cells were cultured in alpha modification of minimal essential medium (α -MEM, Gibco, Invitrogen, Carlsbad, CA, USA) supplemented with 10% fetal bovine serum (FBS) (characterized, HyClone, Logan, UT, USA), 2 mM glutamine, 100 units/mL penicillin and 100 μ g/mL streptomycin (GIBCO, Invitrogen, Carlsbad, CA, USA). HaCaT cells were transfected with pEP-hsa-miR-186 expression vector (Cell Biolabs) or empty vector and maintained with 0.9 μ g/mL puromycin (P7255, Sigma-Aldrich, St Louis, MO, USA) [5]. The clones were isolated and characterized for hsa-miR-186 expression [5]. Three hsa-miR-186 transfected clones with the highest expression and three empty vector transfectants with lowest expression were selected for study [5]. The six clones were propagated independently for 8 weeks in complete α -MEM with 0 or 100 nm sodium arsenite (NaAsO_2) (CAS 7784-46-5, ThermoFisher Scientific, Waltham, MA, USA) [5]. This concentration of NaAsO_2 was selected based on the average blood arsenic level observed in an epidemiological study in China where people used tube wells of high concentration of arsenic [57]. Chronic arsenic intoxication and arsenic-induced skin

lesions and epidermal cancers were observed in this population [35]. The six clones cultured for 8 weeks were established from frozen stocks of cells and further propagated until they reached 29 weeks (Figure 5).

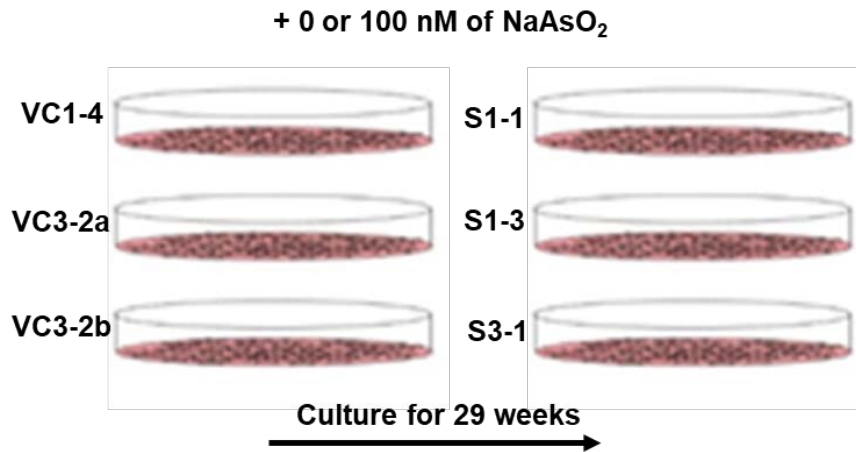


Figure 5: Schematic overview of chronic culture and exposure to 0 or 100 nM of NaAsO₂ of vector control and hsa-miR186 overexpressing HaCaT cells. VC1-4, VC3-2a, VC3-2b are the three vector control clones with the lowest miR-186 expression and S1-1, S1-3, S3-1 are the three miR-186 transfected clones with the highest miR-186 expression levels [5].

Each clone was also exposed to 0 or 100 nM of NaAsO₂ for 29 weeks (Figure 5). So, there are twelve total cultures of the following four different conditions: 1) vector control HaCaT + 0 nM NaAsO₂, 2) vector control HaCaT+ 100 nM NaAsO₂, 3) miR-186 transfected HaCaT + 0 nM NaAsO₂, 4) miR-186 transfected HaCaT + 100 nM NaAsO₂. Cultures were grown at 37°C in humidified atmosphere of 95% air and 5% CO₂. Cells were passaged twice per week (every 3-4 days) and a million cells were plated per 100 mm dish at every passage. Every month, cells were frozen down at 1 x 10⁶ cells/ml in Nunc™ cryovials and stored in liquid nitrogen.

2.1.2 HeLa cells

HeLa cells were cultured in DMEM (Dulbecco's Modified Eagle Media) (ThermoFisher Scientific) supplemented with 10% fetal bovine serum (FBS) (characterized, HyClone, Logan, UT, USA), 2 mM glutamine, 100 units/mL penicillin and 100 µg/mL streptomycin (GIBCO, Invitrogen, Carlsbad, CA, USA). Cultures were grown at 37°C in humidified atmosphere of 95% air and 5% CO₂. Cells were passaged twice per week (every 3-4 days) and a million cells were plated per 100 mm dish at every passage. HeLa cells were used in triplicates as a positive control in soft agar colony formation assay (see 2.6).

2.2 Cytogenetic analysis

HaCaT clones either transfected with empty vector or overexpressing hsa-miR-186 and exposed to 0 or 100 nM of NaAsO₂, were seeded into 100 mm dishes with 7 mL complete α-MEM. Cells were allowed to acclimate for 48 h and re-enter normal cell cycle pattern. Cells were arrested at metaphase after addition of demecolchicine solution (#D1925, Sigma, St. Louis, MO, USA) to final concentration of 0.2 µg/mL. The cultures

were then incubated at 37°C for 1 h. At the end of treatment, media were collected to include any loosely adherent mitotic cells. Then, after collecting the media, the attached cells in the dish were washed with phosphate buffered saline (PBS) and dissociated with 0.25% trypsin /1 mM EDTA (Ethylenediaminetetraacetic acid). Media was added to the trypsinized cells to stop the trypsin. The trypsinized cells with the collected media were then added to the media collected prior to trypsinization (which includes the loosely adherent cells). Then, cells were pelleted by centrifugation at 1000 rpm for 5 min at 4 °C. The pellets were resuspended and incubated in 10 mL of 0.075 M potassium chloride (KCL) hypotonic solution for 17 min to swell the cells and the nuclei. At the end of 17 min, 1 mL of freshly mixed methanol-glacial acetic acid (3:1, v:v) was added to the tubes and cells collected by centrifugation at 1000 rpm for 5 min at 4 °C. Subsequently, pellets were suspended gradually in 10 mL methanol-acetic acid and incubated at room temperature for at least 20 min, collected by centrifugation at 1000 rpm for 5 min at 4 °C and resuspended in methanol-acetic acid. Then, the cells were dropped on microscope slides to provide a suitable density of metaphases for microscopic analysis.

2.2.1 Chromosomal damage staining

The goal is to stain solid chromosomes for the purpose of scoring chromosome damage (ring chromosomes, double minutes, dicentrics) and/or aneuploidy. The slides were stained with 5% Giemsa for 5 min and then washed several times in deionized water, dried overnight and then sealed with microscope cover glass.

2.2.2 Karyotype analysis

The goal is to stain slides for G-banding of chromosomes. The banding pattern can distinguish chromosomal abnormalities or structural rearrangements, such as deletions, translocations, insertions, and inversions. G-banding involves trypsin treatment followed

by staining with Giemsa or Wrights stain to create characteristic light and dark bands. Trypsin degrades euchromatic histones in DNA. After Giemsa staining, highly transcriptional active regions (euchromatin) which have low content of histones will appear as light bands. Highly condensed chromatin with little or no transcriptional activity (heterochromatin) will have a large portion of its histones, which will be digested by trypsin allowing the dye to access to the DNA [326]. The heterochromatin will appear as dark bands. Fetal bovine serum (FBS) is used to inactivate the trypsin activity prior to staining [326]. Specifically, after the cells were fixed, slides were immersed in 0.063% trypsin solution for 30-60 sec at pH 7.2. A 2% FBS wash followed to stop the trypsin digestion. Then, the slides were rinsed with pH 7.0 Gurr's buffer, followed by 70% and 95% ethanol dehydration and rinsed in pH 6.8 Gurr's buffer solution. The slides were then stained for 3 min with 5% Giemsa and slides were coverslipped with cyto seal. Fifteen metaphases were karyotyped for each clone in 9 weeks and 29 weeks timepoint. Metaphases were analyzed using an Olympus light microscope and karyotypes were assembled using Applied Spectral Imaging software.

2.3 RNA extraction

Total RNA was extracted from cells using the mirVana™ RNA Isolation Kit (Ambion, ThermoFisher Scientific) according to the manufacturer's instructions for small RNA enrichment. RNA concentrations were determined using NanoDrop® Spectrophotometer ND-1000 (ThermoFisher Scientific). RNA integrity (RIN) analysis was determined using the Agilent RNA 6000 Pico Kit, Eukaryote, version 2.6 and the Agilent 2100 Bioanalyzer (Agilent Technologies, Inc., Santa Clara, CA, USA). All samples had RIN number greater than 9.

2.4 Western blot analysis

Cells were lysed with a solution of 10 mM Tris-HCl pH 7.4, 1 mM disodium ethylenediaminetetraacetic acid (Na₂EDTA), 0.1% sodium dodecyl sulfate (SDS), 1 mM phenylmethylsulfonyl fluoride (PMSF), 1 mM sodium vanadate (Na₃VO₄) and 1x protease inhibitor cocktail (Complete, Roche, Mannheim, Germany). Insoluble debris was removed from lysates by sonication and centrifugation at 13,000 x g, at 4 °C for 15 min. Protein concentrations were determined with a bicinchoninic acid (BCA) assay (ThermoFisher Scientific). Aliquots of 20 µg of total protein extracts were resolved by electrophoresis in 4-20% Criterion™ TGX™ Precast gradient sodium dodecyl sulfate polyacrylamide gel (SDS-PAGE) (Bio-Rad). The resolved proteins were transferred onto polyvinylidene fluoride membrane (PVDF, Millipore). Staining with Coomassie Brilliant Blue R250 (ThermoFisher Scientific) followed, to ensure loading and transfer of proteins. Membranes were then blocked in 5% milk in TBST (10 mM Tris-HCl pH 7.4, 150 mM NaCl, 0.1% Tween 20) at room temperature for 1 h. The membranes were subsequently probed with antibodies against BUB1 (#ab195268, Abcam, Cambridge, United Kingdom, 1:1000 in 1% skim milk powder in TBST), CDC27 (#ab129085, Abcam, 1:1000 in 1% milk in TBST), BUBR1 (#ab183496, Abcam, 1:1000 in 1% milk in TBST), vimentin (#5741T, Cell Signaling, Danvers, MA, USA, 1:1000 in 1% milk in TBST), n-cadherin (#13116, Cell Signaling, 1:2000 in 1% milk in TBST), slug (#9585, Cell Signaling, 1:2000 in 1% milk in TBST), ZO-1 (#8193, Cell Signaling, 1:2000 in 1% milk in TBST), β-catenin (#8480, Cell Signaling, 1:2000 in 1% milk in TBST), e-cadherin (#3195T, Cell Signaling, 1:3000 in 1% milk in TBST), claudin 1 (#13255, Cell Signaling, 1:1000 in 1% milk in TBST), beta actin (#A5441, Sigma-Aldrich, 1:10000 in 1% milk in TBST) and vinculin (#13901P, Cell Signaling, 1:1000 in 1% milk in TBST). Blots were then incubated with anti-rabbit (#7074, Cell Signaling Technology, 1:1000 in 1% milk in TBST) and anti-mouse (#7076, Cell Signaling Technology, 1:1000 in 1% milk in TBST)

HRP-conjugated secondary antibodies as appropriate. Restore TM Western Blot Stripping Buffer (#21059, ThermoFisher Scientific) was used for stripping between probing with different antibodies. For the detection of signals, blots were incubated with an enhanced chemiluminescent substrate (ECL) (ThermoFisher Scientific). Images were acquired using FOTO/Analyst FX. Densitometry analysis was performed using Image Studio Lite Software version 5.2.5.

2.5 Flow cytometry cell cycle assay

HaCaT clones either transfected with empty vector or overexpressing hsa-miR-186 were seeded at density of 1.5 million cells per 100 mm dish and exposed to 0 or 100 nM NaAsO₂. After 48 hours, the cells were trypsinized, washed twice with phosphate buffered saline (PBS) then fixed in 70% ethanol for 24 hours at 4°C. The cells were then centrifuged at 1500 g for 1 minute, suspended in PBS (400 µl), then RNAase A (10 mg/mL, 50 µL) and propidium iodide (2 mg/mL, 10 µL) were added followed by a 30 minute incubation in the dark at room temperature. Fluorescence was acquired by flow cytometry on a Becton Dickinson FACSCalibur™ (BD Biosciences). Cell cycle distribution was determined using FlowJo™ v10.2 [327].

2.6 Soft agar colony formation assay

Anchorage-independent growth is one of the hallmarks of cell transformation and is considered an accurate *in vitro* assay for detecting malignant transformation [328]. The soft agar colony formation assay is a common method to monitor anchorage independence [328]. It measures proliferation in semisolid culture media after 6-8 weeks by manual counting of colonies. Clones were analyzed at 12, 16, 20, 24 and 29-week timepoints for transformation by colony formation in agar. Three dishes were seeded for each clone. Hela cells, which are known to be malignant cells, were used a positive control. Control and treated clonal cell lines were suspended in 0.4% noble agar onto a

0.8% noble agar base layer in a 30-mm dish at a density of 100,000 cells per dish for HaCaT cells and 30,000 cells per dish for Hela cells and grown for 6-8 weeks. The top and bottom agar layers were made at two times the final concentration in water and diluted 1:1 with 2x concentrated media at the time of plating. Cultures were examined microscopically 24 hours after plating to confirm single cell suspension. During incubation in agar, old media was aspirated, and 0.5 mL of fresh growth media with 0 or 100 nM sodium arsenite was added to the cells twice per week. Colonies were detected by 0.01% crystal violet staining and counted (Figure 6).

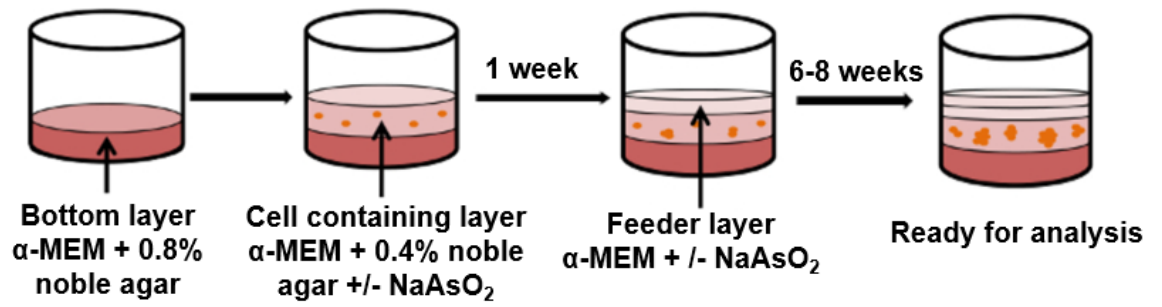


Figure 6: Schematic overview of the protocol for the soft agar colony formation assay

2.7 Mycoplasma PCR assay

MycoSensor PCR Assay kit (#302108, #302109) (Agilent) was used to screen for mycoplasma infection of cell cultures. HaCaT cells transfected with pEP-hsa-miR-186 expression vector or empty vector cultured for 29 weeks and exposed to 0 or 100 nM of NaAsO₂, were tested for Mycoplasma contamination. Fifty µL of test cell culture media, 50 µL of negative control (deionized water) and 50 µL of positive control media (provided by the kit) were used as PCR templates. PCR was performed according to manufacturer's instructions.

2.8 Statistical analysis

Protein expression data were analyzed with two-way ANOVA and Tukey's post-hoc test (for multiple comparisons). Data are expressed as mean +/- SD (Standard Deviation). The level of significance was established at p value ≤ 0.05 . The statistical analyses were all conducted using GraphPad Prism 8.4.2 (679)

CHAPTER 3: RESULTS

3.1 Soft agar colony formation assay

The ability of cells to proliferate in suspension, unattached to any matrix, is a characteristic of transformed cells, correlating with tumorigenic potential *in vivo*. HaCaT overexpressing miR-186 and exposed or not to arsenic were tested *in vitro* for anchorage-independent growth in agar [328]. The assay was performed at an early time point (12 weeks) and at a late time point (29 weeks) to assess if miR-186 overexpression accelerates the arsenic transformation process. We observed that HaCaT overexpressing miR-186 and exposed to arsenite showed increased growth ability in agar at 12 weeks in contrast to vector control unexposed and exposed cells (Panel A, Figure 7). Specifically, single cells formed clusters of cells in all miR-186 transfected clones also exposed to arsenite (S1-1, S1-3, S3-1), as indicated by red arrows (Panel A, Figure 7). We also observed that all arsenite-exposed cells formed colonies in agar at 29 weeks (Panel B, Figure 7). Specifically, single cells formed colonies (more than 50 cells [329]) in agar in vector control and exposed to arsenite clones (VC1-4, VC3-2a, VC3-2b) as well as in miR-186 overexpressing and exposed to arsenite clones (S1-1, S1-3, S3-1), as indicated by red arrows (Panel B, Figure 7). Specifically, we visually observed (not measured) that the miR-186 overexpressing cells and exposed to arsenite formed slightly bigger colonies (as observed visually) compared with vector control and exposed to arsenite clones (Panel B, Figure 7). No quantification of data nor statistical analysis were performed since only one colony was formed per replicate.

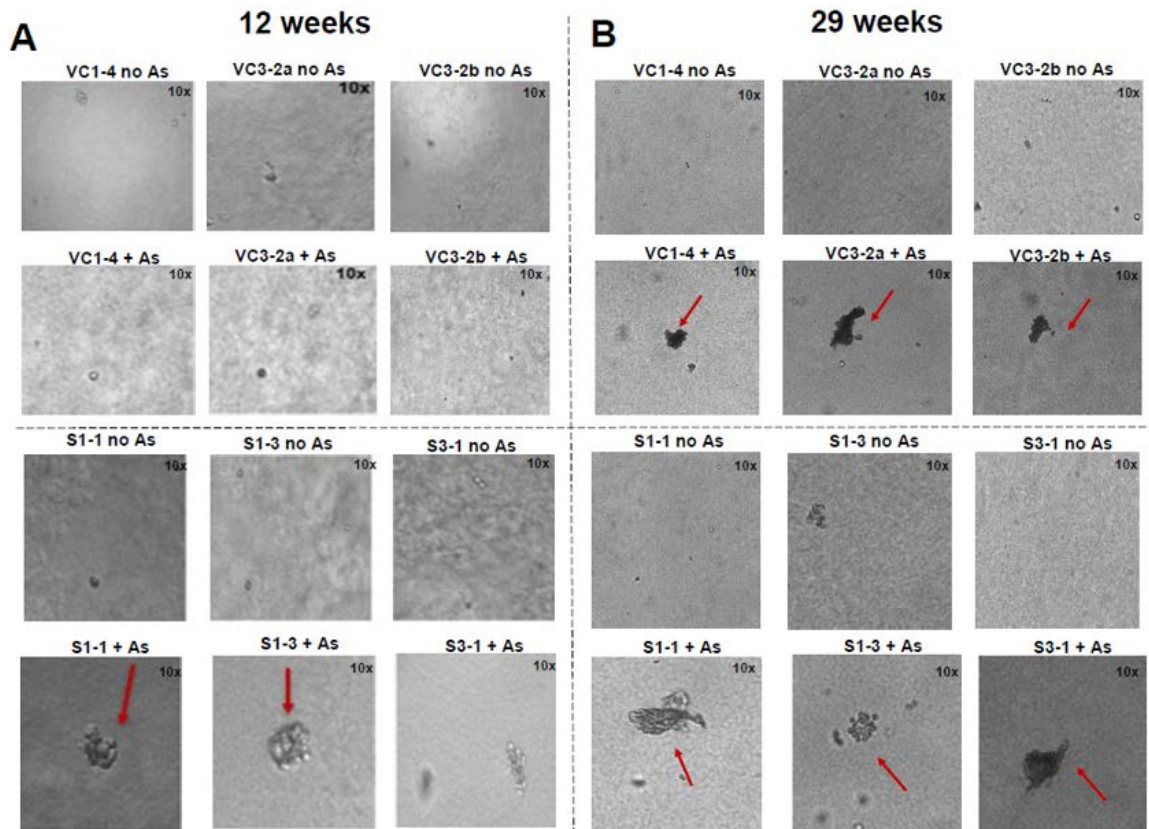


Figure 7: Soft agar colony formation assay. Representative phase contrast images, using 10x magnification: VC: Vector Control HaCaT, VC1-4, VC3-2a, VC3-2b are the three vector control clones (see section 2.1.1), S: miR-186 overexpressing HaCaT, S1-1, S1-3, S3-1 are the three miR-186 overexpressing clones (see section 2.1.1), A. HaCaT overexpressing miR-186 and exposed to arsenite formed clusters of cells indicating ability to grow in agar at 12 weeks, B. HaCaT transfected with vector control and exposed to arsenite and HaCaT overexpressing miR-186 and exposed to arsenite formed colonies from single cells at 29 weeks.

We used HeLa cells as positive control because they are known transformed cells and they formed multiple big colonies in agar, as it is shown after staining with crystal violet 0.01% (Figure 8).

HeLa cells as positive control

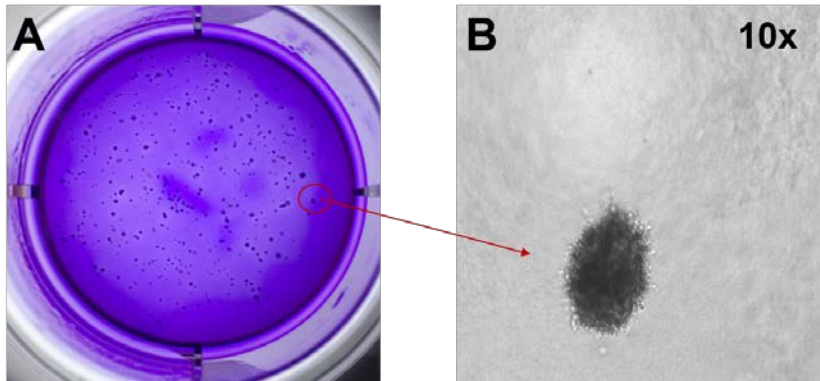


Figure 8: HeLa cells as positive control. A. Representative colonies formed from single cells in agar, stained with 0.01% crystal violet. Image was taken using dissecting microscope. B. Representative image of a colony. Image was taken using phase contrast microscope and 10x magnification.

3.2 Protein levels of epithelial-mesenchymal transition

The results from the soft agar colony formation assay (see section 3.1) showed that HaCaT overexpressing miR-186 and exposed to arsenite exhibited increased growth ability in agar at 12 weeks in contrast to vector control cells (exposed or not to arsenite) (Panel A, Figure 7). The soft agar assay also showed that colonies were formed in HaCaT transfected with vector control and exposed to arsenite clones as well as in HaCaT overexpressing miR-186 and exposed to arsenite clones at 29 weeks (Panel B, Figure 7). In this section, we present another assay to assess the transformation potential of these cells.

The induction of epithelial-to-mesenchymal transition (EMT) is an important mechanism for the progression of carcinomas to a metastatic stage [330]. During EMT, the levels of the epithelial markers are suppressed, and the levels of the mesenchymal markers are induced [330]. We screened HaCaT cells overexpressing miR-186 and exposed or not to arsenite, for the expression levels of epithelial and mesenchymal markers. This approach might elucidate the association of miR-186 overexpression with the progression to carcinoma.

We first determined the levels of the epithelial markers e-cadherin, β -catenin, claudin 1, and ZO-1 [330]. Then, we determined the levels of the mesenchymal markers n-cadherin and slug [330]. We also screened for the mesenchymal marker vimentin [330], but this protein was not expressed in our cell line. At 29 weeks, the miR-186 transfected HaCaT cells and unexposed to arsenite include protein expression data only from two clones (S1-1, S3-1, see section 2.1.1), because the S1-3 clone did not produce enough cells for protein lysate collection.

After 12 weeks of culturing and exposing to 0 or 100 nM sodium arsenite three clones of HaCaT cells transfected with vector control and three clones of HaCaT

overexpressing miR-186 (see section 2.1.1), we observed no significant changes in expression of the epithelial markers e-cadherin, claudin 1, β -catenin, and ZO-1, in vector control and miR-186 overexpressing HaCaT cells, both in arsenite (100 nM) exposed and unexposed cells (Figure 9).

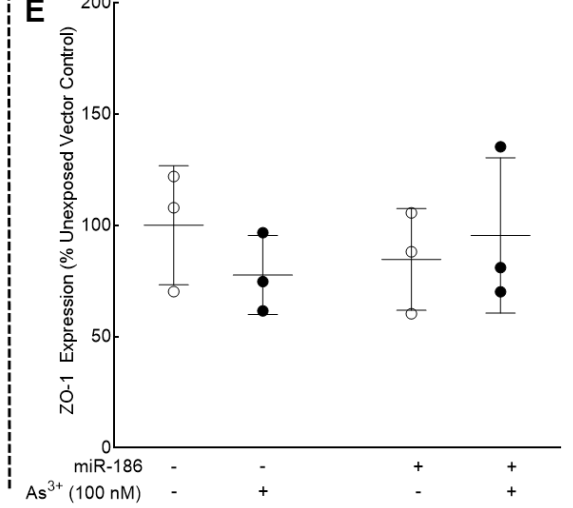
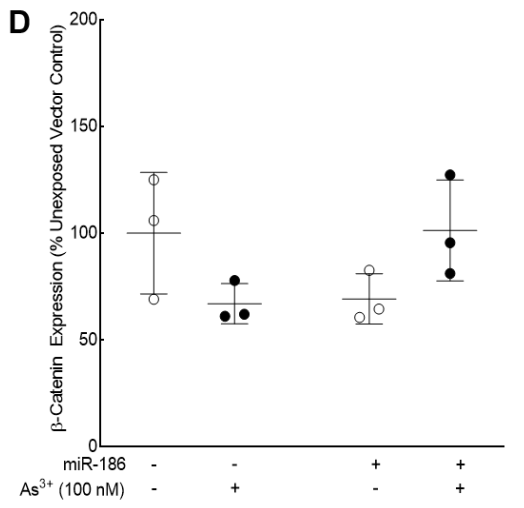
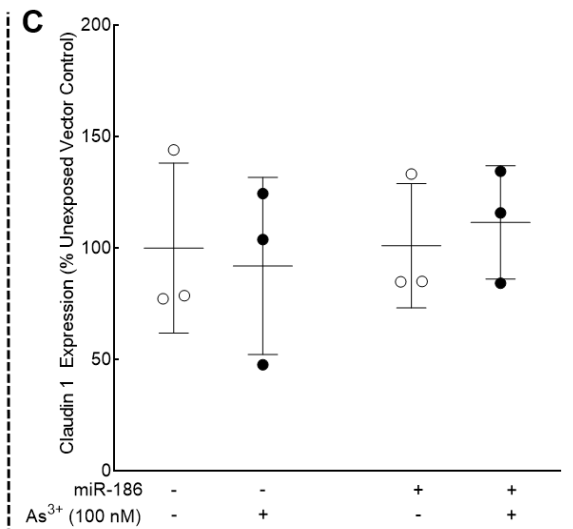
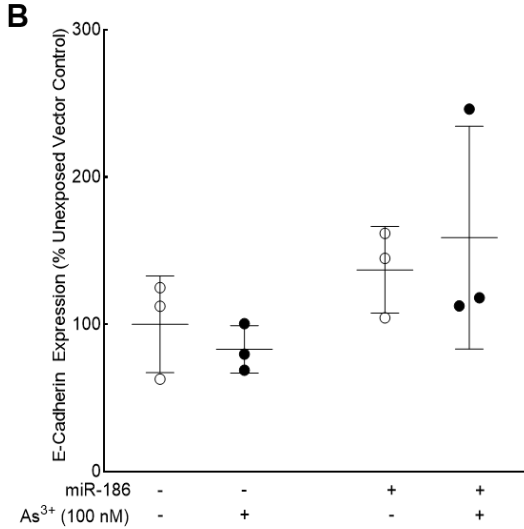
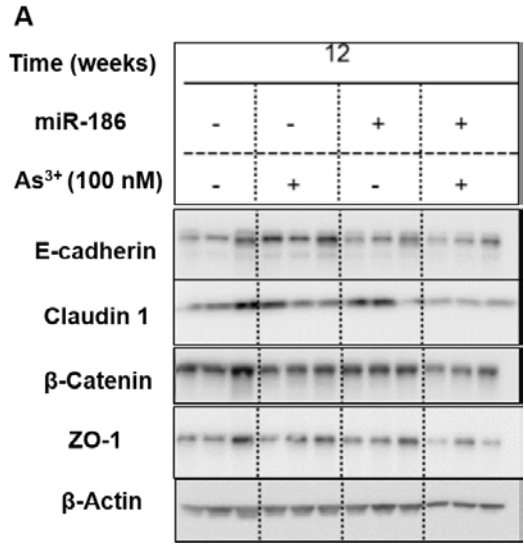


Figure 9 : Western blots for epithelial markers at 12 weeks. A. Western blots for e-cadherin, claudin 1, β -catenin, ZO-1, and β -actin in HaCaT transfected with either vector control or vector overexpressing miR-186 and exposed to 0 or 100 nM sodium arsenite for 12 weeks, B. Quantification of e-cadherin relative to β -actin by densitometric analysis, C. Quantification of claudin 1 relative to β -actin by densitometric analysis, D. Quantification of β -catenin relative to β -actin by densitometric analysis, E. Quantification of ZO-1 relative to β -actin by densitometric analysis. Data are represented as the % of the mean unexposed control expression. Western blot and quantification show no significant changes in expression of e-cadherin, claudin 1, β -catenin, and ZO-1, in vector control and miR-186 overexpressing HaCaT, at 12 weeks. No difference was observed when grouping all the miR-186 overexpressing cells versus the vector control cells. Data are expressed as mean \pm SD. Data were analyzed with two-way ANOVA and Tukey's multiple comparison post hoc test.

Then, we screened the expression levels of mesenchymal markers. Specifically, at 12 weeks, we observed no significant changes in expression of the mesenchymal marker n-cadherin, and slug in vector control and miR-186 overexpressing HaCaT cells, both in arsenite exposed (100 nM) and unexposed cells (

Figure 10).

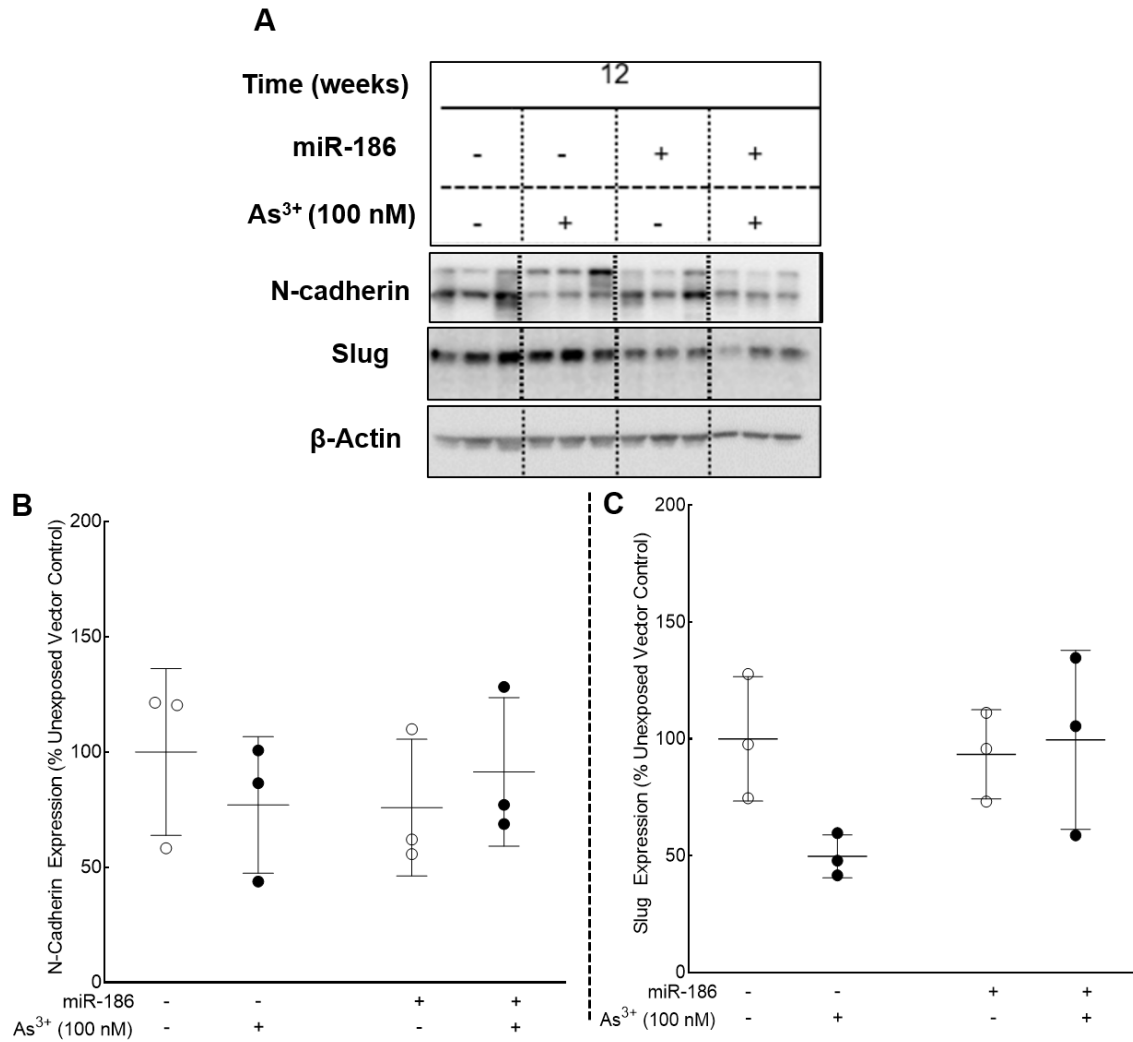


Figure 10 : Western blots for mesenchymal markers at 12 weeks. A. Western blots for n-cadherin, slug, and β -actin in HaCaT transfected with either vector control or vector overexpressing miR-186 and exposed to 0 or 100 nM sodium arsenite for 12 weeks, B. Quantification of n-cadherin relative to β -actin by densitometric analysis, C. Quantification of slug relative to β -actin by densitometric analysis. Data are represented as the % of the mean unexposed control expression. Western blot and quantification show no significant changes in expression of n-cadherin and slug in vector control and

miR-186 overexpressing HaCaT, at 12 weeks. Data are expressed as mean \pm SD.

Data are analyzed with two-way ANOVA and Tukey's multiple comparison post hoc test.

After 29 weeks of culturing three clones of HaCaT cells transfected with vector control and three clones of HaCaT overexpressing miR-186 and 0 or 100 nM sodium arsenite exposure (see section 2.1.1), we observed that the expression of the epithelial marker e-cadherin is significantly decreased in miR-186 overexpressing and exposed to arsenite HaCaT cells ($p < 0.05$), compared to unexposed vector control HaCaT cells (Panel B, Figure 11). Also, the levels of e-cadherin are significantly decreased in miR-186 overexpressing and exposed to arsenite HaCaT cells ($p < 0.05$), compared to miR-186 overexpressing HaCaT cells which were not exposed to arsenite (Panel B, Figure 11). Also, at 29 weeks, we observed that the expression of the epithelial marker claudin 1 is decreased in all arsenite exposed (100 nM) cells (vector control transfected HaCaT and miR-186 overexpressing cells) (Panel C, Figure 11). Specifically, the protein levels of claudin-1 are significantly decreased ($p < 0.05$) in miR-186 overexpressing HaCaT cells and exposed to arsenite (100 nM) compared to unexposed vector control HaCaT cells (Panel C, Figure 11). Additionally, at 29 weeks, we observed that the expression of the epithelial marker β -catenin is significantly decreased in vector control and exposed to arsenite (100 nM) HaCaT cells ($p < 0.05$), compared to unexposed vector control HaCaT cells (Panel D, Figure 11). Also, the protein levels of β -catenin are more significantly decreased in miR-186 overexpressing HaCaT cells and exposed to arsenite (100 nM) ($p < 0.01$), compared to unexposed vector control (Panel D, Figure 11). At 29 weeks, we also observed no significant changes in the expression of the epithelial marker ZO-1 in vector control HaCaT cells and miR-186 overexpressing HaCaT cells, both in exposed (100 nM) and unexposed cells (Panel E, Figure 11).

A

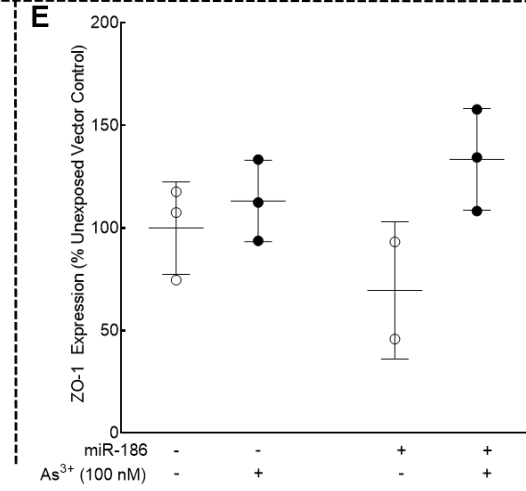
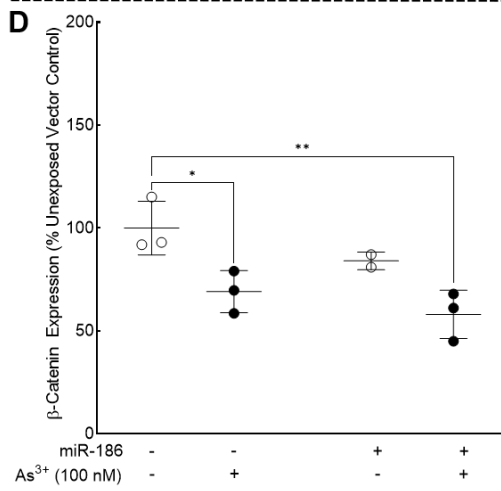
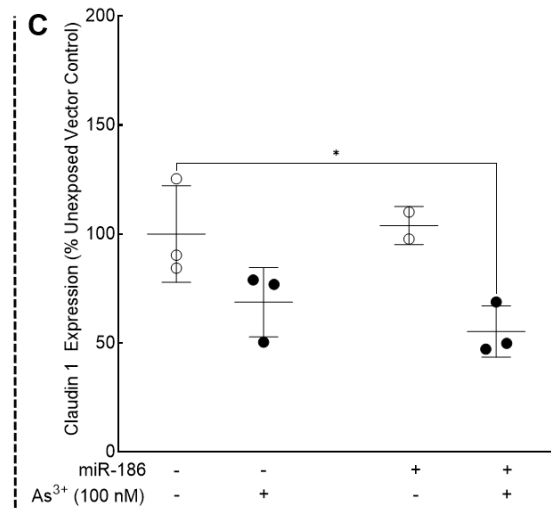
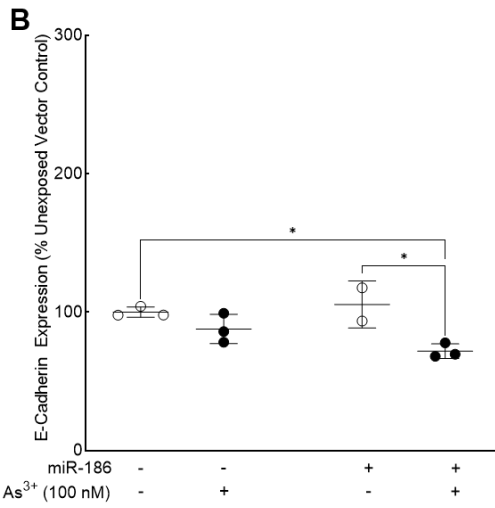
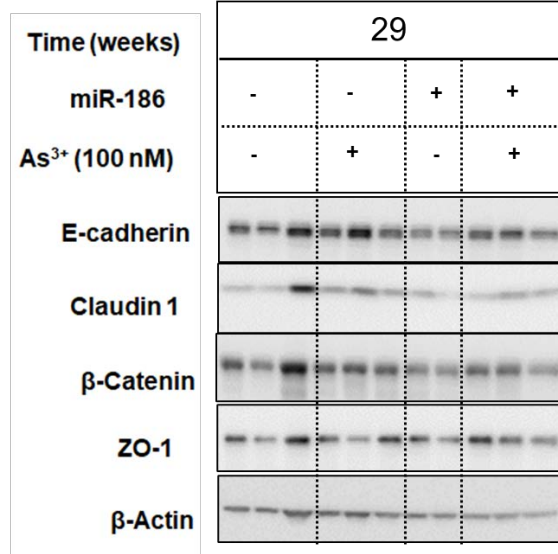


Figure 11 : Western blots for epithelial markers at 29 weeks. Western blots for e-cadherin, claudin 1, β -catenin, ZO-1, and β -actin in HaCaT transfected with either vector control or vector overexpressing miR-186 and exposed to 0 or 100 nM sodium arsenite for 29 weeks, B. Quantification of e-cadherin relative to β -actin by densitometric analysis. Western blot and quantification show that the expression of e-cadherin is significantly ($p < 0.05$) decreased in miR-186 overexpressing HaCaT exposed to arsenite compared to unexposed vector control and compared to miR-186 overexpressing HaCaT unexposed to arsenite, at 29 weeks, C. Quantification of claudin 1 relative to β -actin by densitometric analysis. Western blot and quantification show that the expression of claudin 1 is significantly ($p < 0.05$) decreased in miR-186 overexpressing HaCaT exposed to arsenite compared to unexposed vector control, at 29 weeks, D. Quantification of β -catenin relative to β -actin by densitometric analysis. Western blot and quantification show that the expression of β -catenin is significantly ($p < 0.05$) decreased in vector control exposed to arsenite HaCaT cells compared to unexposed vector control and it is more significantly ($p < 0.01$) decreased in miR-186 overexpressing HaCaT exposed to arsenite compared to unexposed vector control, at 29 weeks, E. Quantification of ZO-1 relative to β -actin by densitometric analysis. Western blot and quantification show no significant changes in expression of ZO-1 in vector control and miR-186 overexpressing HaCaT, at 29 weeks. Data are represented as the % of the mean unexposed control expression Data are expressed as mean \pm SD. Data are analyzed with two-way ANOVA and Tukey's multiple comparison post hoc test. The level of significance is established at p value ≤ 0.05 , * $p < 0.05$. At 29 weeks, the miR-186 transfected HaCaT cells and unexposed to arsenite include protein expression data only from two clones (S1-1, S3-1, see section 2.1.1), because the S1-3 clone did not produce enough cells for protein lysate collection.

Then, we screened the expression levels of mesenchymal markers. Specifically, at 29 weeks, we observed that the expression of the mesenchymal protein n-cadherin is significantly increased in miR-186 overexpressing HaCaT cells and exposed to arsenite (100 nM) ($p < 0.05$), compared to unexposed vector control HaCaT cells (Panel B, Figure 12). Finally, we observed at 29 weeks, that the expression levels of the mesenchymal marker slug are significantly increased in miR-186 overexpressing HaCaT cells and exposed to arsenite (100 nM) ($p < 0.05$), compared to unexposed vector control HaCaT cells (Panel C, Figure 12). Also, the protein levels of slug were more significantly decreased in miR-186 overexpressing HaCaT cells and exposed to arsenite (100 nM) ($p < 0.01$), compared to vector control HaCaT cells and exposed to arsenite (100 nM) (Panel C, Figure 12). Similarly, the levels of slug were significantly decreased in miR-186 overexpressing HaCaT cells and exposed to arsenite (100 nM) ($p < 0.05$), compared to miR-186 overexpressing HaCaT unexposed to arsenite (Panel C, Figure 12).

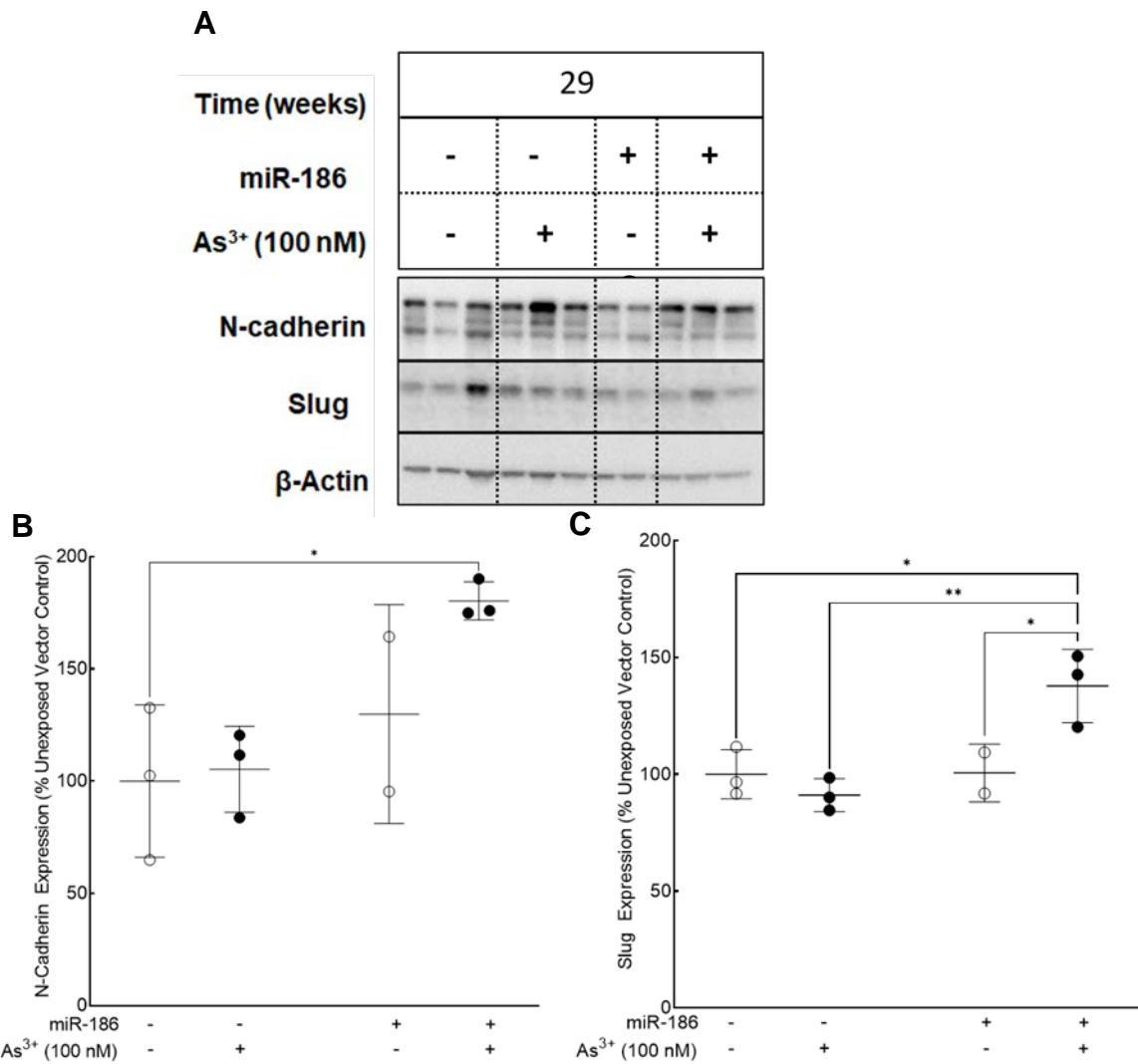


Figure 12 : Western blots for mesenchymal markers at 29 weeks. Western blots for n-cadherin, slug, and β -actin in HaCaT transfected with either vector control or vector overexpressing miR-186 and exposed to 0 or 100 nM sodium arsenite for 29 weeks, B. Quantification of n-cadherin relative to β -actin by densitometric analysis. Western blot and quantification show that the expression of n-cadherin is significantly ($p < 0.05$) increased in miR-186 overexpressing HaCaT exposed to arsenite compared to unexposed vector control, at 29 weeks, C. Quantification of slug relative to β -actin by densitometric analysis. Western blot and quantification show that the expression of slug is significantly ($p < 0.05$) increased in miR-186 overexpressing HaCaT exposed to arsenite compared to unexposed vector control, compared to vector control HaCaT

exposed to arsenite ($p < 0.01$) and compared to miR-186 overexpressing HaCAT unexposed to arsenite ($p < 0.05$), at 29 weeks. Data are represented as the % of the mean unexposed control expression. Data are expressed as mean \pm SD. Data are analyzed with two-way ANOVA and Tukey's multiple comparison post hoc test. The level of significance is established at p value ≤ 0.05 , * $p < 0.05$, ** $p < 0.01$. At 29 weeks, the miR-186 transfected HaCaT cells and unexposed to arsenite include protein expression data only from two clones (S1-1, S3-1, see section 2.1.1), because the S1-3 clone did not produce enough cells for protein lysate collection.

Overall, we observed that all epithelial markers (e-cadherin, β -catenin, claudin 1) examined, apart from ZO-1, were suppressed at 29 weeks in HaCaT overexpressing miR-186 and exposed to arsenite (100 nM) compared to unexposed vector control. Also, both mesenchymal markers (n-cadherin, slug) tested, were induced at 29 weeks in HaCaT overexpressing miR-186 and exposed to arsenite (100 nM) compared to unexposed vector control. We did not observe any changes in any sample at 12 weeks. These observations suggest that HaCaT transfected with miR-186 and exposed to arsenite for 29 weeks undergo EMT.

3.3 Flow cytometry for cell cycle analysis

The results from the soft agar colony formation assay (see section 3.1) showed that HaCaT overexpressing miR-186 and exposed to arsenite exhibited increased growth ability in agar at 12 weeks in contrast to vector control cells (exposed or not to arsenite) (Panel A, Figure 7). The soft agar assay also showed that colonies were formed in HaCaT transfected with vector control and exposed to arsenite clones as well as in HaCaT overexpressing miR-186 and exposed to arsenite clones at 29 weeks (Panel B, Figure 7). Additionally, the western blot analysis for epithelial and mesenchymal markers at 29 weeks, showed that HaCaT overexpressing miR-186 and exposed to arsenite had reduced levels of epithelial markers (see section 3.2) (Panels A, B, C, D, Figure 11) and increased levels of mesenchymal markers (see section 3.2) (Panels A, B, C, Figure 12). Thus, there is an indication that these cells acquire hallmarks of malignant transformation, and specifically the transformation process might be accelerated when the cells overexpress miR-186 and are exposed to sodium arsenite simultaneously.

Cell cycle dysregulation underlies the aberrant cell proliferation that characterizes cancer cells, and loss of cell cycle checkpoint control promotes chromosomal instability [331]. The focus of this thesis is to assess the role of arsenic exposure and miR-186

overexpression in chromosomal instability as a driver force of skin carcinogenesis. Thus, we wanted to determine if there are any changes in the cell cycle patterns of our three clones of HaCaT cells transfected with vector control and three clones of HaCaT overexpressing miR-186 (see section 2.1.1), either exposed to 0 or to 100 nM sodium arsenite. For this purpose, we performed a flow cytometry analysis as described in section 2.5 of the methods, at 14 weeks (an intermediated time point during our chronic cell culture for 29 weeks). No changes in the cell cycle patterns were found, but we observed that all the six clones exposed to 0 or 100 nM sodium arsenite exhibited similar levels of aneuploidy (Figure 13).

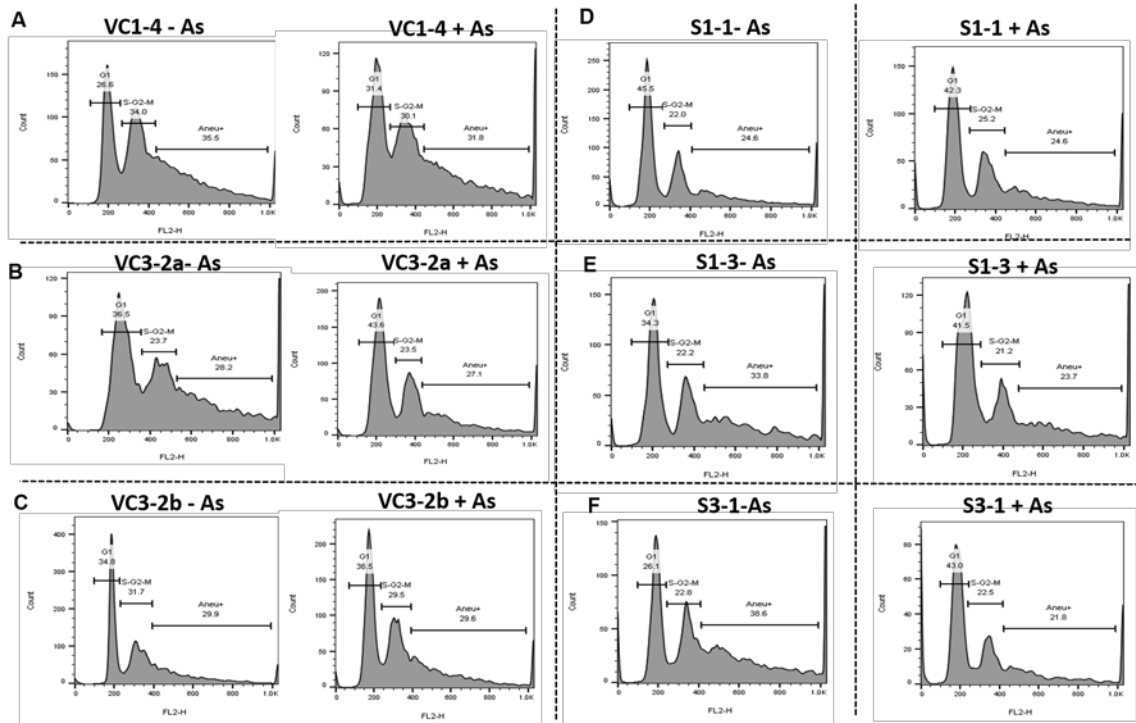


Figure 13 : Flow cytometry for cell cycle analysis. X-axis: DNA content from fluorescence emission (FL2-H channel) after propidium iodide staining, y-axis: count (intensity) A. vector clone (VC1-4) exposed to 0 nM (left) or 100 nM (right) sodium arsenite, B. vector control clone (VC3-2a) exposed to 0 nM (left) or 100 nM (right) sodium arsenite, C. vector control clone (VC3-2b) exposed to 0 nM (left) or 100 nM (right) sodium arsenite, D. miR-186 overexpressing clone (S1-1) exposed to 0 nM (left) or 100 nM (right) sodium arsenite, E. miR-186 overexpressing clone (S1-3) exposed to 0 nM (left) or 100 nM (right) sodium arsenite, F. miR-186 overexpressing clone (S3-1) exposed to 0 nM (left) or 100 nM (right) sodium arsenite. Approximately, 22%-35% cells in each clone, exposed to 0 or 100 nM of sodium arsenite for 14 weeks, exhibited aneuploidy, as indicated in the aneuploid S-phase of the histograms. No statistical difference was observed between any of the clones.

Specifically, 22%-35% cells in each clone, exhibited aneuploidy, as indicated by the percentage of cells with aneuploid DNA content, observed in the aneuploid phase of the histograms (Figure 13).

These data suggest that HaCaT transfected with vector control or overexpressing miR-186 and exposed to 0 or 100 nM sodium arsenite have increased levels of chromosomal instability, that could contribute to their transformation process. Thus, we wanted to further determine the specific types of chromosomal instability that occur and to investigate how arsenic exposure, miR-186 or the combination of both treatments leads to chromosomal instability during carcinogenesis.

3.4 Protein levels of cell cycle proteins

Bioinformatic analysis using the DIANA miRPath V3.0, has shown that miR-186 is predicted to target mRNAs of proteins that regulate the cell cycle and are components of the spindle assembly checkpoint (SAC) and anaphase promoting complex (APC), including: budding uninhibited by benzimidazoles 1 (BUB1), and cell division cycle 27, (CDC27) [194] (see section 1.15). According to the bioinformatic prediction, miR-186 targets and suppresses BUB1 and CDC27, which play a role in the establishment of the mitotic spindle checkpoint and proper chromosome segregation. Also, ectopic expression of miR-186 in HaCaT cells induces significant increase in numerical and structural chromosomal abnormalities and these aberrations are further increased with chronic arsenite exposure at 8 weeks of culture [5].

The focus of this thesis is to assess the role of arsenic exposure and miR-186 in chromosomal instability and skin carcinogenesis. As described in sections 3.1 and 3.2, there is indication that HaCaT overexpressing miR-186 and exposed to arsenite for 29 weeks acquire hallmarks of malignant transformation. Also, we observed that all vector control and miR-186 overexpressing clones exhibited aneuploidy based on the results of PI flow cytometry analysis (see section 3.3). Thus, we wanted to validate if the levels of cell cycle proteins, which are crucial for proper chromosome segregation, are dysregulated, because of miR-186 overexpression and arsenite exposure. Thus, we tested the protein levels of two predicted targets of miR-186: BUB1 and CDC27, after 12 and 29 weeks of arsenite exposure. Also, we determined the protein levels of a downstream target of BUB1, the BUB1-related protein 1 (BUBR1), which is also a crucial component of the spindle assembly checkpoint (see section 1.16).

At 12 weeks, we did not observe any significant difference in BUB1, CDC27, or BUBR1 levels, in vector control and miR-186 overexpressing HaCaT clones (Figure 14). BUB1 protein levels were modestly increased in the arsenite exposed clones (100 nM),

when compared with the unexposed clones, ($p_{\text{arsenite}} = 0.043 < 0.05$) (Panels A, B, Figure 14).

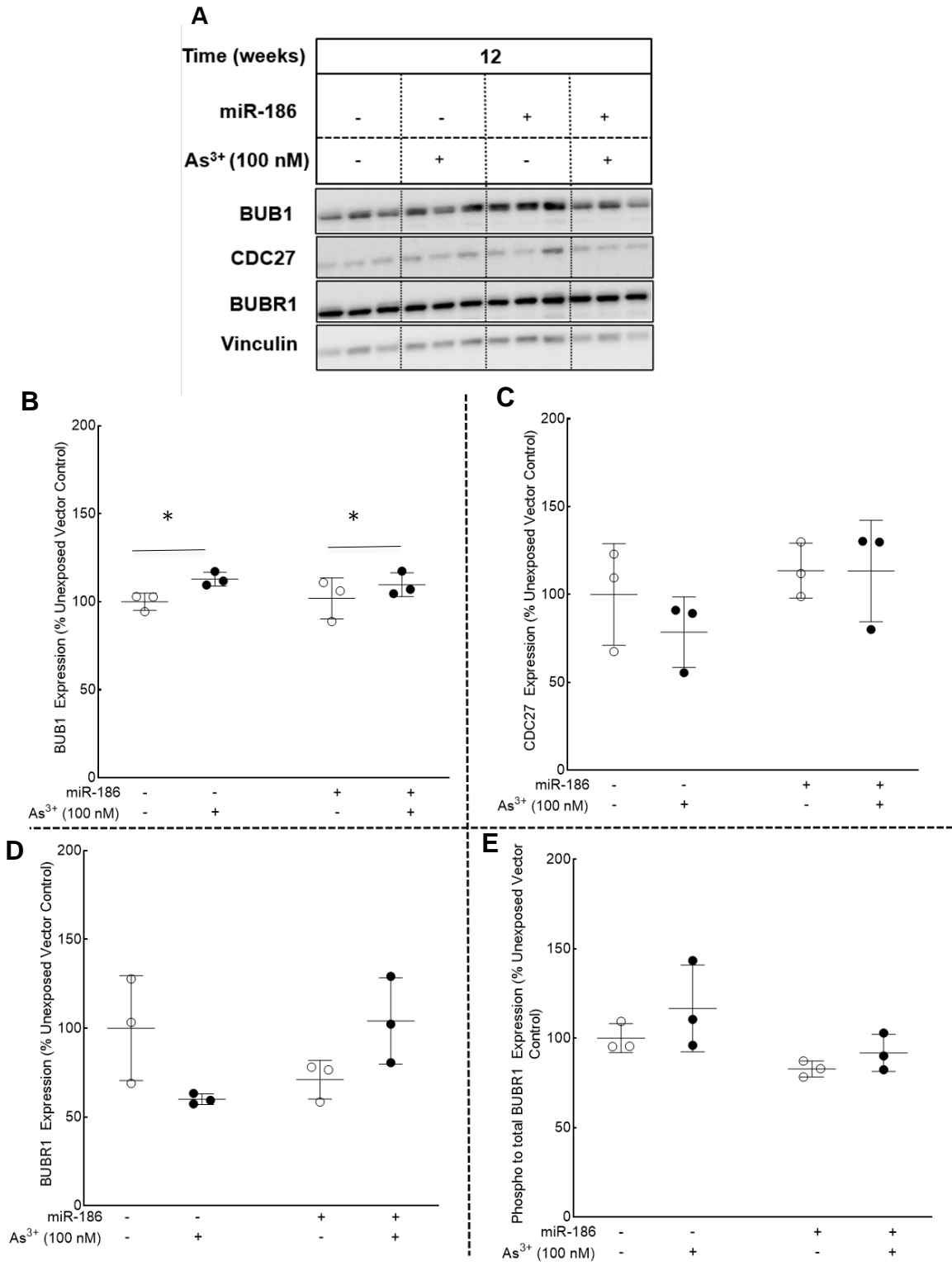


Figure 14 :Western blots for cell cycle proteins at 12 weeks. Western blots for BUB1, CDC27, BUBR1, and vinculin in HaCaT transfected with either vector control or vector overexpressing miR-186 and exposed to 0 or 100 nM sodium arsenite for 12 weeks, B. Quantification of BUB1 relative to vinculin by densitometric analysis. Western blot and quantification show that the levels of BUB1 are slightly increased in all arsenite exposed cells (100 nM), ($p_{\text{arsenite}} = 0.043 < 0.05$), at 12 weeks, C. Quantification of CDC27 relative to vinculin by densitometric analysis. Western blot and quantification show no significant changes in expression of CDC27 in vector control and miR-186 overexpressing HaCaT, at 12 weeks, D. Quantification of BUBR1 relative to vinculin by densitometric analysis. Western blot and quantification show no significant changes in expression of BUBR1 in vector control and miR-186 overexpressing HaCaT, at 12 weeks. E. Quantification of the ratio of phosphorylated BUBR1 to total BUR1, relative to vinculin by densitometric analysis. Western blot and quantification show no significant changes in the levels of phosphorylated BUBR1 in vector control and miR-186 overexpressing HaCaT, at 12 weeks. Data are represented as the % of the mean unexposed control expression Data are expressed as mean +/- SD. Data are analyzed with two-way ANOVA and Tukey's multiple comparison post hoc test. The level of significance is established at $p \text{ value} \leq 0.05$.

Also, CDC27 protein levels did not change significantly in all vector control and miR-186 overexpressing HaCaT clones, at 12 weeks (Panels A, C, Figure 14). Similarly, the levels of BUBR1 were slightly reduced in vector control and exposed (100 nM) cells, as well as in miR-186 overexpressing and unexposed cells, but this difference was not statistically significant (Panels A, D, Figure 14). Additionally, the levels of the phosphorylated BUBR1 were slightly reduced in miR-186 overexpressing cells exposed to 0 or 100 nM sodium arsenite, however no significant changes were observed at 12 weeks (Panels A, E, Figure 14).

At 29 weeks, we did not observe any significant difference in BUB1 levels, in vector control and miR-186 overexpressing HaCaT clones (Figure 14). Overall, BUB1 protein levels were stable in all clones (Panels A, B, Figure 15). CDC27 protein levels were increased in all arsenite exposed cells (100 nM), when compared with the unexposed clones, ($p_{\text{arsenite}} = 0.01 < 0.05$), at 29 weeks (Panels, A, C, Figure 15). Although the levels of BUBR1 in HaCaT overexpressing miR-186 and exposed to arsenite appeared slightly increased, the difference was not statistically significant, when compared to unexposed vector control cells, at 29 weeks (Panels, A, D, Figure 15). Also, the phosphorylated levels of BUBR1 did not significantly change, but we observed a slight decrease in the vector control and exposed to arsenite (100 nM) cells compared to unexposed cells (Panels, A, E, Figure 15).

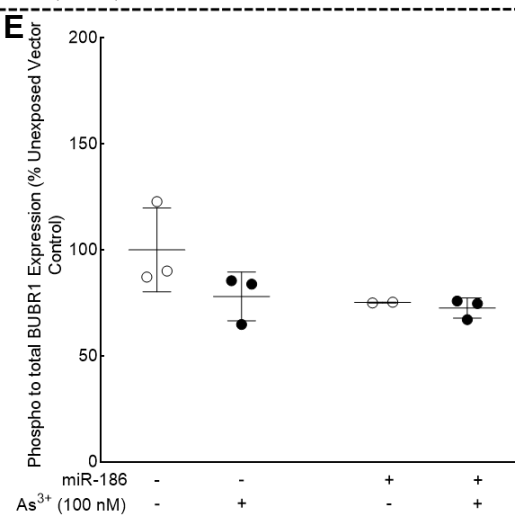
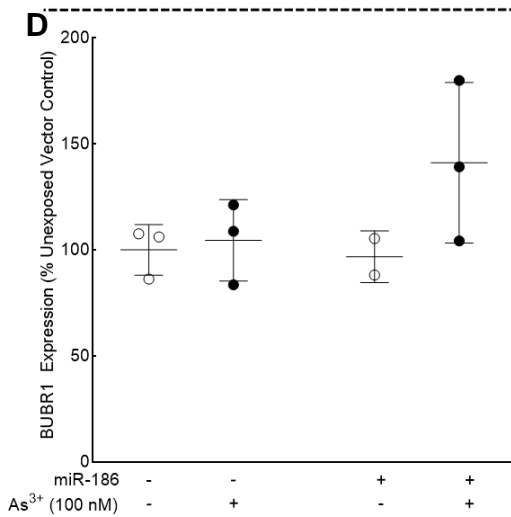
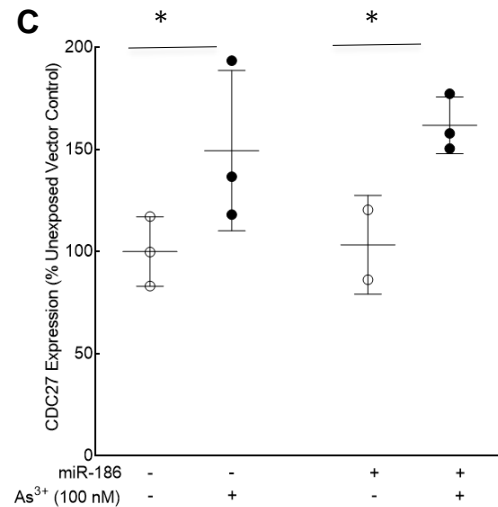
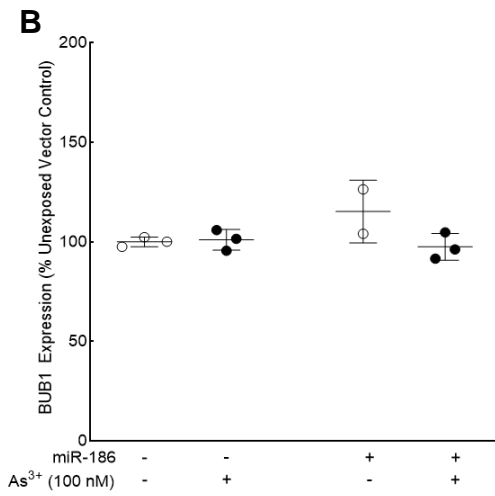
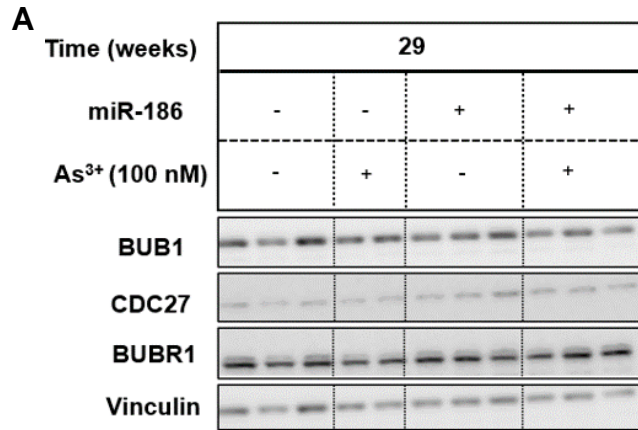


Figure 15 : Western blots for cell cycle proteins at 29 weeks. Western blots for BUB1, CDC27, BUBR1, and vinculin in HaCaT transfected with either vector control or vector overexpressing miR-186 and exposed to 0 or 100 nM sodium arsenite for 29 weeks, B. Quantification of BUB1 relative to vinculin by densitometric analysis. Western blot and quantification show no significant changes in expression of BUB1 in vector control and miR-186 overexpressing HaCaT, at 29 weeks, C. Quantification of CDC27 relative to vinculin by densitometric analysis. Western blot and quantification show that the levels of CDC27 are slightly increased in all arsenite exposed cells (100 nM), ($p_{\text{arsenite}} = 0.01 < 0.05$), at 29 weeks, D. Quantification of BUBR1 relative to vinculin by densitometric analysis. Western blot and quantification show no significant changes in expression of BUBR1 in vector control and miR-186 overexpressing HaCaT, at 29 weeks. E. Quantification of the ratio of phosphorylated BUBR1 to total BUR1, relative to vinculin by densitometric analysis. Western blot and quantification show no significant changes in the levels of phosphorylated BUBR1 in vector control and miR-186 overexpressing HaCaT, at 29 weeks. Data are represented as the % of the mean control expression. Data are expressed as mean \pm SD. Data are analyzed with two-way ANOVA and Tukey's multiple comparison post hoc test. The level of significance is established at p value ≤ 0.05 . At 29 weeks, the miR-186 transfected HaCaT cells and unexposed to arsenite include protein expression data only from two clones (S1-1, S3-1, see section 2.1.1), because the S1-3 clone did not produce enough cells for protein lysate collection.

3.5 Cytogenetic analysis for numerical and structural chromosomal alterations

HaCaT overexpressing miR-186 and exposed to arsenite for 29 weeks acquire hallmarks of malignant transformation (see sections 3.1 and 3.2). We also observed by flow cytometry that all vector control and miR-186 overexpressing clones exhibited aneuploidy (see section 3.3). Also, chromosomal instability is a hallmark of carcinogenesis (see sections 1.19, 1.20) and the role of miR-186 in carcinogenesis via regulation of cell cycle has been reported (see section 1.14). As mentioned in section 1.1, arsenic is clastogenic and it causes CIN both *in vitro* and *in vivo* [3] but the molecular mechanism by which arsenic induces CIN-mediated carcinogenesis is yet to be delineated (see section 1.23). Thus, we wanted to screen for specific structural and numerical chromosomal abnormalities due to arsenic exposure, miR-186 overexpression or combination of both treatments, that could drive transformation process of HaCaT overexpressing miR-186 and exposed to arsenite (100 nM). For this purpose, we performed karyotypic analysis at 9 weeks of culture, as described in section 2.2.2 of methods. HaCaT cells already have endogenous levels of chromosomal aberrations (see section 1.18). HaCaT cells are hypotetraploid with a range of 72-88 chromosomes, and the presence of marker chromosomes M1: t(3q4q), M2: i[9q], and M4: [4p18q] (see section 1.18). We validated the authenticity of the cell line by observing the presence of marker chromosomes. Since HaCaT cells exhibit intrinsic levels of chromosomal instability, we compared our karyotypes with the human normal karyotype (46 chromosomes). We analyzed twenty metaphases for each of the three vector control HaCaT clones exposed to 0 or 100 nM sodium arsenite and each of the three miR-186 overexpressing HaCaT clones exposed to 0 or 100 nM sodium arsenite. Analysis of the structural abnormalities showed that, all clones exhibited structural chromosomal abnormalities, but statistically significant changes were not observed (Panel A,

Figure 16).

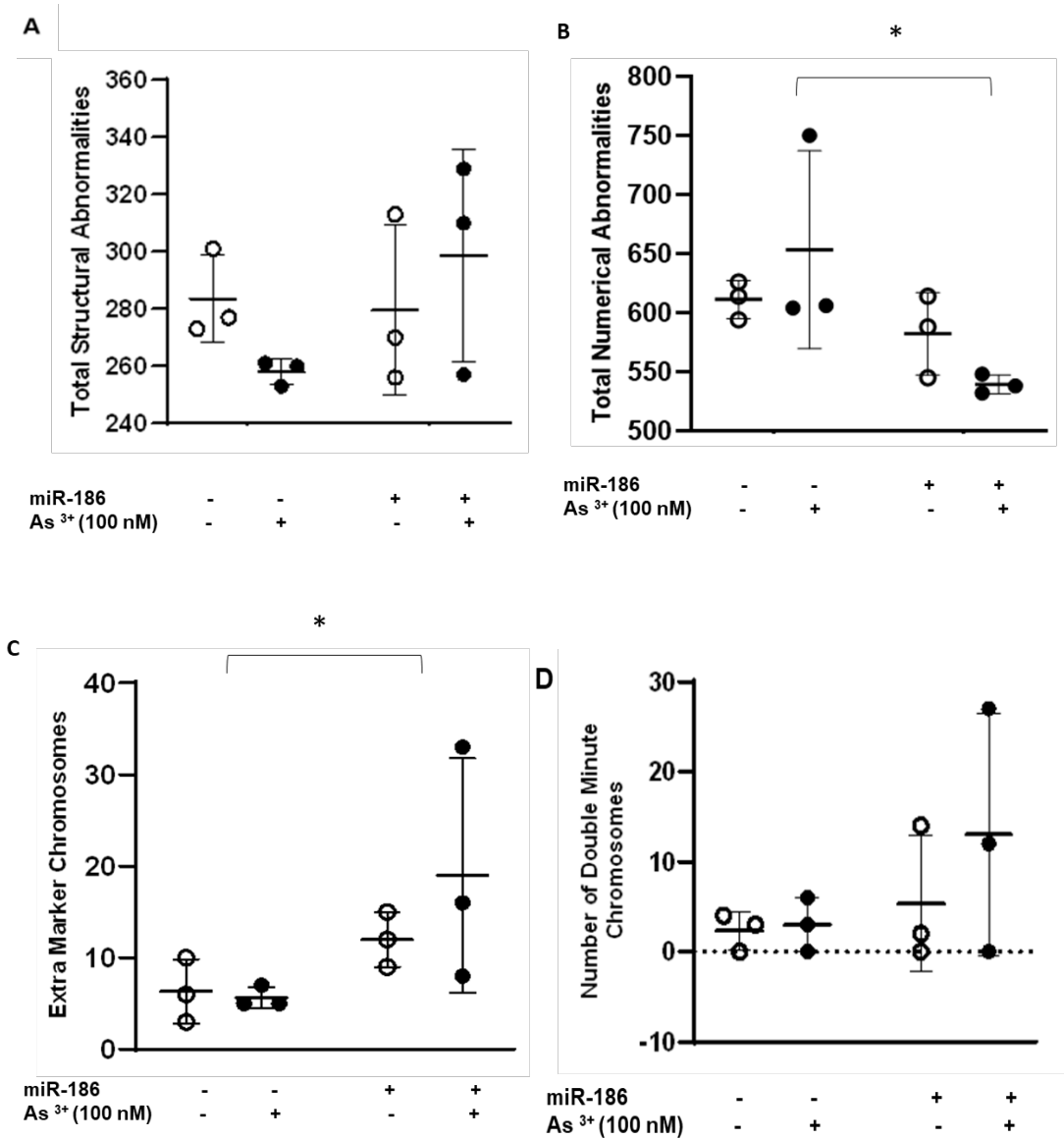


Figure 16 : Total structural and numerical chromosomal abnormalities. A. Total structural chromosomal abnormalities, no statistically significant changes were observed, B. Total numerical abnormalities were plotted and statistically significant changes were observed in cells overexpressing miR-186 and exposed or not sodium arsenite ($p=0.02$), C. Number of extra marker chromosomes, statistically significant changes were observed in

in cells overexpressing miR-186 and exposed or not sodium arsenite ($p=0.04$), D. Number of double minute chromosomes, no statistically significant changes were observed. Data are represented as the % of the mean control expression. Data are expressed as mean \pm SD. Data are analyzed with two-way ANOVA and Tukey's multiple comparison post hoc test. The level of significance is established at p value ≤ 0.05 .

The levels of chromosomal instability varied among clones of the same group (Panel A, Figure 16). Specifically, we observed that one clone from the miR-186 overexpressing cells (S1-3) exhibited higher number of total structural chromosomal abnormalities when compared to unexposed vector control cells (Panel A, Figure 16). Two clones (S1-1 and S1-3) from the miR-186 overexpressing cells and exposed to arsenite (100 nM) exhibited higher number of total structural chromosomal abnormalities when compared to unexposed vector control cells (Panel A, Figure 16). Furthermore, analysis of the numerical abnormalities showed that, all clones exhibited numerical chromosomal aberrations. Specifically, cells overexpressing miR-186 and exposed to arsenite exhibited statistically significant reduced number of numerical chromosomal abnormalities ($p=0.02$) (Panel B, Figure 16). Additionally, cells overexpressing miR-186 and exposed to arsenite exhibited statistically significant increase in the presence of extra marker chromosomes in all clones (Panel C, Figure 16). No statistically significant changes were observed in the presence of double minute chromosomes in all clones (Panel D, Figure 16). However, karyotypic analysis showed that one clone (S3-1) overexpressing miR-186 showed increased number of double minute chromosomes compared to unexposed vector control cells (Panel D, Figure 16). Also, two clones (S1-1 and S3-1) overexpressing miR-186 and exposed to arsenite (100 nM) showed increased number of double minute chromosomes compared to unexposed vector control cells (Panel D, Figure 16). Overall, HaCaT cells overexpressing miR-186 and exposed to arsenite (100 nM) showed a trend towards increased structural chromosomal abnormalities, including the presence of double minute chromosomes. A detailed analysis of karyotypes showed which structural abnormalities frequently occurred.

We observed that HaCaT overexpressing miR-186 and exposed to arsenite (100 nM) more frequently exhibited structural abnormalities (Figure 16). Karyotypic analysis of the structural abnormalities showed that, all clones exhibited structural chromosomal aberrations as depicted in the representative karyotypes for each clone (Figure 17), (Figure 18).

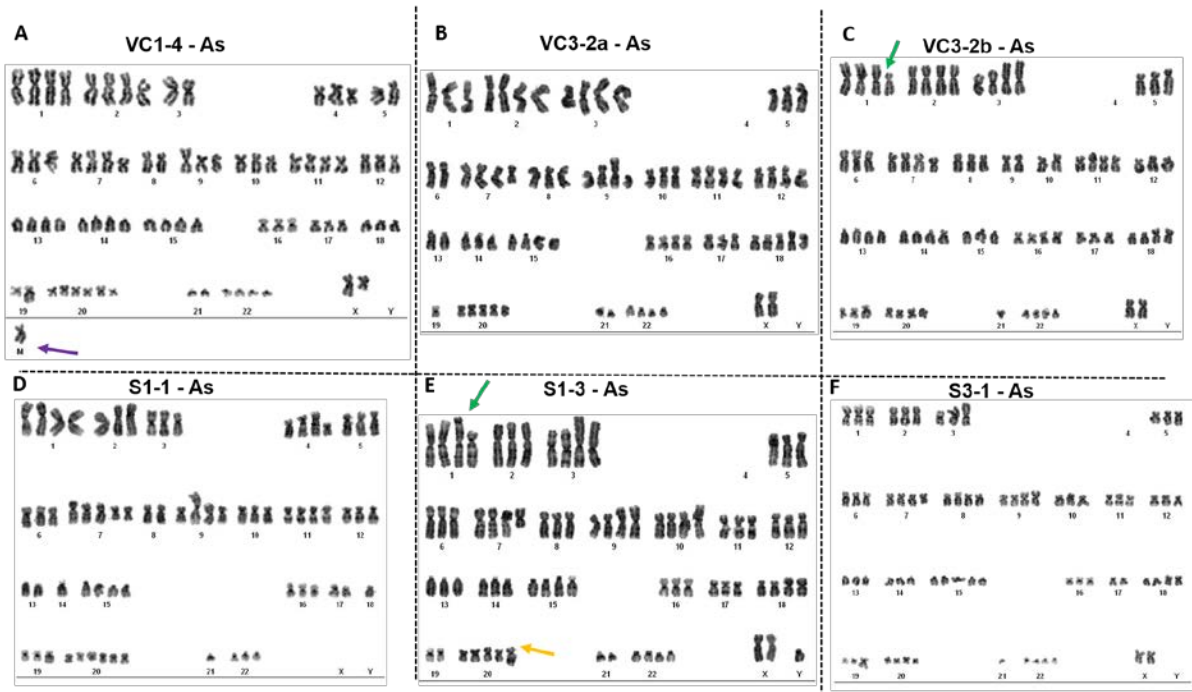


Figure 17: Representative karyotypes of unexposed cells at 9 weeks. A. Representative karyotype of vector control, VC1-4 clone, B. Representative karyotype of vector control, VC3-2a clone, C. Representative karyotype of vector control, VC3-2b clone, D. Representative karyotype of miR-186 overexpressing clone, S1-1 clone, E. Representative karyotype of miR-186 overexpressing clone, S1-3 clone, F. Representative karyotype of miR-186 overexpressing clone, S3-1 clone. Green arrow: shows structural chromosomal instability (deletion) in chromosome 1p, purple arrow: shows the presence of marker chromosomes, yellow (or orange) arrow: shows the structural chromosomal instability (gain of unidentified chromosomal material) in chromosome 20.

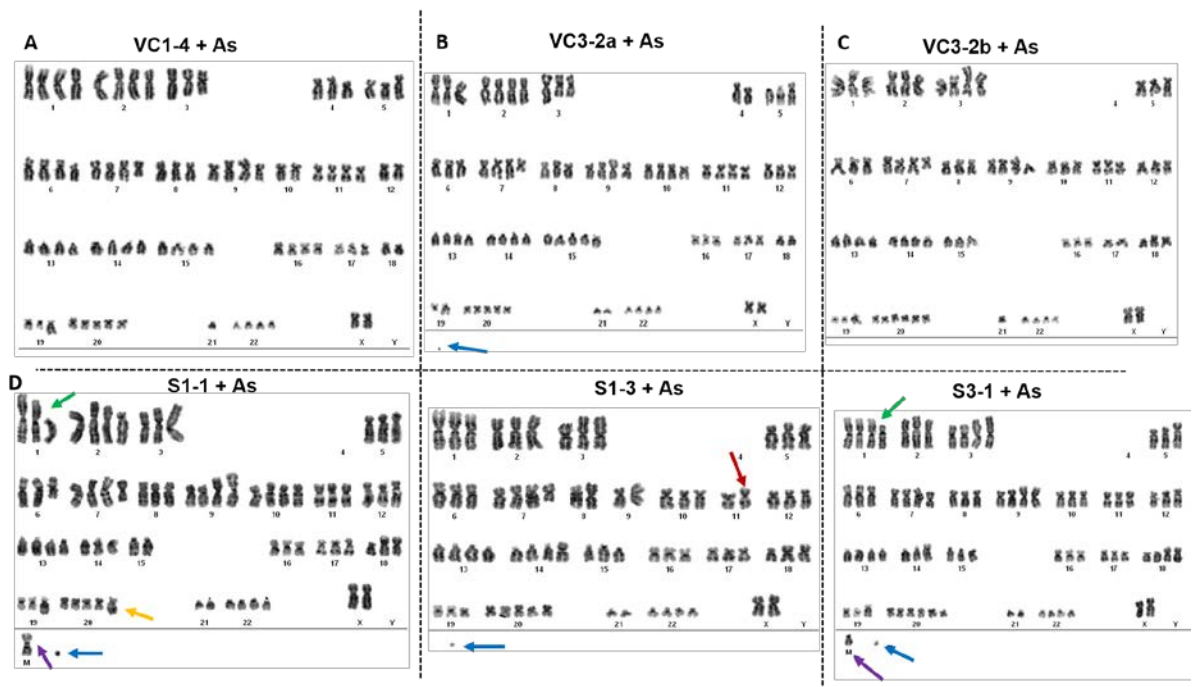


Figure 18: Representative karyotypes of arsenic exposed cells at 9 weeks. A. Representative karyotype of vector control, VC1-4 clone, B. Representative karyotype of vector control, VC3-2a clone, C. Representative karyotype of vector control, VC3-2b clone, D. Representative karyotype of miR-186 overexpressing clone, S1-1 clone, E. Representative karyotype of miR-186 overexpressing clone, S1-3 clone, F. Representative karyotype of miR-186 overexpressing clone, S3-1 clone. Green arrow: shows structural chromosomal instability (deletion) in chromosome 1, blue arrow: shows double minute chromosomes, red arrow: shows structural chromosomal instability (gain of unidentified chromosomal material) in chromosome 11, purple arrow: shows the presence of marker chromosomes, yellow (or orange) arrow: shows the structural chromosomal instability (gain of unidentified chromosomal material) in chromosome 20.

However, the miR-186 overexpressing clones and exposed to arsenite (100 nM) exhibited some structural chromosomal abnormalities more frequently compared to unexposed vector control cells. These abnormalities included deletion of chromosomal material in chromosome 1p, extra chromosomal material of unknown origin in chromosomes 11 and 20 and extra marker chromosomes (Figure 20) (Figure 21). These observations suggest that miR-186 overexpression causes chromosomal instability which is further exacerbated by arsenic exposure.

MiR-186 induces structural chromosomal instability

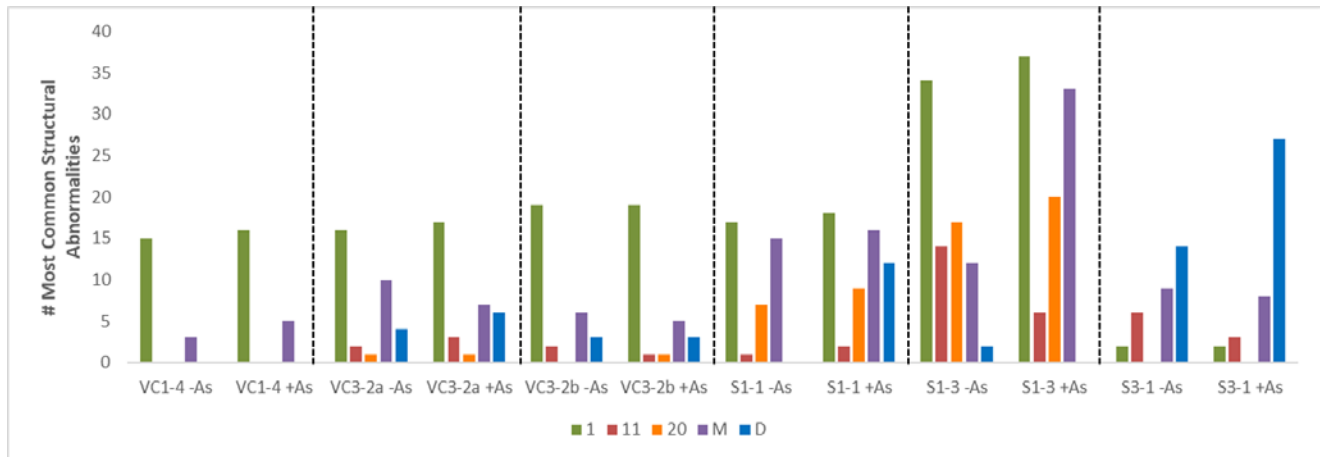


Figure 19: Most common structural chromosomal abnormalities in vector control and miR-186 overexpressing clones at 9 weeks. Number of the most common structural chromosomal abnormalities for the three vector control clones (VC1-4, VC3-2a, VC3-2b) exposed to 0 or 100 nM sodium arsenite (As) and for the three miR-186 overexpressing clones (S1-1, S1-3, S3-1) exposed to 0 or 100 nM sodium arsenite (As) (Figure 17, Figure 18). M indicates marker chromosomes. Green bar: shows structural chromosomal instability (deletion) in chromosome 1p, blue bar: shows double minute chromosomes, red arrow: shows structural chromosomal instability (gain of chromosomal material) in chromosome 11, purple bar: shows the presence of marker chromosomes, orange bar: shows the structural chromosomal instability (gain of chromosomal material) in chromosome 20.

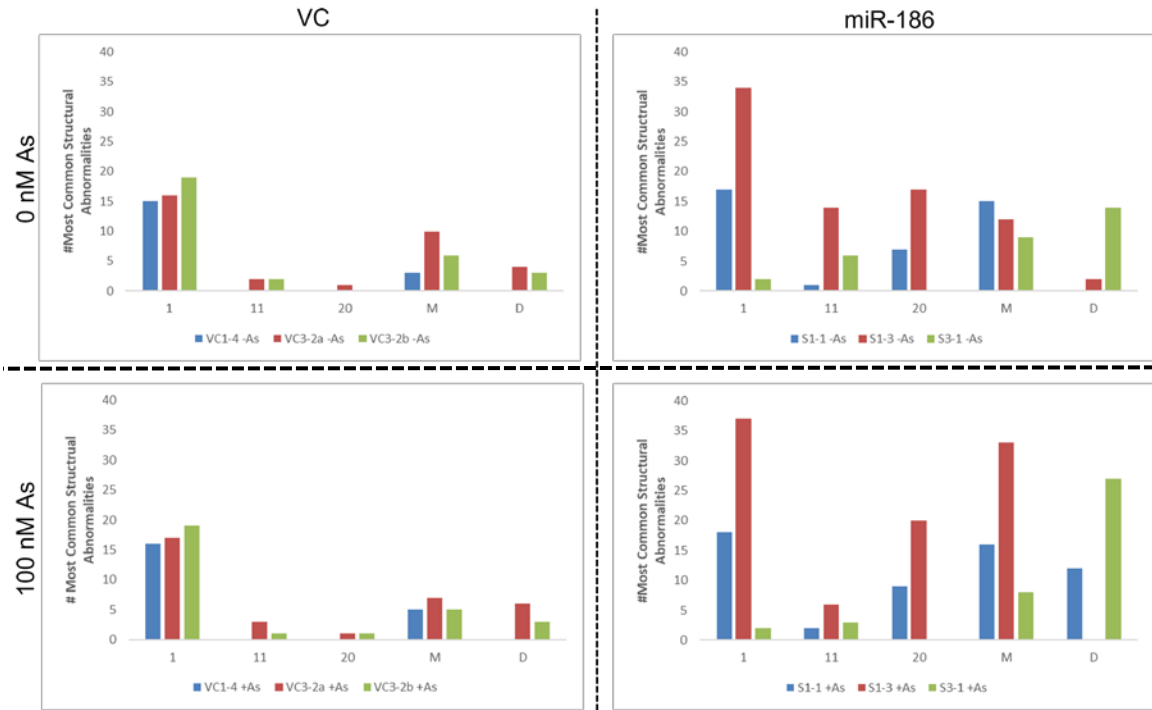


Figure 20: MiRNA-186 induces structural chromosomal instability and this effect is even more pronounced in arsenite (100 nM) exposed keratinocytes.

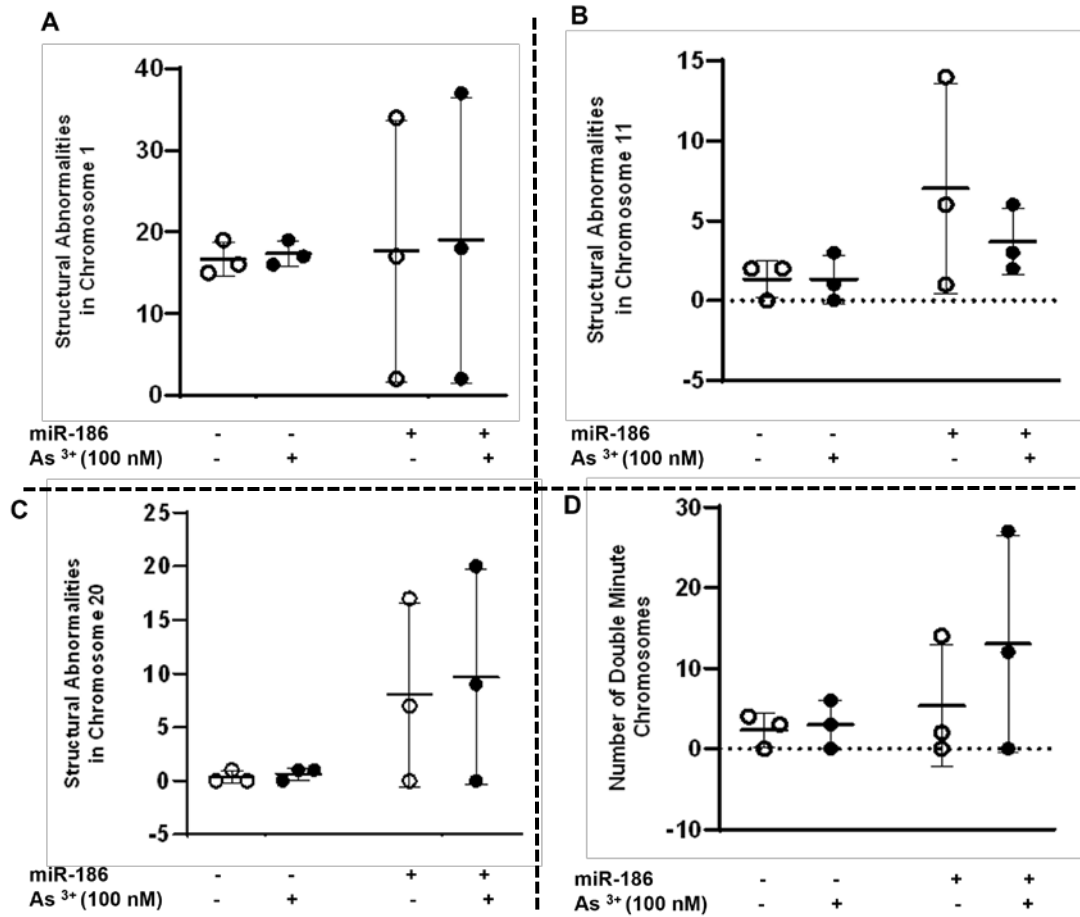


Figure 21: Clonal variability in miR-186 induced structural chromosomal instability

CHAPTER 4: DISCUSSION

Chronic arsenic exposure is a serious public health concern and arsenic poisoning is the cause of many fatal diseases [65]. Arsenic is a toxic metalloid and established carcinogen [2]. It is classified as a group I human carcinogen by the International Agency of Research on Cancer (IARC) since 1980 [89]. The latter means that there is sufficient evidence of carcinogenicity to humans [90]. Arsenic is also clastogenic and causes chromosomal instability (CIN) both *in vitro* and *in vivo* [3]. CIN is a hallmark of carcinogenesis, and is associated with poor prognosis, metastasis, and therapeutic resistance [4]. However, the molecular mechanism by which arsenic induces CIN-mediated carcinogenesis is yet to be elucidated [5].

Arsenic causes several cancers, such as lung, bladder, kidney, liver and non-melanoma skin cancer [2]. Specifically, chronic arsenic exposure is the second most common cause of skin cancer, following sunlight-induced skin cancer [98]. Despite evidence in humans, animal models fail to replicate these observations. The lack of an animal model has made it difficult to determine the exact mode(s) of action underlying arsenic-induced carcinogenicity [90]. However, human immortalized keratinocytes (HaCaT) malignantly transformed by chronic incubation in low concentration of sodium arsenite are a very well-established *in vitro* model to study arsenic-induced skin carcinogenesis [215] [161]. Specifically, continuous exposure of HaCaT cells to toxicologically relevant concentration [57] (100 nM) sodium arsenite for 28 weeks induced malignant transformation [215] [161]. HaCaT cells are a spontaneously immortalized human keratinocyte cell line with unlimited growth potential which

maintains full epidermal differentiation capacity [214]. They are hypotetraploid with a range of 72-88 chromosomes, and the presence of marker chromosomes (M1: t(3q4q), M2: i[9q], and M4:[4p18q] [214]. The presence of these marker chromosomes could be used to validate the authenticity of the cells and exclude cross-contamination with other human cell lines [214].

MiR-186 was found to be highly upregulated in some cases of squamous cell carcinoma induced by chronic arsenic exposure via drinking water, relative to non-malignant hyperkeratosis [109] [183]. MiR-186 plays a crucial role in various biological processes and may act as an oncogenic or tumor-suppressor miRNA. The likely role of miR-186 in carcinogenesis has been reported and dysregulated miR-186 levels can either promote or inhibit tumorigenesis [184] [150].

Upregulated miR-186 suppresses securin, which is one of its targets [185] [109]. Normally, securin binds to and inhibits a protease called separase, which, when released, following securin degradation, cleaves cohesins that hold the sister chromatids together, thus initiating anaphase [192]. Therefore, suppressed securin levels, because of overexpression of miR-186, would allow anaphase progression and contribute to aneuploidy by promoting premature chromatid separation [109]. Analysis using the bioinformatic tool DIANA miRPath V3.0 predicted that miR-186 also targets mRNAs of other proteins that regulate the cell cycle and are components of the spindle assembly checkpoint (SAC) and anaphase promoting complex (APC), including: budding uninhibited by benzimidazoles 1 (BUB1) and cell division cycle 27, (CDC27) [194]. According to the bioinformatic prediction, miR-186 targets and suppresses BUB1 and CDC27, which play a role in the establishment of the mitotic spindle checkpoint and proper chromosome segregation., Ectopic expression of miR-186 in HaCaT cells induces significant increase in numerical and structural chromosomal abnormalities and these aberrations are further increased with chronic arsenite exposure at 8 weeks of

culture [5]. Overall, the studies described above, suggest that upregulated levels of miR-186 cause chromosomal instability and exacerbate the arsenic-induced chromosomal instability associated with skin carcinogenesis.

The focus of this study was to assess the role of miR-186 overexpression in skin carcinogenesis and chromosomal instability in the presence or absence of chronic arsenite exposure. We hypothesized that miR-186 overexpression contributes to malignant transformation of HaCaT cells by induction of chromosomal instability and that chromosomal instability and transformation will be accelerated in HaCaT cells overexpressing miR-186 and exposed to arsenite compared to just arsenite exposed HaCaT cells. To test this hypothesis, we had two main goals. First, we wanted to compare timing of transformation of HaCaT cells overexpressing miR-186 and exposed to arsenite with cells exposed to arsenite without miR-186 overexpression. Second, we wanted to characterize the chromosomal instability in HaCaT overexpressing miR-186 with or without chronic arsenite exposure.

During tumorigenesis, EMT may increase the motility and invasiveness of cancer cells. Malignant transformation is associated with signaling pathways promoting EMT [330]. Specifically, during carcinogenesis cadherin switching may occur [330]. The latter refers to a switch from expression of e-cadherin (an epithelial marker) to expression of n-cadherin (a mesenchymal marker) [330]. One mechanism that most likely operates cadherin switching is transcriptional repression of e-cadherin by transcriptional repressor proteins (e.g. snail, slug) [330]. Also, b-catenin is a transcription factor in the Wnt signaling pathway and is involved in the regulation of cell adhesion [332]. B-catenin is typically more abundant in epithelial-like cells and it is reduced in mesenchymal-like cells, such as cancer cells [332]. Claudin 1 is membrane protein involved in the formation of tight junctions, mainly found in epithelial cells [330]. Claudin 1 regulates transepithelial transport and plays a critical role for cell growth and differentiation [330].

The protein levels of claudin 1 are frequently reduced in many cancers through transcriptional repression by snail or slug, during EMT [330]. Also, zona-occludens 1 (ZO-1) is a tight junction protein that is usually located at cell-cell adhesion membrane complexes in normal epithelial cells [333]. The cytoplasmic/nuclear delocalization of ZO-1 from the tight junctions is common process of EMT and associated with tumor invasion [332]. To elucidate the association of miR-186 overexpression with the progression to arsenic-induced skin cancer, we tested HaCaT that overexpress miR-186 and exposed to 0 or 100 nM sodium arsenite, for the protein expression levels of epithelial and mesenchymal markers.

At 12 weeks, we observed no significant changes in expression of the epithelial markers, e-cadherin, claudin 1, β -catenin, and ZO-1, and in expression of mesenchymal markers, n-cadherin, and slug, in vector control and miR-186 overexpressing HaCaT cells, exposed to 0 or 100 nM sodium arsenite (Figure 9). Thus, the cells did not undergo EMT after 12 weeks. After 29 weeks under selective arsenite pressure, we observed that the protein expression levels of the epithelial markers e-cadherin, claudin 1, β -catenin are significantly decreased in miR-186 overexpressing and exposed to arsenite HaCaT cells ($p < 0.05$), compared to unexposed vector control HaCaT cells (Figure 11). At 29 weeks, we also observed no significant changes in the expression of the epithelial marker ZO-1 in vector control HaCaT cells and miR-186 overexpressing HaCaT cells, both in exposed and unexposed cells (Panel E, Figure 11). Hence, ZO-1 might not play a role during the EMT process of arsenite exposed and miR-186 overexpressing cells, or reduction of ZO-1 protein levels might be a later event of transformation process. Then, we screened the expression levels of mesenchymal markers. We observed that the protein expression levels of the mesenchymal proteins n-cadherin and slug, are significantly increased in miR-186 overexpressing HaCaT cells and exposed to arsenite ($p < 0.05$), compared to unexposed vector control HaCaT cells (Figure 12). The

increased levels of slug could transcriptionally repress e-cadherin and claudin 1 and contribute to EMT. Specifically, the protein levels of slug were more decreased in miR-186 overexpressing HaCaT cells and exposed to arsenite ($p < 0.01$), compared to vector control HaCaT cells and exposed to arsenite (Panel C, Figure 12). Analysis using bioinformatic tools (miRbase, TargetScan) does not predict slug as a target of miR-186, thus, miR-186 might induce slug overexpression indirectly. Thus, these data indicate that the combination of arsenite exposure and miR-186 overexpression results cadherin switching and EMT at 29 weeks, which is linked to invasive and metastatic phenotype.

Neoplastic transformation occurs via a series of alterations that yield a cell population that is capable of proliferating independently of signals that restrain growth [328]. Anchorage-independent growth is one of the hallmarks of cell transformation, which is considered an accurate *in vitro* assay for detecting malignant transformation of cells and correlates with tumorigenic potential *in vivo* [328]. The soft agar colony formation assay is a common method to monitor anchorage-independent growth [328]. It measures proliferation in a semisolid culture media after 4-6 weeks by manual counting of colonies. HaCaT that overexpress miR-186 and exposed to 0 or 100 nM sodium arsenite were tested for anchorage-independent growth in agar. The assay was performed at an early time point (12 weeks) and at a late time point (29 weeks) to assess if miR-186 overexpression accelerates the arsenic transformation process. We observed that HaCaT overexpressing miR-186 and exposed to arsenite showed increased growth ability in agar at 12 weeks in contrast to vector control unexposed and exposed cells (Panel A, Figure 7). Specifically, single cells formed clusters of cells in all miR-186 transfected clones exposed to arsenite (S1-1, S1-3, S3-1) (Panel A, Figure 7). We also observed that all arsenite-exposed clones formed colonies in agar at 29 weeks (Panel B, Figure 7). Specifically, the miR-186 overexpressing cells and exposed to arsenite formed slightly bigger colonies compared with vector control and exposed to

arsenite clones (Panel B, Figure 7). These observations suggest that miR-186 overexpression accelerates the arsenite-induced transformation process, since clusters were formed only in this group of cells, at 12 weeks, and slightly bigger colonies were produced at 29 weeks, compared to vector control and exposed to arsenite cells. However, our data is not robust, since only one colony was formed per technical replicate per clone. Repetition of this assay is crucial. In the future, we propose to design an experiment in which we will optimize the culturing conditions. Specifically, we plan to seed different concentrations of cells in the upper layer of agar. In addition to modifying conditions and repeating this assay with 12 and 29 week cells, it will be important to assay cells from intermediate times, since we want to demonstrate if accelerated transformation occurs in miR-186 overexpressing cells and exposed to arsenite, compared with miR-186 overexpressing cells unexposed to arsenite. Specifically, we want to identify if there is a time when miR-186 overexpressing cells and exposed to arsenite form colonies but miR-186 overexpressing cells unexposed to arsenite do not. Alternatively, we could perform more *in vitro* assays to screen for the transformation potential of cells. Specifically, spheroid formation assay, cell migration (i.e wound healing) and cell invasion assay (i.e transwell assay) could produce more information about the malignant phenotype of arsenite exposed and miR-186 overexpressing HaCaT cells. If the results of these *in vitro* assays support our hypothesis, then we could inoculate these transformed cells into tumor prone athymic nude Balb/c mice (nu/nu) mice with subcutaneous injection into their flank, to evaluate tumorigenesis *in vivo*.

Cell cycle dysregulation underlies the aberrant cell proliferation that characterizes cancer cells, and loss of cell cycle checkpoint control promotes chromosomal instability [331]. Thus, we wanted to determine if there are any changes in the cell cycle patterns of HaCaT cells transfected with vector control and overexpressing miR-186 exposed to 0 or to 100 nM sodium arsenite. Thus, we performed a flow cytometry analysis at 14 weeks

(an intermediated time point during our chronic cell culture for 29 weeks). No changes in the cell cycle patterns were found, but we observed that all the six clones exposed to 0 or 100 nM sodium arsenite exhibited similar levels of aneuploidy (Figure 13).

Bioinformatic analysis using the DIANA miRPath V3.0, has shown that miR-186 is predicted to target mRNAs of proteins that regulate the cell cycle and are crucial for proper chromosome segregation, such as BUB1 and CDC27. Thus, we determined the levels of BUB1 and CDC27 at 12 and 29 weeks. Also, we determined the protein levels of a downstream target of BUB1, the BUB1-related protein 1 (BUBR1), which is also a crucial component of the spindle assembly checkpoint [196]. If BUB1 is targeted by miR-186, we expect decreased phosphorylation of BUBR1. BUB1 is key to proper chromosome segregation, binding to kinetochore and delaying mitosis in response to spindle disruption. [184]. Mutations of BUB1 have been reported in some aneuploid tumor cell lines and primary tumors [204]. Moreover, CDC27 levels are reported to be essential for preventing high levels of chromosomal instability [334], thus increased levels of CDC27 expression would be consistent with the increased chromosomal instability observed in miR-186 overexpressing clones. Also, upregulated levels of CDC27 have been shown to promote EMT, invasion and metastasis in melanoma, colorectal and renal cancers [335] [334]. Additionally, increased expression of BUBR1 has been associated with chromosomal instability and tumor invasion and metastasis in gastric and breast cancers, however the underlying mechanism remains unclear [336] [337].

At 12 weeks, we did not observe any significant difference at the levels of BUB1, CDC27, and BUBR1, in vector control and miR-186 overexpressing HaCaT clones (Figure 14). Thus, the bioinformatic prediction might not be accurate. In the future, a dual-luciferase reporter assay would unravel if miR-186 binds to the 3' untranslated region of the BUB1 and CDC27 mRNAs. BUB1 protein levels were increased in the

arsenite exposed clones, when compared with the unexposed clones (Panels A, B, Figure 14). BUB1 is known to be cell cycle-dependent and a target of the anaphase promoting complex/cyclosome as cyclin B and securin [338]. Also, arsenite exposure increases the proportion of cells in G2 or M phase while stabilizing cyclin B in a fibroblast model [339] and securin in a melanoma model [134]. Arsenite-induced cell cycle arrest at G2/M is not detected in our fourteen weeks flow cytometry data (Figure 13), probably because cells are acclimated to arsenite after long-term exposure. Hence, the arsenite induced BUB1 expression at 9 weeks, may be due to an increase in G2 or M phase via inhibition of the anaphase promoting complex/cyclosome [5]. At 29 weeks, BUB1 protein levels were stable in all clones (Panels A, B, Figure 15). It is possible that cells acclimated to arsenite exposure and overcame the arsenite-induced arrest at G2/M phase, in which BUB1 levels are increased [338]. CDC27 protein levels were increased in all arsenite exposed cells, when compared with the unexposed clones, at 29 weeks (Panels, A, C, Figure 15). The latter is consistent with the knowledge that upregulated levels of CDC27 have been shown to promote EMT, invasion and metastasis [335] [334], since the arsenite-exposed and miR-186-overexpressing cells undergo EMT and exhibit signs of anchorage independent growth at 29 weeks. No significant differences for the levels of BUBR1 were found, but we observed that HaCaT overexpressing miR-186 and exposed to arsenite had slightly increased levels of BUBR1, when compared to unexposed vector control cells, at 29 weeks (Panels, A, D, Figure 15). The latter is consistent with the literature that increased expression of BUBR1 has been associated with chromosomal instability and tumor invasion [336] [337]. This observation could be statistically significant if the cells are exposed to arsenite for more than 29 weeks. Also, the phosphorylated levels of BUBR1 did not significantly change, but we observed a slight decrease in the vector control and exposed to arsenite cells compared to unexposed cells (Panels, A, E, Figure 15). The latter could occur because arsenite

activates phosphatases or inhibits BUBR1 specific kinases. Overall, we observed increased levels of CDC27 and slightly increased levels of BUBR1 in arsenite and miR-186 overexpressing HaCaT cells, which could contribute to chromosomal instability and malignant transformation. Moreover, flow cytometry indicated that all vector control and miR-186 overexpressing clones exhibited aneuploidy (Figure 13). Thus, we wanted to screen for specific structural and numerical chromosomal abnormalities due to arsenic exposure, miR-186 overexpression or combination of both treatments that could drive transformation process of HaCaT overexpressing miR-186 and exposed to arsenite. Analysis of the structural abnormalities showed that, all clones exhibited structural chromosomal abnormalities at 9 weeks. Specifically, we calculated the total number of structural chromosomal abnormalities per clone and we observed that one clone from the miR-186 overexpressing cells (S1-3) unexposed to arsenite exhibited higher number of total structural chromosomal abnormalities when compared to unexposed vector control cells (Panel A, Figure 16). Also, two clones (S1-1 and S3-1) from the miR-186 overexpressing cells and exposed to arsenite group exhibited a higher number of total structural chromosomal abnormalities when compared to unexposed vector control cells (Panel A, Figure 16). Thus, we observe a trend towards increased structural chromosomal instability when there is miR-186 overexpression and concurrent arsenite exposure. We hypothesize that the clones with the higher levels of structural abnormalities might have higher levels of miR-186 expression. Hence, the validation of miR-186 levels with RT-qPCR is crucial for us to interpret these results since the levels of miR-186 might elucidate the correlation of miR-186 with increased structural chromosomal instability. Moreover, karyotypic analysis showed that one clone (S3-1) overexpressing miR-186 and unexposed to arsenite showed increased number of double minute chromosomes compared to unexposed vector control cells (Panel C,

Figure 16). Also, two clones (S1-1 and S3-1) overexpressing miR-186 and exposed to arsenite showed increased number of double minute chromosomes compared to unexposed vector control cells (Panel C, Figure 16). Thus, we observe that there is trend towards increased number of double minutes in arsenite exposed and miR-186 overexpressing cells. Double minute chromosomes lack regulatory elements, and they frequently harbor amplified oncogenes [243]. These data are derived from analysis of twenty metaphases per clone and are therefore preliminary. We intend to analyze fifty metaphases per clone in future studies. Increasing the number of metaphases analyzed, could produce statistically significant data by reducing the standard deviation within the technical replicates. Also fluorescent *in situ* hybridization (FISH) and RNAscope could further produce information about any oncogene amplification events that occur in double minutes of arsenite exposed and miR-186 overexpressing keratinocytes and contribute to their malignant phenotype. Additionally, a detailed karyotypic analysis showed which structural abnormalities frequently occurred. The miR-186 overexpressing clones and exposed to arsenite exhibited some structural chromosomal abnormalities more frequently compared to unexposed vector control cells (Figure) (Figure 20) (Figure 21). These abnormalities included deletion of chromosomal material in chromosome 1, extra chromosomal material of unknown origin in chromosomes 11 and 20 and extra marker chromosomes (Figure) (Figure 20) (Figure 21). Analysis of the genes located in those regions could elucidate gene dosage effects that could be implicated in transformation process as well as unravel pathways that lead to the acquisition of tumorigenic phenotype.

The gains of unidentified chromosomal material in chromosomes 11 and 20, as well as the deletion of chromosomal material in chromosome 1, could be potential sites of chromosomal translocations and gene fusion events (Figure 21). Gene fusions represent an important class of somatic alterations in cancers, and it is estimated that they drive the

development of approximately 17% of cancer cases [4]. We have started a gene fusion analysis from RNA sequencing data obtained from miR-186 overexpressing clones exposed to 0 or 100 nM sodium arsenite. If our ongoing analysis shows evidence of unique gene fusion events, we propose to design primers that will flank the fusion junction in the fused mRNA and perform genomic PCR to validate the presence of these fusions. Overall, our karyotypic observations suggest that miR-186 overexpression causes chromosomal instability which is further exacerbated by arsenic exposure.

The research summarized in this thesis showed that HaCaT cells overexpressing miR-186 and exposed to arsenite had increased chromosomal instability that has been associated with skin cancer progression, since these cells also showed evidence of transformation *in vitro*. We observed that the arsenite exposed and miR-186 overexpressing cells demonstrate hallmarks of EMT at 29 weeks and that concurrent miR-186 overexpression and arsenite exposure probably accelerates the transformation process since miR-186 overexpressing cells and exposed to arsenite exhibited signs of anchorage independent growth at 12 weeks, and formed slightly bigger colonies at 29 weeks compared to vector control and exposed to arsenite cells. Also, arsenite exposed and miR-186 overexpressing cells had increased levels of structural chromosomal aberrations and CDC27 and BUBR1 protein levels, which are known to promote chromosomal instability, invasion, and metastasis. Carcinogenesis is a multistage process, in which cancer cells evolve in response to multiple hits. Overexpression of miR-186 could be a second hit that exacerbates the effect of the first hit, which is the arsenite exposure. Not all cells within each clone are going to transform simultaneously since the transformation process is a stochastic event. The latter explains the karyotypic variability that we observed (Figure 21). Cells that will acquire beneficial phenotypic traits, such as sustained proliferative signaling or resistance to death, will clonally expand and outcompete less fit neighboring cells [340].

The novelty of this study is the emerging link of miRNA dysregulation and chromosomal instability, as a suggested mechanism of arsenic-induced carcinogenesis, which could serve miR-186 as a potential biomarker for the progression from premalignant hyperkeratosis to metastatic squamous cell carcinoma.

REFERENCES

1. Paranjape, T., F.J. Slack, and J.B. Weidhaas, *MicroRNAs: tools for cancer diagnostics*. Gut, 2009. **58**(11): p. 1546-54.
2. Martinez, V.D., et al., *Arsenic Exposure and the Induction of Human Cancers*. Journal of Toxicology, 2011. **2011**: p. 431287.
3. Council, N.R., *Arsenic in Drinking Water: 2001 Update*. 2001, Washington, DC: The National Academies Press. 241.
4. Sansregret, L., B. Vanhaesebroeck, and C. Swanton, *Determinants and clinical implications of chromosomal instability in cancer*. Nat Rev Clin Oncol, 2018. **15**(3): p. 139-150.
5. Wu, J., et al., *Overexpression of hsa-miR-186 induces chromosomal instability in arsenic-exposed human keratinocytes*. Toxicol Appl Pharmacol, 2019. **378**: p. 114614.
6. Simeonova, P.P., et al., *Arsenic exposure accelerates atherogenesis in apolipoprotein E(-/-) mice*. Environ Health Perspect, 2003. **111**(14): p. 1744-8.
7. States, J.C., et al., *Arsenic and Cardiovascular Disease*. Toxicological Sciences, 2009. **107**(2): p. 312-323.
8. Hanlon, D.P. and V.H. Ferm, *Concentration and chemical status of arsenic in the blood of pregnant hamsters during critical embryogenesis. 1. Subchronic exposure to arsenate utilizing constant rate administration*. Environ Res, 1986. **40**(2): p. 372-9.
9. Khandpur, S., et al., *Chronic arsenic toxicity from Ayurvedic medicines*. Int J Dermatol, 2008. **47**(6): p. 618-21.
10. Waxman, S. and K.C. Anderson, *History of the development of arsenic derivatives in cancer therapy*. Oncologist, 2001. **6 Suppl 2**: p. 3-10.
11. Haller, J.S., *Therapeutic mule: the use of arsenic in the nineteenth century materia medica*. Pharm Hist, 1975. **17**(3): p. 87-100.
12. Barrett, M.P., et al., *Human African trypanosomiasis: pharmacological re-engagement with a neglected disease*. Br J Pharmacol, 2007. **152**(8): p. 1155-71.
13. Cohen, N., et al., *PML RING suppresses oncogenic transformation by reducing the affinity of eIF4E for mRNA*. Embo j, 2001. **20**(16): p. 4547-59.
14. Wang, W., et al., *Experimental study on antitumor effect of arsenic trioxide in combination with cisplatin or doxorubicin on hepatocellular carcinoma*. World J Gastroenterol, 2001. **7**(5): p. 702-5.

15. Wang, G., et al., *The initiative role of XPC protein in cisplatin DNA damaging treatment-mediated cell cycle regulation*. Nucleic Acids Res, 2004. **32**(7): p. 2231-40.
16. Petruseva, I.O., A.N. Evdokimov, and O.I. Lavrik, *Molecular mechanism of global genome nucleotide excision repair*. Acta Naturae, 2014. **6**(1): p. 23-34.
17. Ford, J.M., *Regulation of DNA damage recognition and nucleotide excision repair: another role for p53*. Mutat Res, 2005. **577**(1-2): p. 195-202.
18. Muenyi, C.S., et al., *Sodium arsenite ± hyperthermia sensitizes p53-expressing human ovarian cancer cells to cisplatin by modulating platinum-DNA damage responses*. Toxicol Sci, 2012. **127**(1): p. 139-49.
19. Mondal, D., et al., *Comparison of drinking water, raw rice and cooking of rice as arsenic exposure routes in three contrasting areas of West Bengal, India*. Environ Geochem Health, 2010. **32**(6): p. 463-77.
20. Naujokas, M.F., et al., *The broad scope of health effects from chronic arsenic exposure: update on a worldwide public health problem*. Environ Health Perspect, 2013. **121**(3): p. 295-302.
21. Majumdar, K.K., et al., *Effect of Safe Water on Arsenicosis: A Follow-up Study*. J Family Med Prim Care, 2014. **3**(2): p. 124-8.
22. Sun, G., et al., *Current research problems of chronic arsenicosis in China*. J Health Popul Nutr, 2006. **24**(2): p. 176-81.
23. Mukherjee, A., et al., *Arsenic contamination in groundwater: a global perspective with emphasis on the Asian scenario*. J Health Popul Nutr, 2006. **24**(2): p. 142-63.
24. Zaldívar, R., L. Prunés, and G.L. Ghai, *Arsenic dose in patients with cutaneous carcinomata and hepatic hemangio-endothelioma after environmental and occupational exposure*. Arch Toxicol, 1981. **47**(2): p. 145-54.
25. Marshall, G., et al., *Fifty-year study of lung and bladder cancer mortality in Chile related to arsenic in drinking water*. J Natl Cancer Inst, 2007. **99**(12): p. 920-8.
26. Guo, H., et al., *Contrasting distributions of groundwater arsenic and uranium in the western Hetao basin, Inner Mongolia: Implication for origins and fate controls*. Sci Total Environ, 2016. **541**: p. 1172-1190.
27. Fu, S., et al., *Urinary arsenic metabolism in a Western Chinese population exposed to high-dose inorganic arsenic in drinking water: influence of ethnicity and genetic polymorphisms*. Toxicol Appl Pharmacol, 2014. **274**(1): p. 117-23.
28. Paul, S., et al., *Arsenic-induced toxicity and carcinogenicity: a two-wave cross-sectional study in arsenicosis individuals in West Bengal, India*. J Expo Sci Environ Epidemiol, 2013. **23**(2): p. 156-62.
29. Chowdhury, T.R., et al., *Arsenic poisoning in the Ganges delta*. Nature, 1999. **401**(6753): p. 545-6; discussion 546-7.
30. Tseng, C.H., et al., *Arsenic exposure, urinary arsenic speciation, and peripheral vascular disease in blackfoot disease-hyperendemic villages in Taiwan*. Toxicol Appl Pharmacol, 2005. **206**(3): p. 299-308.

31. Knobeloch, L.M., K.M. Zierold, and H.A. Anderson, *Association of arsenic-contaminated drinking-water with prevalence of skin cancer in Wisconsin's Fox River Valley*. J Health Popul Nutr, 2006. **24**(2): p. 206-13.
32. George, C.M., et al., *Reverse osmosis filter use and high arsenic levels in private well water*. Arch Environ Occup Health, 2006. **61**(4): p. 171-5.
33. Ayotte, J.D., et al., *Estimating the High-Arsenic Domestic-Well Population in the Conterminous United States*. Environ Sci Technol, 2017. **51**(21): p. 12443-12454.
34. States, J.C., et al., *Arsenic toxicology: translating between experimental models and human pathology*. Environ Health Perspect, 2011. **119**(10): p. 1356-63.
35. Pi, J., et al., *Decreased serum concentrations of nitric oxide metabolites among Chinese in an endemic area of chronic arsenic poisoning in inner Mongolia*. Free Radic Biol Med, 2000. **28**(7): p. 1137-42.
36. Challenger, F. and P.T. Charlton, *Studies on biological methylation; the fission of the mono- and di-sulphide links by moulds*. J Chem Soc, 1947. **169**: p. 424-9.
37. Marafante, E., M. Vahter, and J. Envall, *The role of the methylation in the detoxication of arsenate in the rabbit*. Chem Biol Interact, 1985. **56**(2-3): p. 225-38.
38. Dong, H., et al., *Identification of Small Molecule Inhibitors of Human As(III) S-Adenosylmethionine Methyltransferase (AS3MT)*. Chem Res Toxicol, 2015. **28**(12): p. 2419-25.
39. Kim, Y.J. and J.M. Kim, *Arsenic Toxicity in Male Reproduction and Development*. Dev Reprod, 2015. **19**(4): p. 167-80.
40. Wei, S., H. Zhang, and S. Tao, *A review of arsenic exposure and lung cancer*. Toxicol Res (Camb), 2019. **8**(3): p. 319-327.
41. Khairul, I., et al., *Metabolism, toxicity and anticancer activities of arsenic compounds*. Oncotarget, 2017. **8**(14): p. 23905-23926.
42. Hayakawa, T., et al., *A new metabolic pathway of arsenite: arsenic-glutathione complexes are substrates for human arsenic methyltransferase Cyt19*. Arch Toxicol, 2005. **79**(4): p. 183-91.
43. Petrick, J.S., et al., *Monomethylarsonous acid (MMA(III)) is more toxic than arsenite in Chang human hepatocytes*. Toxicol Appl Pharmacol, 2000. **163**(2): p. 203-7.
44. Styblo, M., et al., *Comparative toxicity of trivalent and pentavalent inorganic and methylated arsenicals in rat and human cells*. Arch Toxicol, 2000. **74**(6): p. 289-99.
45. Zhou, X., et al., *Differential binding of monomethylarsonous acid compared to arsenite and arsenic trioxide with zinc finger peptides and proteins*. Chem Res Toxicol, 2014. **27**(4): p. 690-8.
46. De Loma, J., et al., *Arsenite methyltransferase (AS3MT) polymorphisms and arsenic methylation in children in rural Bangladesh*. Toxicol Appl Pharmacol, 2018. **357**: p. 80-87.
47. Dopp, E., A.D. Kligerman, and R.A. Diaz-Bone, *Organoarsenicals. Uptake, metabolism, and toxicity*. Met Ions Life Sci, 2010. **7**: p. 231-65.

48. Aposhian, H.V., *Enzymatic methylation of arsenic species and other new approaches to arsenic toxicity*. *Annu Rev Pharmacol Toxicol*, 1997. **37**: p. 397-419.
49. Healy, S.M., et al., *Enzymatic methylation of arsenic compounds. V. Arsenite methyltransferase activity in tissues of mice*. *Toxicol Appl Pharmacol*, 1998. **148**(1): p. 65-70.
50. Cullen, W.R., *Chemical mechanism of arsenic biomethylation*. *Chem Res Toxicol*, 2014. **27**(4): p. 457-61.
51. Wu, R., et al., *Strain differences in arsenic-induced oxidative lesion via arsenic biomethylation between C57BL/6J and 129X1/SvJ mice*. *Sci Rep*, 2017. **7**: p. 44424.
52. Ratnaike, R.N., *Acute and chronic arsenic toxicity*. *Postgrad Med J*, 2003. **79**(933): p. 391-6.
53. Ghariani, M., et al., *[Subacute arsenic poisoning]*. *Ann Fr Anesth Reanim*, 1991. **10**(3): p. 304-7.
54. Campbell, J.P. and J.A. Alvarez, *Acute arsenic intoxication*. *Am Fam Physician*, 1989. **40**(6): p. 93-7.
55. Schoolmeester, W.L. and D.R. White, *Arsenic poisoning*. *South Med J*, 1980. **73**(2): p. 198-208.
56. Middleton, D.R.S., et al., *Urinary arsenic profiles reveal exposures to inorganic arsenic from private drinking water supplies in Cornwall, UK*. *Sci Rep*, 2016. **6**: p. 25656.
57. Chen, Y., et al., *Arsenic exposure from drinking water and mortality from cardiovascular disease in Bangladesh: prospective cohort study*. *Bmj*, 2011. **342**: p. d2431.
58. Hostýnek, J.J., et al., *Metals and the skin*. *Crit Rev Toxicol*, 1993. **23**(2): p. 171-235.
59. Curry, A.S. and C.A. Pounds, *Arsenic in hair*. *J Forensic Sci Soc*, 1977. **17**(1): p. 37-44.
60. Katz, S.A., *On the Use of Hair Analysis for Assessing Arsenic Intoxication*. *Int J Environ Res Public Health*, 2019. **16**(6).
61. Valentine, J.L., H.K. Kang, and G. Spivey, *Arsenic levels in human blood, urine, and hair in response to exposure via drinking water*. *Environ Res*, 1979. **20**(1): p. 24-32.
62. Takagi, Y., et al., *Survey of trace elements in human nails: an international comparison*. *Bull Environ Contam Toxicol*, 1988. **41**(5): p. 690-5.
63. Das, D., et al., *Arsenic in ground water in six districts of West bengal, India: the biggest arsenic calamity in the world. Part 2. Arsenic concentration in drinking water, hair, nails, urine, skin-scale and liver tissue (biopsy) of the affected people*. *Analyst*, 1995. **120**(3): p. 917-24.
64. Guha Mazumder, D.N., *Chronic arsenic toxicity & human health*. *Indian J Med Res*, 2008. **128**(4): p. 436-47.
65. Smith, A.H., E.O. Lingas, and M. Rahman, *Contamination of drinking-water by arsenic in Bangladesh: a public health emergency*. *Bull World Health Organ*, 2000. **78**(9): p. 1093-103.

66. Crinnion, W., *Arsenic: The Underrecognized Common Disease-inducing Toxin*. Integr Med (Encinitas), 2017. **16**(2): p. 8-13.
67. D'Ippoliti, D., et al., *Arsenic in Drinking Water and Mortality for Cancer and Chronic Diseases in Central Italy, 1990-2010*. PLoS One, 2015. **10**(9): p. e0138182.
68. Moon, K.A., et al., *Association between exposure to low to moderate arsenic levels and incident cardiovascular disease. A prospective cohort study*. Ann Intern Med, 2013. **159**(10): p. 649-59.
69. Srivastava, S., et al., *In utero arsenic exposure induces early onset of atherosclerosis in ApoE^{-/-} mice*. Reprod Toxicol, 2007. **23**(3): p. 449-56.
70. Srivastava, S., et al., *Arsenic exacerbates atherosclerotic lesion formation and inflammation in ApoE^{-/-} mice*. Toxicol Appl Pharmacol, 2009. **241**(1): p. 90-100.
71. Negro Silva, L.F., et al., *Effects of Inorganic Arsenic, Methylated Arsenicals, and Arsenobetaine on Atherosclerosis in the Mouse Model and the Role of As3mt-Mediated Methylation*. Environ Health Perspect, 2017. **125**(7): p. 077001.
72. Waalkes, M.P., J. Liu, and B.A. Diwan, *Transplacental arsenic carcinogenesis in mice*. Toxicol Appl Pharmacol, 2007. **222**(3): p. 271-80.
73. Smith, A.H., et al., *Mortality in young adults following in utero and childhood exposure to arsenic in drinking water*. Environ Health Perspect, 2012. **120**(11): p. 1527-31.
74. Smith, A.H., et al., *Increased mortality from lung cancer and bronchiectasis in young adults after exposure to arsenic in utero and in early childhood*. Environ Health Perspect, 2006. **114**(8): p. 1293-6.
75. Yuan, Y., et al., *Kidney cancer mortality: fifty-year latency patterns related to arsenic exposure*. Epidemiology, 2010. **21**(1): p. 103-8.
76. Yuan, Y., et al., *Acute myocardial infarction mortality in comparison with lung and bladder cancer mortality in arsenic-exposed region II of Chile from 1950 to 2000*. Am J Epidemiol, 2007. **166**(12): p. 1381-91.
77. Rosenberg, H.G., *Systemic arterial disease with myocardial infarction. Report on two infants*. Circulation, 1973. **47**(2): p. 270-5.
78. Spivey, A., *Arsenic and infectious disease: a potential factor in morbidity among Bangladeshi children*. Environ Health Perspect, 2011. **119**(5): p. A218.
79. Mochizuki, H., et al., *Peripheral neuropathy induced by drinking water contaminated with low-dose arsenic in Myanmar*. Environ Health Prev Med, 2019. **24**(1): p. 23.
80. Ishii, N., et al., *Clinical Symptoms, Neurological Signs, and Electrophysiological Findings in Surviving Residents with Probable Arsenic Exposure in Toroku, Japan*. Arch Environ Contam Toxicol, 2018. **75**(4): p. 521-529.
81. Le Quesne, P.M. and J.G. McLeod, *Peripheral neuropathy following a single exposure to arsenic. Clinical course in four patients with electrophysiological and histological studies*. J Neurol Sci, 1977. **32**(3): p. 437-51.
82. Patlolla, A.K. and P.B. Tchounwou, *Serum acetyl cholinesterase as a biomarker of arsenic induced neurotoxicity in sprague-dawley rats*. Int J Environ Res Public Health, 2005. **2**(1): p. 80-3.

83. Singh, A.P., R.K. Goel, and T. Kaur, *Mechanisms pertaining to arsenic toxicity*. Toxicol Int, 2011. **18**(2): p. 87-93.
84. Amitai, Y. and G. Koren, *High risk for neural tube defects; the role of arsenic in drinking water and rice in Asia*. Med Hypotheses, 2018. **119**: p. 88-90.
85. Ren, A.G., *Prevention of neural tube defects with folic acid: The Chinese experience*. World J Clin Pediatr, 2015. **4**(3): p. 41-4.
86. Wlodarczyk, B.J., et al., *Arsenic-induced gene expression changes in the neural tube of folate transport defective mouse embryos*. Neurotoxicology, 2006. **27**(4): p. 547-57.
87. Schmidt, C.W., *In search of "just right": the challenge of regulating arsenic in rice*. Environ Health Perspect, 2015. **123**(1): p. A16-9.
88. Wang, M., et al., *Maternal consumption of non-staple food in the first trimester and risk of neural tube defects in offspring*. Nutrients, 2015. **7**(5): p. 3067-77.
89. Kapaj, S., et al., *Human health effects from chronic arsenic poisoning--a review*. J Environ Sci Health A Tox Hazard Subst Environ Eng, 2006. **41**(10): p. 2399-428.
90. Martinez, V.D., et al., *Arsenic exposure and the induction of human cancers*. J Toxicol, 2011. **2011**: p. 431287.
91. Bates, M.N., et al., *Case-control study of bladder cancer and exposure to arsenic in Argentina*. Am J Epidemiol, 2004. **159**(4): p. 381-9.
92. Steinmaus, C., et al., *Case-control study of bladder cancer and drinking water arsenic in the western United States*. Am J Epidemiol, 2003. **158**(12): p. 1193-201.
93. Ferreccio, C., et al., *Lung cancer and arsenic concentrations in drinking water in Chile*. Epidemiology, 2000. **11**(6): p. 673-9.
94. Wu, M.M., et al., *Dose-response relation between arsenic concentration in well water and mortality from cancers and vascular diseases*. Am J Epidemiol, 1989. **130**(6): p. 1123-32.
95. Mostafa, M.G., J.C. McDonald, and N.M. Cherry, *Lung cancer and exposure to arsenic in rural Bangladesh*. Occup Environ Med, 2008. **65**(11): p. 765-8.
96. Hutchinson, J., *SALVARSAN ("606") AND ARSENIC CANCER*. Br Med J, 1911. **1**(2626): p. 976-7.
97. Wong, S.S., K.C. Tan, and C.L. Goh, *Cutaneous manifestations of chronic arsenicism: review of seventeen cases*. J Am Acad Dermatol, 1998. **38**(2 Pt 1): p. 179-85.
98. Hunt, K.M., et al., *The mechanistic basis of arsenicosis: pathogenesis of skin cancer*. Cancer Lett, 2014. **354**(2): p. 211-9.
99. Cuzick, J., et al., *Medicinal arsenic and internal malignancies*. Br J Cancer, 1982. **45**(6): p. 904-11.
100. Mazumder, D., *Chapter 4 : Diagnosis and treatment of chronic arsenic poisoning*. Drinking-water Quality, 2000.
101. Guha Mazumder, D.N., et al., *Arsenic levels in drinking water and the prevalence of skin lesions in West Bengal, India*. Int J Epidemiol, 1998. **27**(5): p. 871-7.
102. Siefring, M.L., et al. *Rapid onset of multiple concurrent squamous cell carcinomas associated with the use of an arsenic-containing traditional*

- medicine for chronic plaque psoriasis*. BMJ case reports, 2018. **2018**, DOI: 10.1136/bcr-2017-222645.
103. Centeno, J.A., et al., *Pathology related to chronic arsenic exposure*. Environ Health Perspect, 2002. **110 Suppl 5**(Suppl 5): p. 883-6.
 104. Yoshida, T., H. Yamauchi, and G. Fan Sun, *Chronic health effects in people exposed to arsenic via the drinking water: dose-response relationships in review*. Toxicol Appl Pharmacol, 2004. **198**(3): p. 243-52.
 105. Bailey, K.A., et al., *Gene expression of normal human epidermal keratinocytes modulated by trivalent arsenicals*. Mol Carcinog, 2010. **49**(12): p. 981-98.
 106. Sun, Y., et al., *Arsenic transformation predisposes human skin keratinocytes to UV-induced DNA damage yet enhances their survival apparently by diminishing oxidant response*. Toxicol Appl Pharmacol, 2011. **255**(3): p. 242-50.
 107. Melkonian, S., et al., *A prospective study of the synergistic effects of arsenic exposure and smoking, sun exposure, fertilizer use, and pesticide use on risk of premalignant skin lesions in Bangladeshi men*. Am J Epidemiol, 2011. **173**(2): p. 183-91.
 108. Rossman, T.G., et al., *Arsenite is a cocarcinogen with solar ultraviolet radiation for mouse skin: an animal model for arsenic carcinogenesis*. Toxicol Appl Pharmacol, 2001. **176**(1): p. 64-71.
 109. States, J.C., *Disruption of Mitotic Progression by Arsenic*. Biol Trace Elem Res, 2015. **166**(1): p. 34-40.
 110. Thomas-Schoemann, A., et al., *Arsenic trioxide exerts antitumor activity through regulatory T cell depletion mediated by oxidative stress in a murine model of colon cancer*. J Immunol, 2012. **189**(11): p. 5171-7.
 111. Liu, S.X., et al., *Induction of oxyradicals by arsenic: implication for mechanism of genotoxicity*. Proc Natl Acad Sci U S A, 2001. **98**(4): p. 1643-8.
 112. Liu, S.X., et al., *Mitochondrial damage mediates genotoxicity of arsenic in mammalian cells*. Cancer Res, 2005. **65**(8): p. 3236-42.
 113. Ushio-Fukai, M., et al., *p22phox is a critical component of the superoxide-generating NADH/NADPH oxidase system and regulates angiotensin II-induced hypertrophy in vascular smooth muscle cells*. J Biol Chem, 1996. **271**(38): p. 23317-21.
 114. Di-Poi, N., et al., *Mechanism of NADPH oxidase activation by the Rac/Rho-GDI complex*. Biochemistry, 2001. **40**(34): p. 10014-22.
 115. Kumagai, Y. and D. Sumi, *Arsenic: signal transduction, transcription factor, and biotransformation involved in cellular response and toxicity*. Annu Rev Pharmacol Toxicol, 2007. **47**: p. 243-62.
 116. Lynn, S., et al., *NADH oxidase activation is involved in arsenite-induced oxidative DNA damage in human vascular smooth muscle cells*. Circ Res, 2000. **86**(5): p. 514-9.
 117. Bhattacharjee, P., M. Banerjee, and A.K. Giri, *Role of genomic instability in arsenic-induced carcinogenicity. A review*. Environ Int, 2013. **53**: p. 29-40.
 118. Mahata, J., et al., *Chromosomal aberrations and sister chromatid exchanges in individuals exposed to arsenic through drinking water in West Bengal, India*. Mutat Res, 2003. **534**(1-2): p. 133-43.

119. Niedzwiecki, M.M., et al., *A dose-response study of arsenic exposure and global methylation of peripheral blood mononuclear cell DNA in Bangladeshi adults*. Environ Health Perspect, 2013. **121**(11-12): p. 1306-12.
120. Coppin, J.F., W. Qu, and M.P. Waalkes, *Interplay between cellular methyl metabolism and adaptive efflux during oncogenic transformation from chronic arsenic exposure in human cells*. J Biol Chem, 2008. **283**(28): p. 19342-50.
121. Kelsey, K.T., et al., *TP53 alterations and patterns of carcinogen exposure in a U.S. population-based study of bladder cancer*. Int J Cancer, 2005. **117**(3): p. 370-5.
122. Rossman, T.G., A.N. Uddin, and F.J. Burns, *Evidence that arsenite acts as a cocarcinogen in skin cancer*. Toxicol Appl Pharmacol, 2004. **198**(3): p. 394-404.
123. Hsu, C.H., et al., *Mutational spectrum of p53 gene in arsenic-related skin cancers from the blackfoot disease endemic area of Taiwan*. Br J Cancer, 1999. **80**(7): p. 1080-6.
124. Hossain, M.B., et al., *Environmental arsenic exposure and DNA methylation of the tumor suppressor gene p16 and the DNA repair gene MLH1: effect of arsenic metabolism and genotype*. Metallomics, 2012. **4**(11): p. 1167-75.
125. Muenyi, C.S., M. Ljungman, and J.C. States, *Arsenic Disruption of DNA Damage Responses-Potential Role in Carcinogenesis and Chemotherapy*. Biomolecules, 2015. **5**(4): p. 2184-93.
126. Komissarova, E.V. and T.G. Rossman, *Arsenite induced poly(ADP-ribosylation) of tumor suppressor P53 in human skin keratinocytes as a possible mechanism for carcinogenesis associated with arsenic exposure*. Toxicol Appl Pharmacol, 2010. **243**(3): p. 399-404.
127. Ebert, F., et al., *Arsenicals affect base excision repair by several mechanisms*. Mutat Res, 2011. **715**(1-2): p. 32-41.
128. Hartwig, A., et al., *Very low concentrations of arsenite suppress poly(ADP-ribosylation) in mammalian cells*. Int J Cancer, 2003. **104**(1): p. 1-6.
129. Schwerdtle, T., I. Walter, and A. Hartwig, *Arsenite and its biomethylated metabolites interfere with the formation and repair of stable BPDE-induced DNA adducts in human cells and impair XPAzf and Fpg*. DNA Repair (Amst), 2003. **2**(12): p. 1449-63.
130. Zhang, J. and B. Wang, *Arsenic trioxide (As(2)O(3)) inhibits peritoneal invasion of ovarian carcinoma cells in vitro and in vivo*. Gynecol Oncol, 2006. **103**(1): p. 199-206.
131. Ding, W., et al., *Inhibition of poly(ADP-ribose) polymerase-1 by arsenite interferes with repair of oxidative DNA damage*. J Biol Chem, 2009. **284**(11): p. 6809-17.
132. Yu, H.S., W.T. Liao, and C.Y. Chai, *Arsenic carcinogenesis in the skin*. J Biomed Sci, 2006. **13**(5): p. 657-66.
133. States, J.C., et al., *Arsenite disrupts mitosis and induces apoptosis in SV40-transformed human skin fibroblasts*. Toxicol Appl Pharmacol, 2002. **180**(2): p. 83-91.

134. McNeely, S.C., B.F. Taylor, and J.C. States, *Mitotic arrest-associated apoptosis induced by sodium arsenite in A375 melanoma cells is BUBR1-dependent*. Toxicology and applied pharmacology, 2008. **231**(1): p. 61-67.
135. Rancati, G., et al., *Mad3/BubR1 phosphorylation during spindle checkpoint activation depends on both Polo and Aurora kinases in budding yeast*. Cell Cycle, 2005. **4**(7): p. 972-80.
136. D'Angiolella, V., et al., *The spindle checkpoint requires cyclin-dependent kinase activity*. Genes Dev, 2003. **17**(20): p. 2520-5.
137. Rahman, A., et al., *Arsenic exposure in pregnancy increases the risk of lower respiratory tract infection and diarrhea during infancy in Bangladesh*. Environ Health Perspect, 2011. **119**(5): p. 719-24.
138. Srivastava, R.K., et al., *Unfolded protein response (UPR) signaling regulates arsenic trioxide-mediated macrophage innate immune function disruption*. Toxicol Appl Pharmacol, 2013. **272**(3): p. 879-87.
139. Nouri, K., et al., *The incidence of recurrent herpes simplex and herpes zoster infection during treatment with arsenic trioxide*. J Drugs Dermatol, 2006. **5**(2): p. 182-5.
140. Li, C., et al., *Unfolded protein response signaling and MAP kinase pathways underlie pathogenesis of arsenic-induced cutaneous inflammation*. Cancer Prev Res (Phila), 2011. **4**(12): p. 2101-9.
141. Abernathy, C.O., et al., *Arsenic: health effects, mechanisms of actions, and research issues*. Environ Health Perspect, 1999. **107**(7): p. 593-7.
142. Zhao, B., et al., *TEAD mediates YAP-dependent gene induction and growth control*. Genes Dev, 2008. **22**(14): p. 1962-71.
143. Li, C., et al., *Arsenic-induced cutaneous hyperplastic lesions are associated with the dysregulation of Yap, a Hippo signaling-related protein*. Biochem Biophys Res Commun, 2013. **438**(4): p. 607-12.
144. Felix, K., et al., *Low levels of arsenite activates nuclear factor-kappaB and activator protein-1 in immortalized mesencephalic cells*. J Biochem Mol Toxicol, 2005. **19**(2): p. 67-77.
145. Tong, D., et al., *Arsenic Inhibits DNA Mismatch Repair by Promoting EGFR Expression and PCNA Phosphorylation*. J Biol Chem, 2015. **290**(23): p. 14536-41.
146. Kawasaki, H., et al., *Regulation of intestinal myofibroblasts by KRas-mutated colorectal cancer cells through heparin-binding epidermal growth factor-like growth factor*. Oncol Rep, 2017. **37**(5): p. 3128-3136.
147. Sun, J., et al., *Carcinogenic metalloid arsenic induces expression of mdig oncogene through JNK and STAT3 activation*. Cancer Lett, 2014. **346**(2): p. 257-63.
148. Liu, X., et al., *Regulation of microRNAs by epigenetics and their interplay involved in cancer*. J Exp Clin Cancer Res, 2013. **32**(1): p. 96.
149. Alberti, C. and L. Cochella, *A framework for understanding the roles of miRNAs in animal development*. Development, 2017. **144**(14): p. 2548-2559.
150. Cardoso, A.P.F., L. Al-Eryani, and J.C. States, *Arsenic-Induced Carcinogenesis: The Impact of miRNA Dysregulation*. Toxicol Sci, 2018. **165**(2): p. 284-290.

151. Borchert, G.M., W. Lanier, and B.L. Davidson, *RNA polymerase III transcribes human microRNAs*. Nat Struct Mol Biol, 2006. **13**(12): p. 1097-101.
152. Lee, Y., et al., *MicroRNA maturation: stepwise processing and subcellular localization*. Embo j, 2002. **21**(17): p. 4663-70.
153. Peng, Y. and C.M. Croce, *The role of MicroRNAs in human cancer*. Signal Transduct Target Ther, 2016. **1**: p. 15004.
154. Jansson, M.D. and A.H. Lund, *MicroRNA and cancer*. Mol Oncol, 2012. **6**(6): p. 590-610.
155. Hayes, J., P.P. Peruzzi, and S. Lawler, *MicroRNAs in cancer: biomarkers, functions and therapy*. Trends Mol Med, 2014. **20**(8): p. 460-9.
156. Bushati, N. and S.M. Cohen, *microRNA functions*. Annu Rev Cell Dev Biol, 2007. **23**: p. 175-205.
157. Macfarlane, L.A. and P.R. Murphy, *MicroRNA: Biogenesis, Function and Role in Cancer*. Curr Genomics, 2010. **11**(7): p. 537-61.
158. Iorio, M.V. and C.M. Croce, *microRNA involvement in human cancer*. Carcinogenesis, 2012. **33**(6): p. 1126-33.
159. Lagos-Quintana, M., et al., *Identification of novel genes coding for small expressed RNAs*. Science, 2001. **294**(5543): p. 853-8.
160. Huang, S., et al., *MicroRNA-181a modulates gene expression of zinc finger family members by directly targeting their coding regions*. Nucleic Acids Res, 2010. **38**(20): p. 7211-8.
161. Pi, J., et al., *Arsenic-induced malignant transformation of human keratinocytes: involvement of Nrf2*. Free Radic Biol Med, 2008. **45**(5): p. 651-8.
162. Sand, M., et al., *Expression levels of the microRNA processing enzymes Drosha and dicer in epithelial skin cancer*. Cancer Invest, 2010. **28**(6): p. 649-53.
163. Sand, M., et al., *Expression levels of the microRNA maturing microprocessor complex component DGCR8 and the RNA-induced silencing complex (RISC) components argonaute-1, argonaute-2, PACT, TARBP1, and TARBP2 in epithelial skin cancer*. Mol Carcinog, 2012. **51**(11): p. 916-22.
164. Reddy, K.B., *MicroRNA (miRNA) in cancer*. Cancer Cell Int, 2015. **15**: p. 38.
165. Humphries, B., Z. Wang, and C. Yang, *The role of microRNAs in metal carcinogen-induced cell malignant transformation and tumorigenesis*. Food Chem Toxicol, 2016. **98**(Pt A): p. 58-65.
166. Lotterman, C.D., O.A. Kent, and J.T. Mendell, *Functional integration of microRNAs into oncogenic and tumor suppressor pathways*. Cell Cycle, 2008. **7**(16): p. 2493-9.
167. Zhou, K., M. Liu, and Y. Cao, *New Insight into microRNA Functions in Cancer: Oncogene-microRNA-Tumor Suppressor Gene Network*. Front Mol Biosci, 2017. **4**: p. 46.
168. Sampson, V.B., et al., *MicroRNA let-7a down-regulates MYC and reverts MYC-induced growth in Burkitt lymphoma cells*. Cancer Res, 2007. **67**(20): p. 9762-70.
169. Johnson, S.M., et al., *RAS is regulated by the let-7 microRNA family*. Cell, 2005. **120**(5): p. 635-47.

170. Akao, Y., Y. Nakagawa, and T. Naoe, *let-7 microRNA functions as a potential growth suppressor in human colon cancer cells*. Biol Pharm Bull, 2006. **29**(5): p. 903-6.
171. Hu, W., et al., *Negative regulation of tumor suppressor p53 by microRNA miR-504*. Mol Cell, 2010. **38**(5): p. 689-99.
172. Sturchio, E., et al., *Arsenic exposure triggers a shift in microRNA expression*. Sci Total Environ, 2014. **472**: p. 672-80.
173. Michailidi, C., et al., *Involvement of epigenetics and EMT-related miRNA in arsenic-induced neoplastic transformation and their potential clinical use*. Cancer Prev Res (Phila), 2015. **8**(3): p. 208-21.
174. Marsit, C.J., K. Eddy, and K.T. Kelsey, *MicroRNA responses to cellular stress*. Cancer Res, 2006. **66**(22): p. 10843-8.
175. Banerjee, N., et al., *Increased microRNA 21 expression contributes to arsenic induced skin lesions, skin cancers and respiratory distress in chronically exposed individuals*. Toxicology, 2017. **378**: p. 10-16.
176. Gao, S.M., et al., *Synergistic apoptosis induction in leukemic cells by miR-15a/16-1 and arsenic trioxide*. Biochem Biophys Res Commun, 2010. **403**(2): p. 203-8.
177. Li, Y., et al., *Anti-miR-21 oligonucleotide sensitizes leukemic K562 cells to arsenic trioxide by inducing apoptosis*. Cancer Sci, 2010. **101**(4): p. 948-54.
178. Stern, R.S., *Prevalence of a history of skin cancer in 2007: results of an incidence-based model*. Arch Dermatol, 2010. **146**(3): p. 279-82.
179. Gonzalez, H., et al., *Arsenic-exposed Keratinocytes Exhibit Differential microRNAs Expression Profile; Potential Implication of miR-21, miR-200a and miR-141 in Melanoma Pathway*. Clin Cancer Drugs, 2015. **2**(2): p. 138-147.
180. Ye, Q., et al., *MicroRNA-141 inhibits epithelial-mesenchymal transition, and ovarian cancer cell migration and invasion*. Mol Med Rep, 2017. **16**(5): p. 6743-6749.
181. Mizuno, R., K. Kawada, and Y. Sakai, *The Molecular Basis and Therapeutic Potential of Let-7 MicroRNAs against Colorectal Cancer*. Can J Gastroenterol Hepatol, 2018. **2018**: p. 5769591.
182. Jiang, R., et al., *The acquisition of cancer stem cell-like properties and neoplastic transformation of human keratinocytes induced by arsenite involves epigenetic silencing of let-7c via Ras/NF- κ B*. Toxicol Lett, 2014. **227**(2): p. 91-8.
183. Al-Eryani, L., et al., *Differentially Expressed mRNA Targets of Differentially Expressed miRNAs Predict Changes in the TP53 Axis and Carcinogenesis-Related Pathways in Human Keratinocytes Chronically Exposed to Arsenic*. Toxicol Sci, 2018. **162**(2): p. 645-654.
184. Su, B.B., et al., *MiR-186 inhibits cell proliferation and invasion in human cutaneous malignant melanoma*. J Cancer Res Ther, 2018. **14**(Supplement): p. S60-s64.
185. Li, H., et al., *PTTG1 promotes migration and invasion of human non-small cell lung cancer cells and is modulated by miR-186*. Carcinogenesis, 2013. **34**(9): p. 2145-55.

186. Qi, M., et al., *Identification of differentially expressed microRNAs in metastatic melanoma using next-generation sequencing technology*. Int J Mol Med, 2014. **33**(5): p. 1117-21.
187. Zhang, Y., et al., *Profiling of 95 microRNAs in pancreatic cancer cell lines and surgical specimens by real-time PCR analysis*. World J Surg, 2009. **33**(4): p. 698-709.
188. Baffa, R., et al., *MicroRNA expression profiling of human metastatic cancers identifies cancer gene targets*. J Pathol, 2009. **219**(2): p. 214-21.
189. Leidinger, P., et al., *High-throughput miRNA profiling of human melanoma blood samples*. BMC Cancer, 2010. **10**: p. 262.
190. Yang, J., et al., *miR-186 downregulates protein phosphatase PPM1B in bladder cancer and mediates G1-S phase transition*. Tumour Biol, 2016. **37**(4): p. 4331-41.
191. Sun, P., et al., *miR-186 regulates glycolysis through Glut1 during the formation of cancer-associated fibroblasts*. Asian Pac J Cancer Prev, 2014. **15**(10): p. 4245-50.
192. Solomon, M.J. and J.L. Burton, *Securin' M-phase entry*. Nat Cell Biol, 2008. **10**(4): p. 381-3.
193. Nowak, M.A., et al., *The role of chromosomal instability in tumor initiation*. Proc Natl Acad Sci U S A, 2002. **99**(25): p. 16226-31.
194. Vlachos, I.S., et al., *DIANA-miRPath v3.0: deciphering microRNA function with experimental support*. Nucleic Acids Res, 2015. **43**(W1): p. W460-6.
195. Foley, E.A. and T.M. Kapoor, *Microtubule attachment and spindle assembly checkpoint signalling at the kinetochore*. Nat Rev Mol Cell Biol, 2013. **14**(1): p. 25-37.
196. Teixeira, J.H., et al., *An overview of the spindle assembly checkpoint status in oral cancer*. Biomed Res Int, 2014. **2014**: p. 145289.
197. Sudakin, V., G.K. Chan, and T.J. Yen, *Checkpoint inhibition of the APC/C in HeLa cells is mediated by a complex of BUBR1, BUB3, CDC20, and MAD2*. J Cell Biol, 2001. **154**(5): p. 925-36.
198. Rieder, C.L., et al., *The checkpoint delaying anaphase in response to chromosome monoorientation is mediated by an inhibitory signal produced by unattached kinetochores*. J Cell Biol, 1995. **130**(4): p. 941-8.
199. Mapelli, M., et al., *The Mad2 conformational dimer: structure and implications for the spindle assembly checkpoint*. Cell, 2007. **131**(4): p. 730-43.
200. Hara, M., et al., *Structure of an intermediate conformer of the spindle checkpoint protein Mad2*. Proc Natl Acad Sci U S A, 2015. **112**(36): p. 11252-7.
201. Han, J.S., et al., *Catalytic assembly of the mitotic checkpoint inhibitor BubR1-Cdc20 by a Mad2-induced functional switch in Cdc20*. Mol Cell, 2013. **51**(1): p. 92-104.
202. Johnson, V.L., et al., *Bub1 is required for kinetochore localization of BubR1, Cenp-E, Cenp-F and Mad2, and chromosome congression*. J Cell Sci, 2004. **117**(Pt 8): p. 1577-89.
203. Tang, Z., et al., *Phosphorylation of Cdc20 by Bub1 provides a catalytic mechanism for APC/C inhibition by the spindle checkpoint*. Mol Cell, 2004. **16**(3): p. 387-97.

204. Sasaki, M., et al., *Spindle checkpoint protein Bub1 corrects mitotic aberrancy induced by human T-cell leukemia virus type I Tax*. *Oncogene*, 2006. **25**(26): p. 3621-7.
205. Abrieu, A., et al., *Mps1 is a kinetochore-associated kinase essential for the vertebrate mitotic checkpoint*. *Cell*, 2001. **106**(1): p. 83-93.
206. Carmena, M., et al., *The chromosomal passenger complex (CPC): from easy rider to the godfather of mitosis*. *Nat Rev Mol Cell Biol*, 2012. **13**(12): p. 789-803.
207. Tanaka, T.U., et al., *Evidence that the Ipl1-Sli15 (Aurora kinase-INCENP) complex promotes chromosome bi-orientation by altering kinetochore-spindle pole connections*. *Cell*, 2002. **108**(3): p. 317-29.
208. Kops, G.J., B.A. Weaver, and D.W. Cleveland, *On the road to cancer: aneuploidy and the mitotic checkpoint*. *Nat Rev Cancer*, 2005. **5**(10): p. 773-85.
209. Mc Gee, M.M., *Targeting the Mitotic Catastrophe Signaling Pathway in Cancer*. *Mediators Inflamm*, 2015. **2015**: p. 146282.
210. Janssen, A. and R.H. Medema, *Mitosis as an anti-cancer target*. *Oncogene*, 2011. **30**(25): p. 2799-809.
211. Chan, K.S., C.G. Koh, and H.Y. Li, *Mitosis-targeted anti-cancer therapies: where they stand*. *Cell Death Dis*, 2012. **3**(10): p. e411.
212. Brito, D.A. and C.L. Rieder, *Mitotic checkpoint slippage in humans occurs via cyclin B destruction in the presence of an active checkpoint*. *Curr Biol*, 2006. **16**(12): p. 1194-200.
213. Gascoigne, K.E. and S.S. Taylor, *Cancer cells display profound intra- and interline variation following prolonged exposure to antimetabolic drugs*. *Cancer Cell*, 2008. **14**(2): p. 111-22.
214. Boukamp, P., et al., *Normal keratinization in a spontaneously immortalized aneuploid human keratinocyte cell line*. *J Cell Biol*, 1988. **106**(3): p. 761-71.
215. Sun, Y., et al., *Aberrant cytokeratin expression during arsenic-induced acquired malignant phenotype in human HaCaT keratinocytes consistent with epidermal carcinogenesis*. *Toxicology*, 2009. **262**(2): p. 162-70.
216. Bershadsky, A.D., V.I. Gelfand, and J.M. Vasiliev, *Multinucleation of transformed cells normalizes their spreading on the substratum and their cytoskeleton structure*. *Cell Biol Int Rep*, 1981. **5**(2): p. 143-50.
217. Barajas-Olmos, F.M., et al., *Analysis of the dynamic aberrant landscape of DNA methylation and gene expression during arsenic-induced cell transformation*. *Gene*, 2019. **711**: p. 143941.
218. Huang, S., et al., *CD44v6 expression in human skin keratinocytes as a possible mechanism for carcinogenesis associated with chronic arsenic exposure*. *Eur J Histochem*, 2013. **57**(1): p. e1.
219. Alexander, E.T., et al., *Polyamine-stimulation of arsenic-transformed keratinocytes*. *Carcinogenesis*, 2019. **40**(8): p. 1042-1051.
220. Rajput, M., et al., *Flavonoids inhibit chronically exposed arsenic-induced proliferation and malignant transformation of HaCaT cells*. *Photodermatol Photoimmunol Photomed*, 2018. **34**(1): p. 91-101.
221. Thompson, S.L., S.F. Bakhoun, and D.A. Compton, *Mechanisms of chromosomal instability*. *Curr Biol*, 2010. **20**(6): p. R285-95.

222. Tijhuis, A.E., S.C. Johnson, and S.E. McClelland, *The emerging links between chromosomal instability (CIN), metastasis, inflammation and tumour immunity*. Mol Cytogenet, 2019. **12**: p. 17.
223. Schukken, K.M. and F. Foijer, *CIN and Aneuploidy: Different Concepts, Different Consequences*. Bioessays, 2018. **40**(1).
224. Orr, B., K.M. Godek, and D. Compton, *Aneuploidy*. Curr Biol, 2015. **25**(13): p. R538-42.
225. Burrell, R.A., et al., *Replication stress links structural and numerical cancer chromosomal instability*. Nature, 2013. **494**(7438): p. 492-496.
226. Janssen, A., et al., *Chromosome segregation errors as a cause of DNA damage and structural chromosome aberrations*. Science, 2011. **333**(6051): p. 1895-8.
227. Novo, F.J., *Chromosomal Translocations*, in *Encyclopedia of Cancer*, M. Schwab, Editor. 2009, Springer Berlin Heidelberg: Berlin, Heidelberg. p. 679-680.
228. Morris, C.M. and S.M. Benjes, *BCR-ABL1*, in *Encyclopedia of Cancer*, M. Schwab, Editor. 2009, Springer Berlin Heidelberg: Berlin, Heidelberg. p. 318-323.
229. Stimpson, K.M., J.E. Matheny, and B.A. Sullivan, *Dicentric chromosomes: unique models to study centromere function and inactivation*. Chromosome Res, 2012. **20**(5): p. 595-605.
230. Earnshaw, W.C. and B.R. Migeon, *Three related centromere proteins are absent from the inactive centromere of a stable isodicentric chromosome*. Chromosoma, 1985. **92**(4): p. 290-6.
231. Warburton, D., et al., *A stable human dicentric chromosome, t dic (12;14)(p13;p13) including an intercalary satellite region between centromeres*. Am J Hum Genet, 1973. **25**(4): p. 439-45.
232. Therman, E., B. Susman, and C. Denniston, *The nonrandom participation of human acrocentric chromosomes in Robertsonian translocations*. Ann Hum Genet, 1989. **53**(1): p. 49-65.
233. Pristyazhnyuk, I.E. and A.G. Menzorov, *Ring chromosomes: from formation to clinical potential*. Protoplasma, 2018. **255**(2): p. 439-449.
234. Rhoades, M.M. and B. McClintock, *The cytogenetics of maize*. The Botanical Review, 1935. **1**(8): p. 292-325.
235. McClintock, B., *The Stability of Broken Ends of Chromosomes in Zea Mays*. Genetics, 1941. **26**(2): p. 234-82.
236. Fucic, A., et al., *Follow-up studies on genome damage in children after Chernobyl nuclear power plant accident*. Archives of Toxicology, 2016. **90**(9): p. 2147-2159.
237. Arnedo, N., et al., *Mitotic and meiotic behaviour of a naturally transmitted ring Y chromosome: reproductive risk evaluation*. Human Reproduction, 2005. **20**(2): p. 462-468.
238. Surace, C., et al., *Telomere shortening and telomere position effect in mild ring 17 syndrome*. Epigenetics & Chromatin, 2014. **7**(1): p. 1.
239. Jacobs, P.A., et al., *The effect of structural aberrations of the chromosomes on reproductive fitness in man. II. Results*. Clin Genet, 1975. **8**(3): p. 169-78.
240. Kosztolányi, G., *Does "ring syndrome" exist? An analysis of 207 case reports on patients with a ring autosome*. Hum Genet, 1987. **75**(2): p. 174-9.

241. Leibowitz, M.L., C.Z. Zhang, and D. Pellman, *Chromothripsis: A New Mechanism for Rapid Karyotype Evolution*. *Annu Rev Genet*, 2015. **49**: p. 183-211.
242. Xu, K., et al., *Structure and evolution of double minutes in diagnosis and relapse brain tumors*. *Acta Neuropathol*, 2019. **137**(1): p. 123-137.
243. Turner, K.M., et al., *Extrachromosomal oncogene amplification drives tumour evolution and genetic heterogeneity*. *Nature*, 2017. **543**(7643): p. 122-125.
244. Gerlinger, M., et al., *Intratumor heterogeneity and branched evolution revealed by multiregion sequencing*. *N Engl J Med*, 2012. **366**(10): p. 883-892.
245. McGranahan, N., et al., *Cancer chromosomal instability: therapeutic and diagnostic challenges*. *EMBO Rep*, 2012. **13**(6): p. 528-38.
246. Ichijima, Y., et al., *DNA lesions induced by replication stress trigger mitotic aberration and tetraploidy development*. *PLoS One*, 2010. **5**(1): p. e8821.
247. Barber, T.D., et al., *Chromatid cohesion defects may underlie chromosome instability in human colorectal cancers*. *Proc Natl Acad Sci U S A*, 2008. **105**(9): p. 3443-8.
248. Yu, R., et al., *Overexpressed pituitary tumor-transforming gene causes aneuploidy in live human cells*. *Endocrinology*, 2003. **144**(11): p. 4991-8.
249. Zhang, N., et al., *Overexpression of Separase induces aneuploidy and mammary tumorigenesis*. *Proc Natl Acad Sci U S A*, 2008. **105**(35): p. 13033-8.
250. Jones, S., et al., *Core signaling pathways in human pancreatic cancers revealed by global genomic analyses*. *Science*, 2008. **321**(5897): p. 1801-6.
251. Li, Y. and R. Benezra, *Identification of a human mitotic checkpoint gene: hsMAD2*. *Science*, 1996. **274**(5285): p. 246-8.
252. Cahill, D.P., et al., *Mutations of mitotic checkpoint genes in human cancers*. *Nature*, 1998. **392**(6673): p. 300-3.
253. Michel, L.S., et al., *MAD2 haplo-insufficiency causes premature anaphase and chromosome instability in mammalian cells*. *Nature*, 2001. **409**(6818): p. 355-9.
254. Iwanaga, Y., et al., *Heterozygous deletion of mitotic arrest-deficient protein 1 (MAD1) increases the incidence of tumors in mice*. *Cancer Res*, 2007. **67**(1): p. 160-6.
255. Jeganathan, K., et al., *Bub1 mediates cell death in response to chromosome missegregation and acts to suppress spontaneous tumorigenesis*. *J Cell Biol*, 2007. **179**(2): p. 255-67.
256. Cimini, D., et al., *Aurora kinase promotes turnover of kinetochore microtubules to reduce chromosome segregation errors*. *Curr Biol*, 2006. **16**(17): p. 1711-8.
257. Bakhom, S.F., et al., *Genome stability is ensured by temporal control of kinetochore-microtubule dynamics*. *Nat Cell Biol*, 2009. **11**(1): p. 27-35.
258. Green, R.A. and K.B. Kaplan, *Chromosome instability in colorectal tumor cells is associated with defects in microtubule plus-end attachments caused by a dominant mutation in APC*. *J Cell Biol*, 2003. **163**(5): p. 949-61.
259. Rajagopalan, H., et al., *Inactivation of hCDC4 can cause chromosomal instability*. *Nature*, 2004. **428**(6978): p. 77-81.
260. Hernando, E., et al., *Rb inactivation promotes genomic instability by uncoupling cell cycle progression from mitotic control*. *Nature*, 2004. **430**(7001): p. 797-802.

261. Patsouris, C., P.M. Michael, and L.J. Campbell, *A new nonrandom unbalanced t(17;20) in myeloid malignancies*. *Cancer Genet Cytogenet*, 2002. **138**(1): p. 32-7.
262. Wang, P., et al., *dic(5;17): a recurring abnormality in malignant myeloid disorders associated with mutations of TP53*. *Genes Chromosomes Cancer*, 1997. **20**(3): p. 282-91.
263. Heerema, N.A., et al., *Dicentric (9;20)(p11;q11) identified by fluorescence in situ hybridization in four pediatric acute lymphoblastic leukemia patients*. *Cancer Genet Cytogenet*, 1996. **92**(2): p. 111-5.
264. Mackinnon, R.N. and L.J. Campbell, *The role of dicentric chromosome formation and secondary centromere deletion in the evolution of myeloid malignancy*. *Genet Res Int*, 2011. **2011**: p. 643628.
265. Andersen, M.K. and J. Pedersen-Bjergaard, *Increased frequency of dicentric chromosomes in therapy-related MDS and AML compared to de novo disease is significantly related to previous treatment with alkylating agents and suggests a specific susceptibility to chromosome breakage at the centromere*. *Leukemia*, 2000. **14**(1): p. 105-11.
266. An, Q., et al., *Variable breakpoints target PAX5 in patients with dicentric chromosomes: a model for the basis of unbalanced translocations in cancer*. *Proc Natl Acad Sci U S A*, 2008. **105**(44): p. 17050-4.
267. Amor, D.J. and K.H. Choo, *Neocentromeres: role in human disease, evolution, and centromere study*. *Am J Hum Genet*, 2002. **71**(4): p. 695-714.
268. Gebhart, E., *Ring chromosomes in human neoplasias*. *Cytogenet Genome Res*, 2008. **121**(3-4): p. 149-73.
269. Gisselsson, D., et al., *The structure and dynamics of ring chromosomes in human neoplastic and non-neoplastic cells*. *Human Genetics*, 1999. **104**(4): p. 315-325.
270. Kazmierczak, B., et al., *A high frequency of tumors with rearrangements of genes of the HMGI(Y) family in a series of 191 pulmonary chondroid hamartomas*. *Genes Chromosomes Cancer*, 1999. **26**(2): p. 125-33.
271. Barker, P.E., *Double minutes in human tumor cells*. *Cancer Genet Cytogenet*, 1982. **5**(1): p. 81-94.
272. Nathanson, D.A., et al., *Targeted therapy resistance mediated by dynamic regulation of extrachromosomal mutant EGFR DNA*. *Science*, 2014. **343**(6166): p. 72-6.
273. Biedler, J.L. and B.A. Spengler, *Metaphase chromosome anomaly: association with drug resistance and cell-specific products*. *Science*, 1976. **191**(4223): p. 185-7.
274. Balaban-Malenbaum, G. and F. Gilbert, *Double minute chromosomes and the homogeneously staining regions in chromosomes of a human neuroblastoma cell line*. *Science*, 1977. **198**(4318): p. 739-41.
275. Levan, A., G. Levan, and N. Mandahl, *A new chromosome type replacing the double minutes in a mouse tumor*. *Cytogenet Cell Genet*, 1978. **20**(1-6): p. 12-23.
276. Nunberg, J.H., et al., *Amplified dihydrofolate reductase genes are localized to a homogeneously staining region of a single chromosome in a methotrexate-*

- resistant Chinese hamster ovary cell line. Proc Natl Acad Sci U S A, 1978. 75(11): p. 5553-6.*
277. Dolnick, B.J., et al., *Correlation of dihydrofolate reductase elevation with gene amplification in a homogeneously staining chromosomal region in L5178Y cells. J Cell Biol, 1979. 83(2 Pt 1): p. 394-402.*
 278. Kaufman, R.J., P.C. Brown, and R.T. Schimke, *Amplified dihydrofolate reductase genes in unstably methotrexate-resistant cells are associated with double minute chromosomes. Proc Natl Acad Sci U S A, 1979. 76(11): p. 5669-73.*
 279. Gebhart, E., *Double minutes, cytogenetic equivalents of gene amplification, in human neoplasia - a review. Clin Transl Oncol, 2005. 7(11): p. 477-85.*
 280. Testa, J.R., et al., *Advances in the analysis of chromosome alterations in human lung carcinomas. Cancer Genet Cytogenet, 1997. 95(1): p. 20-32.*
 281. Schwab, M., *MYCN Amplification in Neuroblastoma: a Paradigm for the Clinical Use of an Oncogene. Pathol Oncol Res, 1997. 3(1): p. 3-7.*
 282. Marinello, M.J., et al., *Double minute chromosomes in human leukemia. N Engl J Med, 1980. 303(12): p. 704.*
 283. Tavares, A.S., et al., *Tumour ploidy and prognosis in carcinomas of the bladder and prostate. Br J Cancer, 1966. 20(3): p. 438-41.*
 284. Porschen, R., et al., *Prognostic significance of DNA ploidy in adenocarcinoma of the pancreas. A flow cytometric study of paraffin-embedded specimens. Cancer, 1993. 71(12): p. 3846-50.*
 285. Xu, J., L. Huang, and J. Li, *DNA aneuploidy and breast cancer: a meta-analysis of 141,163 cases. Oncotarget, 2016. 7(37): p. 60218-60229.*
 286. Laubert, T., et al., *Stage-specific frequency and prognostic significance of aneuploidy in patients with sporadic colorectal cancer--a meta-analysis and current overview. Int J Colorectal Dis, 2015. 30(8): p. 1015-28.*
 287. de Aretxabala, X., et al., *DNA ploidy pattern and tumour spread in gastric cancer. Br J Surg, 1988. 75(8): p. 770-3.*
 288. Iarmarcovai, G., A. Botta, and T. Orsière, *Number of centromeric signals in micronuclei and mechanisms of aneuploidy. Toxicol Lett, 2006. 166(1): p. 1-10.*
 289. Wise, S.S. and J.P. Wise, *Aneuploidy as an early mechanistic event in metal carcinogenesis. Biochem Soc Trans, 2010. 38(6): p. 1650-4.*
 290. Wu, C.L., L.Y. Huang, and C.L. Chang, *Linking arsenite- and cadmium-generated oxidative stress to microsatellite instability in vitro and in vivo. Free Radic Biol Med, 2017. 112: p. 12-23.*
 291. Filipič, M., *Mechanisms of cadmium induced genomic instability. Mutat Res, 2012. 733(1-2): p. 69-77.*
 292. Hartwig, A., *Mechanisms in cadmium-induced carcinogenicity: recent insights. Biometals, 2010. 23(5): p. 951-60.*
 293. Wang, Z. and D.M. Templeton, *Cellular factors mediate cadmium-dependent actin depolymerization. Toxicol Appl Pharmacol, 1996. 139(1): p. 115-21.*
 294. Güerci, A., A. Seoane, and F.N. Dulout, *Aneugenic effects of some metal compounds assessed by chromosome counting in MRC-5 human cells. Mutat Res, 2000. 469(1): p. 35-40.*

295. Wise, S.S., et al., *Hexavalent Chromium-Induced Chromosome Instability Drives Permanent and Heritable Numerical and Structural Changes and a DNA Repair-Deficient Phenotype*. *Cancer Res*, 2018. **78**(15): p. 4203-4214.
296. Hirose, T., et al., *Frequent microsatellite instability in lung cancer from chromate-exposed workers*. *Mol Carcinog*, 2002. **33**(3): p. 172-80.
297. Xiaohua, L., et al., *Evaluation of the correlation between genetic damage and occupational chromate exposure through BNMN frequencies*. *J Occup Environ Med*, 2012. **54**(2): p. 166-70.
298. Holmes, A.L., S.S. Wise, and J.P. Wise, Sr., *Carcinogenicity of hexavalent chromium*. *Indian J Med Res*, 2008. **128**(4): p. 353-72.
299. Wise, S.S., et al., *Chronic exposure to particulate chromate induces spindle assembly checkpoint bypass in human lung cells*. *Chem Res Toxicol*, 2006. **19**(11): p. 1492-8.
300. Martino, J., et al., *Chronic Exposure to Particulate Chromate Induces Premature Centrosome Separation and Centriole Disengagement in Human Lung Cells*. *Toxicol Sci*, 2015. **147**(2): p. 490-9.
301. Qin, Q., et al., *Homologous recombination repair signaling in chemical carcinogenesis: prolonged particulate hexavalent chromium exposure suppresses the Rad51 response in human lung cells*. *Toxicol Sci*, 2014. **142**(1): p. 117-25.
302. Xie, H., et al., *Neoplastic transformation of human bronchial cells by lead chromate particles*. *Am J Respir Cell Mol Biol*, 2007. **37**(5): p. 544-52.
303. Wise, S.S., et al., *Hexavalent chromium induces chromosome instability in human urothelial cells*. *Toxicol Appl Pharmacol*, 2016. **296**: p. 54-60.
304. Panda, D., H.P. Miller, and L. Wilson, *Determination of the size and chemical nature of the stabilizing "cap" at microtubule ends using modulators of polymerization dynamics*. *Biochemistry*, 2002. **41**(5): p. 1609-17.
305. De Boeck, M., M. Kirsch-Volders, and D. Lison, *Cobalt and antimony: genotoxicity and carcinogenicity*. *Mutat Res*, 2003. **533**(1-2): p. 135-52.
306. Figgitt, M., et al., *The genotoxicity of physiological concentrations of chromium (Cr(III) and Cr(VI)) and cobalt (Co(II)): an in vitro study*. *Mutat Res*, 2010. **688**(1-2): p. 53-61.
307. Bonacker, D., et al., *Genotoxicity of inorganic lead salts and disturbance of microtubule function*. *Environ Mol Mutagen*, 2005. **45**(4): p. 346-53.
308. Kapka, L., et al., *Environmental lead exposure increases micronuclei in children*. *Mutagenesis*, 2007. **22**(3): p. 201-7.
309. Thier, R., et al., *Interaction of metal salts with cytoskeletal motor protein systems*. *Toxicol Lett*, 2003. **140-141**: p. 75-81.
310. Seoane, A.I. and F.N. Dulout, *Genotoxic ability of cadmium, chromium and nickel salts studied by kinetochore staining in the cytokinesis-blocked micronucleus assay*. *Mutat Res*, 2001. **490**(2): p. 99-106.
311. Ohshima, S., *Induction of aneuploidy by nickel sulfate in V79 Chinese hamster cells*. *Mutat Res*, 2001. **492**(1-2): p. 39-50.
312. Ochi, T., et al., *Cytotoxic, genotoxic and cell-cycle disruptive effects of thio-dimethylarsinate in cultured human cells and the role of glutathione*. *Toxicol Appl Pharmacol*, 2008. **228**(1): p. 59-67.

313. Yih, L.H. and T.C. Lee, *Induction of C-anaphase and diplochromosome through dysregulation of spindle assembly checkpoint by sodium arsenite in human fibroblasts*. *Cancer Res*, 2003. **63**(20): p. 6680-8.
314. Hubaux, R., et al., *Molecular features in arsenic-induced lung tumors*. *Mol Cancer*, 2013. **12**: p. 20.
315. Zhao, Y., P. Toselli, and W. Li, *Microtubules as a critical target for arsenic toxicity in lung cells in vitro and in vivo*. *Int J Environ Res Public Health*, 2012. **9**(2): p. 474-95.
316. Yih, L.H., et al., *Induction of centrosome amplification during arsenite-induced mitotic arrest in CGL-2 cells*. *Cancer Res*, 2006. **66**(4): p. 2098-106.
317. Taylor, B.F., et al., *Arsenite-induced mitotic death involves stress response and is independent of tubulin polymerization*. *Toxicol Appl Pharmacol*, 2008. **230**(2): p. 235-46.
318. Salazar, A.M., M. Sordo, and P. Ostrosky-Wegman, *Relationship between micronuclei formation and p53 induction*. *Mutat Res*, 2009. **672**(2): p. 124-8.
319. Moore, L.E., et al., *Arsenic-related chromosomal alterations in bladder cancer*. *J Natl Cancer Inst*, 2002. **94**(22): p. 1688-96.
320. Sciandrello, G., et al., *Arsenic-induced DNA hypomethylation affects chromosomal instability in mammalian cells*. *Carcinogenesis*, 2004. **25**(3): p. 413-7.
321. Ghosh, P., et al., *Cytogenetic damage and genetic variants in the individuals susceptible to arsenic-induced cancer through drinking water*. *Int J Cancer*, 2006. **118**(10): p. 2470-8.
322. Ghosh, P., et al., *Evaluation of cell types for assessment of cytogenetic damage in arsenic exposed population*. *Mol Cancer*, 2008. **7**: p. 45.
323. Liou, S.H., et al., *Increased chromosome-type chromosome aberration frequencies as biomarkers of cancer risk in a blackfoot endemic area*. *Cancer Res*, 1999. **59**(7): p. 1481-4.
324. Boffetta, P., et al., *Chromosomal aberrations and cancer risk: results of a cohort study from Central Europe*. *Am J Epidemiol*, 2007. **165**(1): p. 36-43.
325. Al-Eryani, L., et al., *miRNA expression profiles of premalignant and malignant arsenic-induced skin lesions*. *PLoS One*, 2018. **13**(8): p. e0202579.
326. Howe, B., A. Umrigar, and F. Tsien, *Chromosome preparation from cultured cells*. *J Vis Exp*, 2014(83): p. e50203.
327. Chowdhury, R., et al., *Arsenic-induced cell proliferation is associated with enhanced ROS generation, Erk signaling and CyclinA expression*. *Toxicol Lett*, 2010. **198**(2): p. 263-71.
328. Borowicz, S., et al., *The soft agar colony formation assay*. *J Vis Exp*, 2014(92): p. e51998.
329. Puck, T.T. and P.I. Marcus, *Action of x-rays on mammalian cells*. *J Exp Med*, 1956. **103**(5): p. 653-66.
330. Kalluri, R. and R.A. Weinberg, *The basics of epithelial-mesenchymal transition*. *J Clin Invest*, 2009. **119**(6): p. 1420-8.
331. Williams, G.H. and K. Stoeber, *The cell cycle and cancer*. *J Pathol*, 2012. **226**(2): p. 352-64.

332. Polette, M., et al., *Beta-catenin and ZO-1: shuttle molecules involved in tumor invasion-associated epithelial-mesenchymal transition processes*. Cells Tissues Organs, 2007. **185**(1-3): p. 61-5.
333. Scanlon, C.S., et al., *Biomarkers of epithelial-mesenchymal transition in squamous cell carcinoma*. J Dent Res, 2013. **92**(2): p. 114-21.
334. Burkard, M.E. and B.A. Weaver, *Tuning Chromosomal Instability to Optimize Tumor Fitness*. Cancer Discov, 2017. **7**(2): p. 134-136.
335. Qiu, L., et al., *CDC27 Induces Metastasis and Invasion in Colorectal Cancer via the Promotion of Epithelial-To-Mesenchymal Transition*. J Cancer, 2017. **8**(13): p. 2626-2635.
336. Ando, K., et al., *High expression of BUBR1 is one of the factors for inducing DNA aneuploidy and progression in gastric cancer*. Cancer Sci, 2010. **101**(3): p. 639-45.
337. Maciejczyk, A., et al., *Elevated BUBR1 expression is associated with poor survival in early breast cancer patients: 15-year follow-up analysis*. J Histochem Cytochem, 2013. **61**(5): p. 330-9.
338. Qi, W. and H. Yu, *KEN-box-dependent degradation of the Bub1 spindle checkpoint kinase by the anaphase-promoting complex/cyclosome*. J Biol Chem, 2007. **282**(6): p. 3672-9.
339. McNeely, S.C., et al., *Exit from arsenite-induced mitotic arrest is p53 dependent*. Environ Health Perspect, 2006. **114**(9): p. 1401-6.
340. Giam, M. and G. Rancati, *Aneuploidy and chromosomal instability in cancer: a jackpot to chaos*. Cell Div, 2015. **10**: p. 3.

CURRICULUM VITAE

Angeliki Lykoudi

aglyko01@louisville.edu

Education

- MS in Pharmacology & Toxicology, University of Louisville, KY, USA, Fall 2018-present
- BS in Molecular Biology & Genetics, Democritus University of Thrace, Greece, Fall 2013- Summer 2018

Research Experience

- Dr. J. Christopher States' lab, University of Louisville, KY, USA, involved in projects aimed to investigate mechanisms of arsenic-induced skin carcinogenesis, January 2019- present
- Dr. David W. Hein's lab & Dr Gavin E. Arteel's lab, University of Louisville, KY, USA, the project aimed to investigate how the combination of N-acetyltransferase genetic polymorphisms and diet affects the development of metabolic syndrome, April-June 2017
- Dr. Sotiria Boukouvala' s lab, Democritus University of Thrace, Greece, the project aimed to investigate the metabolic functions of N-acetyltransferases homologues, September-April 201

Working Experience

- Diagnostic Clinical Laboratory Feres, Evros, Greece, carried out administrative tasks involving patients' prescriptions and performed routine biochemical tests from blood and urine samples, June-August 2016
- Technician at Choremio Laboratory, St Sophia's Children's Hospital, Athens, Greece, performed routine cytogenetic analysis of karyotypes for Down, Turner and Klinefelter syndromes, June-July 2014

Awards

- 1st Place Masters Student Award, Virtual Student & Postdoctoral Researchers' Summer Meeting, Ohio Valley Society of Toxicology Regional Chapter, July 2020
- 2nd Place Charles River Travel Award, Society of Toxicology Dermal Toxicology Specialty Section, Anaheim, CA, March 2020
- Graduate Student Council (GSC) Travel Grant Award, University of Louisville, Louisville, KY, USA, January 2019
- 2nd place Masters Basic Science Graduate Student Award, Research!Louisville Conference, University of Louisville, Louisville, KY, USA, September 2019

Presentations

Lykoudi A, Cardoso AP, Wise S, States JC, MiR-186 overexpression exacerbates the arsenic-induced chromosomal instability associated with skin carcinogenesis: Presented at:

- Poster at Ohio Valley Society of Toxicology Regional Chapter Annual Virtual

Meeting, November 2020

- 3 min Tox on the Clock/Graphical Abstract Presentation, Ohio Valley Society of Toxicology Regional Chapter Annual Virtual Meeting, November 2020

Lykoudi A, Cardoso AP, Wu J, Wise S, States JC, Overexpression of hsa-miR-186 induces anchorage- independent growth and chromosomal alterations in arsenic exposed human keratinocytes: A preliminary study. Presented at:

- 3 min Speed Talk/Graphical Abstract Presentation, Virtual Student & Postdoctoral Researchers' Summer Meeting, Ohio Valley Society of Toxicology Regional Chapter, July 2020
- Poster at SOT Annual Meeting Society of Toxicology, Anaheim, CA, USA, March 2020 (accepted for presentation but meeting cancelled because of coronavirus pandemic)
- Poster at Ohio Valley Society of Toxicology Regional Chapter, Procter & Gamble, Cincinnati, OH, USA, October 2019
- Poster at Research!Louisville Conference, University of Louisville, Louisville, KY, USA, September 2019

Published abstracts

- Ohio Valley Society of Toxicology Regional Chapter Annual Virtual Meeting, Lykoudi A, Cardoso AP, Wise S, States JC, MiR-186 overexpression exacerbates the arsenic-induced chromosomal instability associated with skin carcinogenesis, November 2020
- Ohio Valley Society of Toxicology Regional Chapter Annual Virtual Meeting, Hong KU, Doll M, Lykoudi A, Salazar-Gonzalez RA, Habil MR, Walls KM, Bakr AF, Ghare SS, Barve SS, Arteel GE, Hein DW, Acetylator Genotype-Dependent Dyslipidemia in

Rats Congenic for N-Acetyltransferase 2, November 2020

- Lykoudi A, Cardoso AP, Wu J, Wise S, States JC. Overexpression of hsa-miR-186 induces anchorage-independent growth and chromosomal alterations in arsenic exposed human keratinocytes: A preliminary study. In: *The Toxicologist*. Supplement to Toxicological Sciences, 174, 1, Society of Toxicology, 2020, 2622
- Banerjee M, Cardoso AP, Lykoudi A, Wilkey DW, Watson WH, Garbett NC, Merchant ML, Pan J, Rai SN, States JC. Arsenite Alters Structure and Function of alternative Splicing Regulator ZRANB2 by Displacing Zinc from Zinc Finger Motifs. In: *The Toxicologist*. Supplement to Toxicological Sciences, 174, 1, Society of Toxicology, 2020, 2632
- Ohio Valley Society of Toxicology Regional Chapter Procter & Gamble, Lykoudi A, Cardoso AP, Wu J, Wise S, States JC, "Overexpression of hsa-miR-186 induces anchorage-independent growth and chromosomal alterations in arsenic exposed human keratinocytes: A preliminary study", Cincinnati, October 2019
- Research! Louisville Conference, Lykoudi A, Cardoso AP, Wu J, Wise S, States JC, "Overexpression of hsa-miR-186 induces anchorage-independent growth and chromosomal alterations in arsenic exposed human keratinocytes: A preliminary study", University of Louisville, September 2019

Publications

- Cardoso APF, Banerjee M, Nail AN, Lykoudi A, States JC, miRNA dysregulation is an emerging modulator of genomic instability, *Semin Cancer Biol*, 2021, 33979676
- Hong KU, Doll MA, Lykoudi A, Salazar-Gonzalez RA, Habil MR, Walls KM, Bakr AF, Ghare SS, Barve SS, Arteel GE, Hein DW, Acetylator Genotype-Dependent Dyslipidemia in Rats Congenic for N-Acetyltransferase 2, *Toxicol Rep*, 2020,

(7):1319-1330

- Banerjee M, Cardoso APF, Lykoudi A, Wilkey DW, Pan J, Watson WH, Garbett NC, Rai SN, Merchant MM, States JC, Zinc displacement from ZRANB2 by arsenic affects splicing, *Chem Res Toxicol*, 2020, 10.1021
- Salazar-Gonzalez RA, Zhang X, Doll MA, Lykoudi A, Hein DW, Role of the human N-acetyltransferase 2 genetic polymorphism in metabolism and genotoxicity of 4,4'-methylenedianiline, *Arch Toxicol*, 2019, 93(8):2237-2246